

LONGITUDINAL STRENGTH OF SHIPS

A simplified approach

A thesis submitted for the
Degree of Master of Science in
the Faculty of Engineering of
the University of Glasgow

by

José Manuel Antunes Mendes GORDO

Department of Naval Architecture and Ocean Engineering

University of Glasgow

(C) José Gordo, 1993

ProQuest Number: 13832027

All rights reserved

INFORMATION TO ALL USERS

The quality of this reproduction is dependent upon the quality of the copy submitted.

In the unlikely event that the author did not send a complete manuscript and there are missing pages, these will be noted. Also, if material had to be removed, a note will indicate the deletion.



ProQuest 13832027

Published by ProQuest LLC (2019). Copyright of the Dissertation is held by the Author.

All rights reserved.

This work is protected against unauthorized copying under Title 17, United States Code
Microform Edition © ProQuest LLC.

ProQuest LLC.
789 East Eisenhower Parkway
P.O. Box 1346
Ann Arbor, MI 48106 – 1346

LONGITUDINAL STRENGTH OF SHIPS

A simplified approach

A thesis submitted for the
Degree of Master of Science in
The Faculty of Engineering of
The University of Glasgow

Jose Manuel Alvarez Mendez B.Eng.

Department of Naval Architecture and Ocean Engineering

University of Glasgow

1997

Thesis
9582
copy 1



To my Wife and my Children,

Rita and Bernardo.

Contents

Contents	i
Notation	iv
List of Figures	viii
List of Tables	x
Acknowledgements	xi
Summary	xii
1 Introduction	1
2 Strength of Plate Elements	3
2.1 Load-Shortening Curves for Plates under Uniaxial Loading	6
2.1.1 Slenderness and Effective Width	8
2.1.2. Aspect Ratio and Transverse Strength	12
2.2 Effect of Residual Stresses	16
2.2.1 Approach for Design Formulas (DFM)	16
2.2.2 Physical Approach Method (PAM)	20
2.2.3. Comparison between models	24
2.3 Effect of Initial Deformations	27
2.4 Effect of Biaxial Loading	30
2.4.1 Reduction Factor	32
2.4.2 Formulation Adopted	33
2.5 Effect of Lateral Pressure	35
2.6 Effect of Edge Shear	37

3	Strength of Stiffened Plates	40
3.1	Review of the literature	43
3.1.1	Theoretical approaches	43
3.1.2	Tests	44
3.1.2.1	Uniaxial compression	44
3.1.2.2	Compression and lateral pressure	46
3.2	Modes of failure	47
3.2.1	Plate induced failure	47
3.2.2	Flexural buckling of columns	48
3.2.2.1	Faulkner's method	48
3.2.2.2	Carlsen's method	51
3.2.3	Tripping of stiffeners	55
3.2.3.1	Elastic tripping stress	56
3.2.3.2	Inelastic effects	58
3.2.3.3	Behaviour of pre and post tripping	59
3.3	Load-end shortening curves of beam-columns	62
3.3.1	Effect of distortions	64
3.3.1.1	Consequence of plate imperfections on column strength	64
3.3.1.2	Consequence of out-of-plane imperfections of the stiffener	66
3.3.1.3	Consequence of lateral rotational distortions	68
3.3.2	Effect of lateral pressure	69

3.3.3	Load shedding after buckling	70
3.3.4	Effect of the residual stresses	70
4	Longitudinal Strength of the Hull Girder	75
4.1	Moment-Curvature Curves	77
4.1.1	The method	77
4.1.1	Modelling of the ship's cross section	81
4.2	Analysis of 'Energy Concentration'	85
4.2.1	The Ship	85
4.2.2	Modelling of the Ship	87
4.2.3	Moment-Curvature Curve	90
4.3	Effect of corrosion	98
4.4	Effect of Residual Stresses	101
4.5	Effect of distortions	105
4.6	Analysis for combined loading	107
4.7	Efficiency of high strength steel	113
5	Conclusion and Future Development	115
	REFERENCES	119

Notation

a	Plate length, stiffener span
b	Plate width
b_e	Effective width of the plate
b_e'	Reduced effective width of the plate
p_r	Proportional limit stress ratio
r_{ce}	Inertial radii of a column's effective cross-section
t	Plate thickness
A_s	Cross-section area of the stiffener
C_s	Rotational spring stiffness
C_y	Biaxial reduction factor
C_{yQ}	Biaxial and lateral pressure reduction factor
C_τ	Edge shear reduction factor
DFM	Design formulas method
E	Young's modulus of elasticity
E_s	Secant modulus of elasticity
E_t	Tangent modulus of elasticity
E_{tb}	Tangent modulus of elasticity in biaxial loading
I_{ce}'	Reduced moment of inertia
I_p	Moment of inertia of the stiffener about the toe
G	Shear modulus of elasticity
J	St. Venant torsional constant
JO	Johnson-Ostenfeld method to determine column behaviour using Faulkner approach
PAM	Physical approach method

- PR Abreviation of Perry-Robertson method to determine column behaviour using Carlsen approach
- Q_L Non-dimensional lateral pressure parameter
- R_Q Lateral pressure reduction factor
- R_{rd} Initial imperfections reduction factor
- R_x Applied stress normalised by ultimate stress in longitudinal direction
- R_y Applied stress normalised by ultimate stress in transverse direction
- T_p Tripping parameter
- x_i Horizontal distance from the stiffened element i to the base line
- x_{1i} Horizontal position from the stiffened element i to the vertical axis passing over any point of the neutral axis
- x_{NAi} Horizontal position from the stiffened element i to the vertical axis passing over the instantaneous CG
- y_i Vertical distance from the stiffened element i to the center line
- y_{1i} Vertical position from the stiffened element i to the horizontal axis passing over any point of the neutral axis
- y_{NAi} Vertical position from the stiffened element i to the horizontal axis passing over the instantaneous CG
- W Beam-column section modulus
- α Aspect ratio of a plate
- β Plate slenderness
- β_0 Nominal plate slenderness
- δ_p Initial out-of-plane imperfections of the plate

δ_s	Out-of-plane deformation of the stiffener
ε	Strain
ε_0	Yield strain
$\bar{\varepsilon}$	Strain normalised by yield strain
λ	Column slenderness
λ_0	Nominal column slenderness
η	Width of residual stress tension strip normalised by t
σ	In-plane stress
σ_a	Average stress
σ_e	Edge stress
σ_0	Yield stress
σ_E	Euler stress
σ_r	Compressive residual stress
σ_T	Elastic tripping stress
Φ	Stress normalised by yield stress, $\Phi = \bar{\sigma}$
Φ_a	Average long plate stress normalised by yield stress
Φ_{ab}	Average normalised stress due to flexural buckling of the column
Φ_{ac}	Average normalised stress due to plate induced failure
Φ_{ap}	Average normalised stress of a column using Carlsen's method
Φ_{at}	Average wide plate stress normalised by yield stress
Φ_{bQa}	Average strength of the plate at a given strain corrected by biaxial and lateral pressure effects
Φ_e	Edge stress normalised by yield stress

- Φ_{er} Strength of the elasto-perfectly plastic plate with residual stresses
- Φ_{jo} Jonhson-Ostenfeld normalised stress at a given strain
- Φ_r Normalised compressive residual stress
- Φ_{rp} Normalised average stress of the plate with residual stress (PAM)
- Φ_{Ti} Inelastic normalised average tripping stress of a column
- Φ_{Tu} Ultimate normalised average tripping stress of a panel
- Φ_u Ultimate stress normalised by yield stress, ultimate strength
- Φ_{ub} Ultimate normalised stress of the column due to flexural buckling
- Φ_{uc} Ultimate normalised stress of the column due to plate induced failure
- Φ_{ux} Ultimate stress normalised by yield stress in longitudinal direction
- Φ_{uy} Ultimate stress normalised by yield stress in transverse direction
- Φ_{uc} Ultimate normalised stress of the column due to plate induced failure
- Φ_w Longitudinal effective width
- Φ_{wt} Transverse effective width
- Φ_δ Reduction of strength of the perfect plate due to initial distortions

List of Figures

Figure 1 - Stress-Strain Curves Model	10
Figure 2 - Stress-Strain Curves	10
Figure 3 - Plate's Stress Distribution and Model	12
Figure 4 - Transverse Strength of Plates	14
Figure 5 - Transverse Strength of Plates	14
Figure 6 - Residual Stresses Pattern Model	17
Figure 7 - Residual Stresses Effect using DFM	18
Figure 8 - Tangent Modulus Ratio	19
Figure 9 - Residual Stresses Effect in Perfect Plates	20
Figure 10 - Example of a Plate with Residual Stress	21
Figure 11 - Curves for several levels of residual stresses	23
Figure 12 - Ultimate strength and residual stresses	24
Figure 13 - Comparison of stress-strain curves	26
Figure 14 - Ultimate strength and ultimate strain	26
Figure 15 - Comparison between Levels of Distortions	39
Figure 16 - Comparison between effective width formulas	52
Figure 17-Construction of load-shortening curves	63
Figure 18 - Effect of Stiffener Imperfections	67
Figure 19-Load-Shortening Curves of Columns	73
Figure 20-Load-Shortening Curves of Columns	73
Figure 21-Load-Shortening Curves of Columns	74
Figure 22-Load-Shortening Curves of Columns	74
Figure 23-Combined bending of hull	78

Figure 24-Strain State of a Stiffened Plate Element	82
Figure 25-Modelling of Unstiffened Side Girders	83
Figure 26-The 'Energy Concentration' plan and profile	85
Figure 27-Bending Moment Distribution at Failure	86
Figure 28-Modelling of the Failure Cross-Section	87
Figure 29-Geometry and Dimensions of Energy Concentration	88
Figure 30-Scantlings of Plating and Longitudinals	88
Figure 31-Moment-Curvature Curve of 'Energy Concentration'	92
Figure 32-Moment-Curvature Curve of 'Energy Concentration'	93
Figure 33-Moment-Curvature Curve of 'Energy Concentration'	95
Figure 34-Moment-Curvature Curve of 'Energy Concentration'	96
Figure 35-Effect of Corrosion	100
Figure 36- Effect of Residual Stresses	102
Figure 37-Components of Combined Bending at 165°	109
Figure 38-Variation of Moment Angle with Curvature	109
Figure 39- Combined Bending Moment	111

List of Tables

Table 1-Scantlings Dimensions and Material Properties	89
Table 2-Results of Hogging Moment	90
Table 3-Results of Ultimate Moment in Sagging	94
Table 4-Effect of Corrosion (Faulkner Method)	99
Table 5-Effect of Corrosion (Carlsen Method)	99
Table 6-Effect of Residual Stresses on Ultimate Moment	102
Table 7-Effect of Distortions (Carlsen Method)	105
Table 8-Influence of High Strength Steel	114

Acknowledgements

This work was carried out at the Department of Naval Architecture and Ocean Engineering, University of Glasgow and at the Instituto Superior Técnico, Universidade Técnica de Lisboa.

I wish to express my sincere gratitude to Professor D. Faulkner and Professor C. Guedes Soares for their valuable guidance, help, advice and support throughout the project.

I also would like to thank the Junta Nacional de Investigação Científica e Tecnologia - Programa Ciência, who provided me with the necessary financial support during my stay in Glasgow.

José Gordo

June 1993

Author's statement:

All the material in this thesis is original except where reference is made to other sources.

Summary

A simplified method is proposed to predict the behaviour of full cross-sections of ships under longitudinal bending.

The method assumes that plane sections remain plane and thus a linear distribution of strains is considered over the cross-section. The hull girder collapse strength may be calculated for any heeling conditions.

The large panels between the primary framing system of the cross-section are assumed to have the same behaviour as their significant individual elements - stiffener with associated plate.

The load-shortening curves of the stiffened plates is assessed using the Johnson-Ostenfeld or the Perry-Robertson formulation. These formulations are basically used to determine the flexural collapse strength of the stiffened elements, but here, they are extended to cover the whole range of strains, predicting the pre and post buckling behaviour. The reduction of the effective width of the associated plate during the path loading is accounted for by considering approximated average stress-strain curves of the plate elements and the Faulkner proposal is adopted to quantify the impact of this reduction on the load-shortening curve of the column.

The effects of flexural-torsional buckling are considered, applying the methods developed by Adamchak and Faulkner, both in respect to the ultimate carrying capacity of the stiffened plate and the post buckling behaviour.

The stress-strain curves of the plate elements are determined in relation to a design formula of the ultimate strength of simply supported plates and the concept is extended in order to obtain the curve for the whole range of strains.

The method includes the effect of residual stresses in the plate elements by modifying the material properties. So the impact of plate residual stresses on hull girder strength may be investigated.

Also available is a method to incorporate the effect of plate and stiffener distortions and their effects on the ultimate strength of the ships.

An investigation of the effect of secondary load systems in plate elements is made. Formulae to include the effect of biaxial loading, lateral pressure and edge shear are indicated based on a study of the ultimate strength of plate elements.

Concerning to the ultimate bending moment of the hull girder, the effect of residual stresses and stiffener distortions is investigated as well as the consequences of corrosion and the use of high tensile steel. The strength of the hull girder is calculated for any angle of heel by a method that ensures a constant angle between the position of the neutral axis at any curvature and the horizontal.

1 Introduction

The present study has as the main objective of studying the collapse strength of the hull girder and its components. To determine the hull strength requires the development of a program which is able to predict and analyse the behaviour of a mid-ship section under the normal operation loads.

Starting from the definition of the section's geometry, the program must be able to determine the contribution of every element to the total strength by taking into account the variation of the strength as a result of several parameters like slendernesses of plate and column, distortions, residual stresses and corrosion.

The analysis must be as simple as possible, but at the same time applying and satisfying all the concepts, results and theories accepted nowadays as the most representative of structural knowledge.

This simplicity of the formulation and resolution of the tasks is aimed at achieving reliable results in reasonable time and with very low costs. This last point is of special importance as existing methods are usually based on finite element analyses, which are very expensive both in the definition of the models geometry and in the program's running time.

On the other hand, these types of analyses take a long time to develop, making them incompatible with the normal development of a ship's project. They have also very little flexibility to consider the effects of geometric modifica-

tions which are always required when wishing to improve the final design.

In a broad view, the collapse strength of a ship section can be seen as the summation of individual contributions of several panels which are part of the section. The strength of each panel, when submitted to axial strains, will determine the overall strength of the section.

The panel's strength can be calculated analysing, individually, each reinforced element of the panel and assuming certain conditions for the structural behaviour, as will be seen in chapter 3.

There are actually many theories about the behaviour of reinforced elements working as a beam or as a column. However, most of them need to have a clear definition of the effective width of the associated plate which will be used on the model. This then inevitably requires the study of the plate elements in order to clarify the concepts of effective width and breadth under several load conditions.

2 Strength of Plate Elements

Marine structures and more precisely ship hulls are mainly formed of plates reinforced by stiffeners. As a consequence, the study of plate behaviour is of major importance for the structural analysis of ships.

These plates can be subjected to different loadings, from a simple uniaxial loading to a complex case of biaxial loading with lateral pressure and edge shear. Uniaxial loading is predominant on deck plating, while biaxial loading and lateral pressure may be very important on bottom plating and edge shear on side shell and bulkhead plating.

Several studies have been performed to establish an accurate description of the behaviour of rectangular plates under specific loading conditions. The most common approaches to the problem of plate behaviour under uniaxial compression attempt to define the ultimate strength of the plate^{1,2} and its dependence on residual stresses and distortions^{1,3,4,5}, or, analysing the whole load-shortening curves in order to provide a comprehensive understanding of inelastic buckling and post-buckling collapse phenomena⁵⁻¹⁰.

The work on plates may be classified as numerical, experimental or statistical:

- There are many references dealing with numerical solutions to plate behaviour. They may use energy methods¹¹, Ritz' method⁸, finite element analysis^{2,9,12,34} or finite differences methods with dynamic relaxation techniques¹⁰. One is

able, in principle, to use these techniques for studying the behaviour of plates with residual stresses and initial distortions. It is also possible to study the effect of different boundary conditions on plate behaviour, by controlling the degree of restraint imposed on the edges of the plate. In this text the boundary conditions are classified as clamped when all membrane displacements at the edge are fixed to zero, as restrained when the membrane displacement normal to the edge are zero but free to rotate, as constrained when the edges remain straight but are free to pull in or out and to rotate and unrestrained when all in-plane membrane displacements are free.

- Experiments¹³⁻²⁰ represent the best way of testing and calibrating numerical results. However these tests show several difficulties in execution, especially in respect of the control of boundary conditions, residual stresses and distortions. In fact, if it is very difficult to simultaneously control residual stresses and distortions in numerical methods unless the effects of residual stresses are considered by a shift on material properties curve as in PANFEM which is a finite element program for research purposes³⁴, in tests this is almost impossible and the best one can get is the maximum out-of-plane deformation of the unloaded plate and detailed information of the welding process.
- Statistical studies represent an effort to synthesise the available information. Normally two classes may be identified: the first, dealing with primary parameters like slenderness¹ and aspect ratio^{2,8}; the other, concerning the dependence on secondary parameters like residual stresses and distortions^{3,9}.

With respect to the type of loading, these studies may be classified:

- uniaxial compression - longitudinal or transverse
- biaxial in-plane loading
- uniaxial or biaxial with lateral pressure
- uniaxial with edge shear

Attention is called to the fact that some of the uniaxial tests are really biaxial tests where transverse stresses are normally a small part of longitudinal stresses. Most tests and numerical studies on restrained plates are unfortunately of this kind, and usually no record of average transverse stresses is available.

However some studies treat this situation as in Dowling et al⁷ where it is shown that transverse stresses due to restrained boundary conditions may be positive, negative or zero, depending on the geometry of the plate and the level of stresses applied. Moxham⁸ called our attention to the unloaded edge displacement in unrestrained plates during compression.

2.1 Load-Shortening Curves for Plates under Uniaxial Loading

When a ship is subjected to longitudinal bending all longitudinal elements, namely girders, longitudinals and plates, are loaded unidirectionally in their own geometric plane. Simultaneously, there may coexist loadings in other directions as a result of secondary effects like local lateral pressure or shear.

As longitudinal stresses predominate in a ship, it is very important to understand the behaviour of the plate elements loaded longitudinally or transversely, depending the type of stiffening in a ship's structure.

As the plate behaviour under tension does not seem to represent a problem to model since the plate may be considered fully effective, the greatest problem is the plate behaviour under compression due to the loss of effectiveness of part of the plate by elastic and inelastic instability and distortions. Several works were aimed at determining that behaviour for the whole range of average strain, where average strain is defined as the edge strain ($\varepsilon = \varepsilon_e$). Thus, keeping the edge in-plane, it is formally equivalent to talk about average strain or normalised shortening and elongation.

Smith⁹ produced average stress-strain curves based on a finite element analysis and a linear regression of tests. Plates were grouped by slenderness ($\beta = 1.0, 1.5, 2.0, 2.5, 3.0, 3.5$ and 4.0) and three levels of imperfections were considered: slight, average and severe. Linear interpolation was used for intermediate slendernesses. Each increasing level of imperfections was associated simultaneously with both increasing residual stresses and distortions. This does not seem to be very appropriate

because, as Faulkner¹ demonstrated, residual stresses decrease as plate slenderness increases whereas distortions increase with slenderness. There is high correlation between these two imperfections but negative and not positive as considered. Buckling strains were selected approximately at 1, 1.5 and 2 times the yield strain depending on the level of imperfections.

Billingsley²³ based his plate model by considering two main contributions to plate effectiveness: the first, concerned with the edge zones, is based on an effective width; the centre contribution is the loading supported by an infinitely wide plate. Only the first contribution must be considered in long plates. The model does not take into account either residual stresses and distortions or load shedding after buckling, which is very important for ultimate bending moment estimation.

Rhodes²⁴ also used a method based on the effective width concept and post-buckling behaviour based on the assumption that elastically derived effective widths were adequate to describe it. The effects of residual stresses and initial distortions were incorporated.

Lin²² proposed an approximate method to generate average stress-strain curves using cubic splines for representing the load shortening curves of residual stress-free plates, based on the data from a parametric study of Frieze. A simplified procedure was used to derive the curves for plates with residual stresses.

The present work considers that the material has an elastic-perfectly plastic behaviour for every average strain. Of course, this is not completely true since it does not consider either the change in tangent modulus beyond the proportional stress or the hardening after

yielding. However, the approximation is quite accurate for mild steel and structural ship steel in general, especially because there is no interest in strains larger than three or four times yield strain. This behaviour may be represented analytically by:

$$\Phi(\bar{\epsilon}) \equiv \Phi_e = \begin{cases} -1 & \text{when } \bar{\epsilon} < -1 \\ \bar{\epsilon} & \text{when } -1 < \bar{\epsilon} < 1 \\ 1 & \text{when } \bar{\epsilon} > 1 \end{cases} \quad (1)$$

where Φ_e is the normalised edge stress ratio, σ_e/σ_0 , and $\bar{\epsilon}$ is the normalised strain, ϵ/ϵ_0 .

In order to include elastic instability under compression and elasto-plastic effects, it is considered that the quantification of the effective width presented by Faulkner¹ is the most suitable and also that it may be used beyond buckling. With these basic concepts one is able to obtain realistic average stress-strain curves.

2.1.1 Slenderness and Effective Width

Plate strength under compression depends mainly on its geometry and more precisely on its slenderness. Thus, it is necessary to define clearly what is slenderness and how it is related to the plate strength.

For this work, the slenderness, β , is defined for each strain by:

$$\beta = \frac{b}{t} \cdot \sqrt{\epsilon} \quad (2)$$

which is related to the nominal slenderness, β_0 , by:

$$\beta = \beta_0 \cdot \sqrt{\bar{\epsilon}} \quad (3)$$

According to Faulkner, for long plates ($a > b$) with simply supported edges forced to remain straight under longitudinal loading, the effective width, Φ_w , is given

as a function of the average strain by:

$$\Phi_w = \begin{cases} \frac{2}{\beta} - \frac{1}{\beta^2} & \text{for } \beta > 1 \\ 1 & \text{for } \beta < 1 \end{cases} \quad (4)$$

and the nominal effective width, Φ_o , is:

$$\Phi_o = \frac{2}{\beta_o} - \frac{1}{\beta_o^2} \quad \text{for } \beta_o > 1 \quad (5)$$

This expression was derived by Faulkner¹ for the case of plates simply supported with average initial distortions. Guedes Soares³ has shown that for nominally perfect plates the effective width is given by:

$$\Phi_o = \frac{2.16}{\beta_o} - \frac{1.08}{\beta_o^2} \quad \text{for } \beta_o > 1 \quad (6)$$

This expression leads to values higher than 1.0 for stocky plates which has been observed in different experiments and can be attributed to the strengthening effect of the edges remaining straight. Its use is recommended when an explicit influence of distortions is needed and must be associated with a corrective function that accounts for distortions effects on ultimate strength.

Thus, for a given plate and returning to eq. (4), the effective width is changing from a value close to 1 to lower values as the loading is increased. No substantial reduction in effective width takes place when buckling occurs (curve C of Figure 1, for $\beta \equiv \beta_o$, i.e. $\varepsilon = \varepsilon_o$). The discontinuity of the structural tangent modulus at the buckling point (curve A of fig. 1) is only due to the yielding of edge strips, i.e., because of the change of the material behaviour from elastic to plastic range ($\bar{\varepsilon} = 1$, curve B of fig. 1).

The normalised average stress of the plate is given

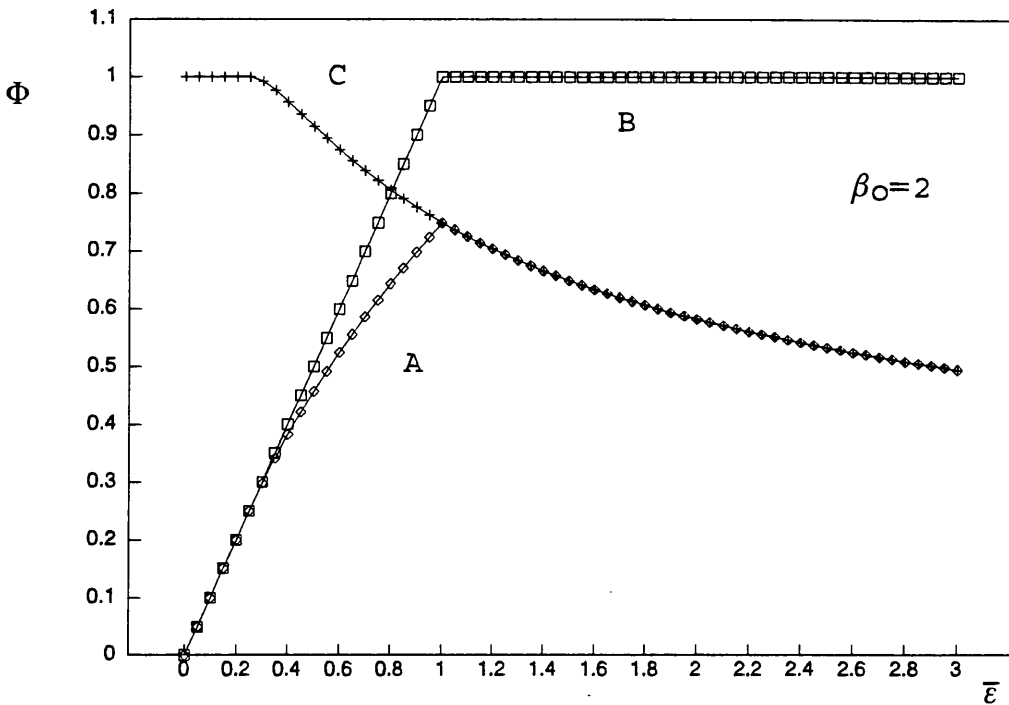


Figure 1 - Stress-Strain Curves Model

Normalised average stress-strain relationship (A) for a plate under compression, with representation of the auxiliary curves of edge stress (B) and effective width (C).

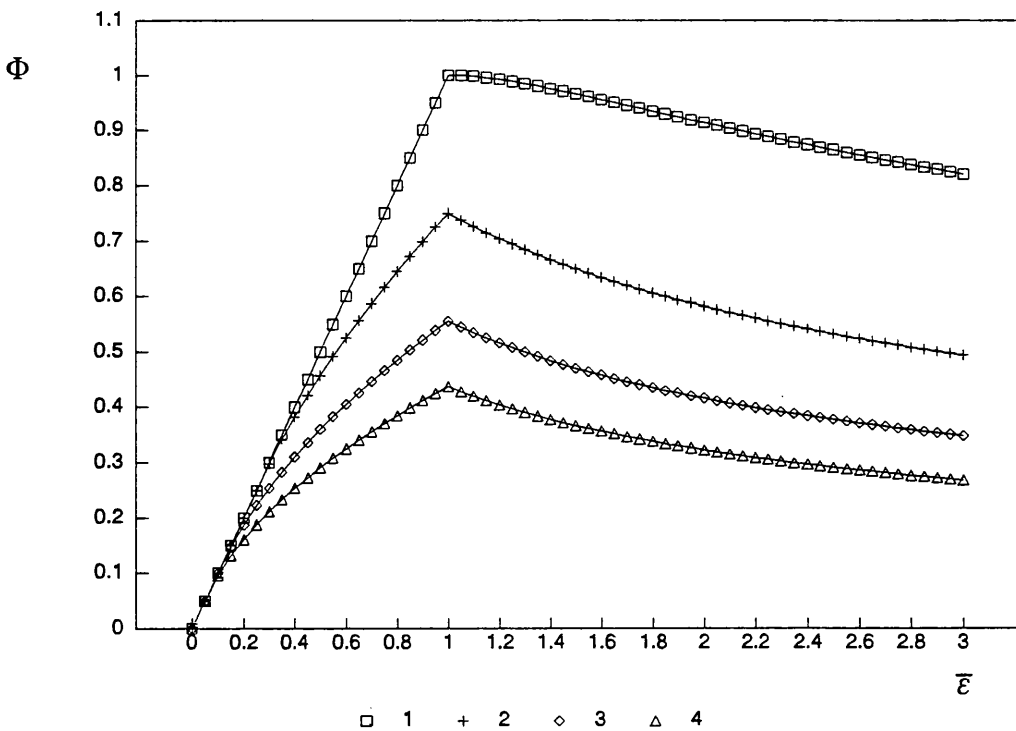


Figure 2 - Stress-Strain Curves

Normalised average stress-strain curves for plates under compression, for $\beta_0 = 1, 2, 3, 4$, without considering residual stresses.

by the product of the edge stress (1) and the effective width corresponding to this stress level (4), fig. 1:

$$\Phi_a = \Phi_e \cdot \Phi_w \quad (7)$$

where:

$$\Phi_e = \frac{\sigma_e}{\sigma_0} \quad (8)$$

As can be seen in fig. 1, stress-strain curves have their maximum at yield strain, if residual stresses are not considered.

Figure 2 shows average stress-strain curves for several levels of slendernesses. It is important to underline that it is possible to create two different kinds of curves for post-buckling behaviour with a small change in the formulation:

- a constant loading capacity of the plate after buckling, which corresponds to a consideration that there is not any reduction in effective width beyond ϵ_0 .
- a decreasing loading capacity after buckling, if it is considered that there is an increased reduction on effective width after yielding of the plate's edges.

Obviously the results obtained for the ultimate bending moment of the ship are very different for each plate model. Using the first model, the ultimate moment is never reached if buckling of stiffened plate is not considered, and predictions will be more optimistic than with the second. Nevertheless both models are considered to allow comparisons between them.

Figure 3 shows the real distribution of stresses in a plate and compares it with the effective width model which satisfies the relation:

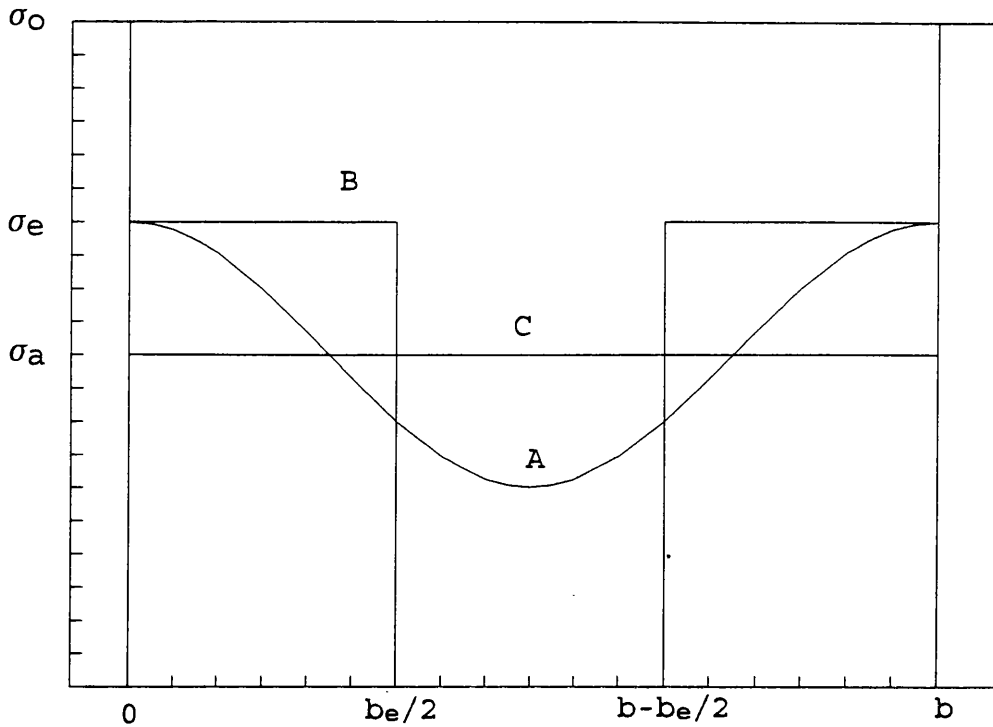


Figure 3 - Plate's Stress Distribution and Model
 Distribution of compressive stresses in a plate (A) and adopted models to defined effective width (B) and average stress (C).

$$\sigma_e \cdot b_e = \int_0^b \sigma(x) dx$$

where it is considered that all of the plate loading is sustained by the two edge strips with a width of $b_e/2$ subjected to the edge stress σ_e .

One can also say that the concepts of effective width and average stress are similar since:

$$\sigma_e \cdot b_e = \sigma_a \cdot b$$

and thus:

$$\frac{\sigma_a}{\sigma_e} = \frac{b_e}{b}$$

2.1.2. Aspect Ratio and Transverse Strength

For ships with transverse stiffening, it is more relevant to know the behaviour of plates loaded transver-

sely, i. e., loaded along the long edges. Transverse strength of plates has a greater degree of complexity than longitudinal strength, because the aspect ratio, α , becomes an important parameter in the strength predictions.

The longitudinal strength of a plate is almost independent of aspect ratio, as shown by Moxham⁸ who detected a variation of less 2% and as confirmed recently by Soares and Kmieciak⁷⁸. In transverse loaded plates the average strength decreases quickly with the increase of aspect ratio. The justification of this dependence is due to the fact that in a plate with $\alpha \gg 1$ most part of the plate is unsupported laterally. Thus, it behaves like a plate of infinite width in the center part, but differently at the two strips near the unloaded edges. These strips show an increased rigidity due to the presence of the supports (which are the stiffeners in ship plating).

Several formulations of ultimate transverse strength are based on this interpretation of the plate behaviour^{2,25,26}.

The model adopted in this work follows the same form as is used in longitudinal strength, that is that the average transverse stress is:

$$\Phi_{at} = \Phi_e \cdot \Phi_{wt} \quad (9)$$

The effective width, Φ_{wt} , is given, for every stress level, by:

$$\Phi_{wt} = \frac{\Phi_w}{\alpha} + \left(1 - \frac{1}{\alpha}\right) \cdot \Phi_i \quad (10)$$

where Φ_i represents the strength of the central part of the plate, which, according to Valsgard², is:

$$\Phi_i = 0.08 \cdot \left(1 + \frac{1}{\beta^2}\right)^2 \quad (11)$$

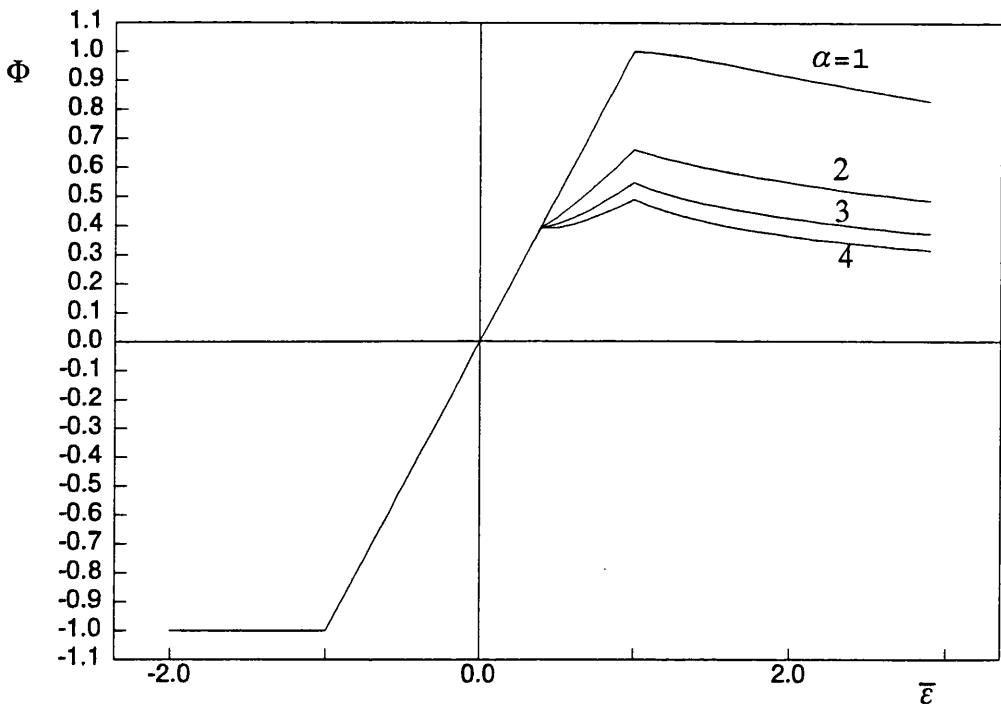


Figure 4 - Transverse Strength of Plates
Average stress-strain curves for plates under transverse loading, varying α and $\beta_0=1$.

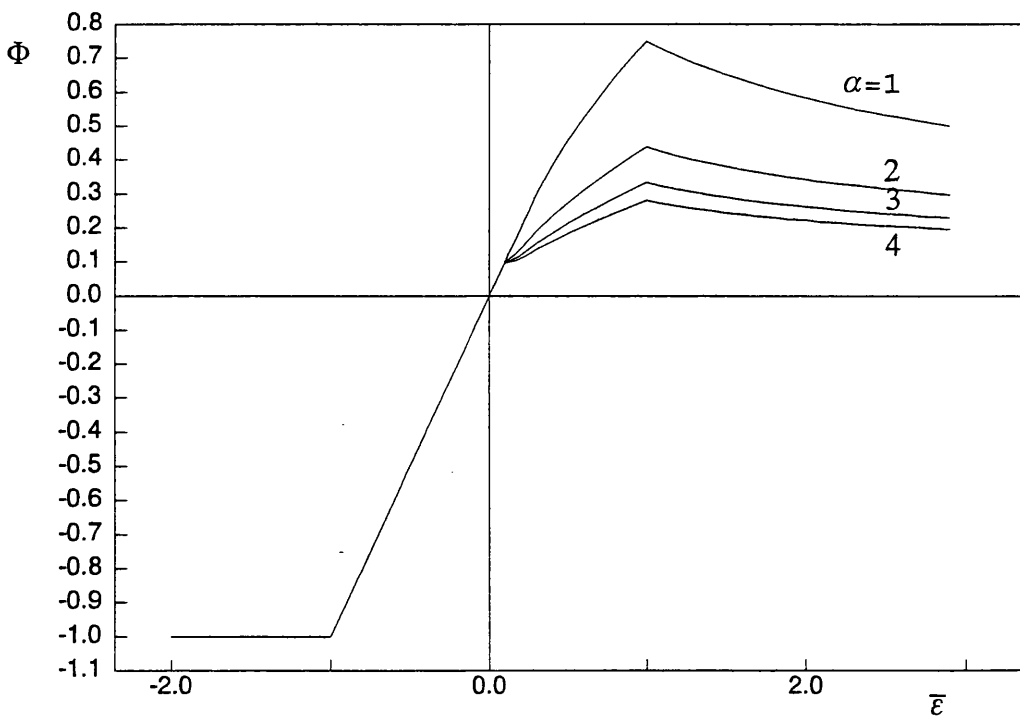


Figure 5 - Transverse Strength of Plates
Average stress-strain curves for plates under transverse loading, varying α and $\beta_0=2$.

and Φ_w is given by equation (4).

Equation (11) was obtained from a fitting of numerical calculations and is used instead of the buckling strength of an infinitely wide plate²⁷.

Figures 4 and 5 show the average stress-strain curves varying the aspect ratio for slenderness of 1 and 2.

However it must be noticed that these curves have very little applicability since most ships have a longitudinally stiffened structure, and so their plates will be loaded longitudinally, due to bending.

2.2 Effect of Residual Stresses

The effect of residual stresses on the strength of simply supported plates has been the subject of several studies. Some of them tried to determine the effect on the ultimate strength of the level of residual stresses^{1,4} incorporating an explicit formula for that variation in the strength prediction equation. Others were more interested in the impact of residual stresses in the whole stress-strain curve^{8,9,22} and, in these cases, no expression is given to compute the variation of the strength.

In this work both effects are very important: stress-strain curves must include the effect of residual stresses but also the ultimate strength must obey the statistically derived corrections. Because of the difficulty to satisfy both simultaneously two different approaches will be used:

- the first one is based on Faulkner's work that considered the effect of residual stresses on plate strength to be dependent on the nominal slenderness.
- the other is similar to the Crisfield approach, which explicitly takes into consideration the effect of the tension strips near the edges.

2.2.1 Approach for Design Formulas (DFM)

Following Faulkner¹, the ultimate strength of a plate is affected by residual stresses as a function of the nominal slenderness. The reduction of strength is approximated by:

$$\Delta\bar{\sigma}_r \equiv \frac{\Delta\sigma_r}{\sigma_o} = \frac{E_t}{E} \cdot \frac{\sigma_r}{\sigma_o} \quad (12)$$

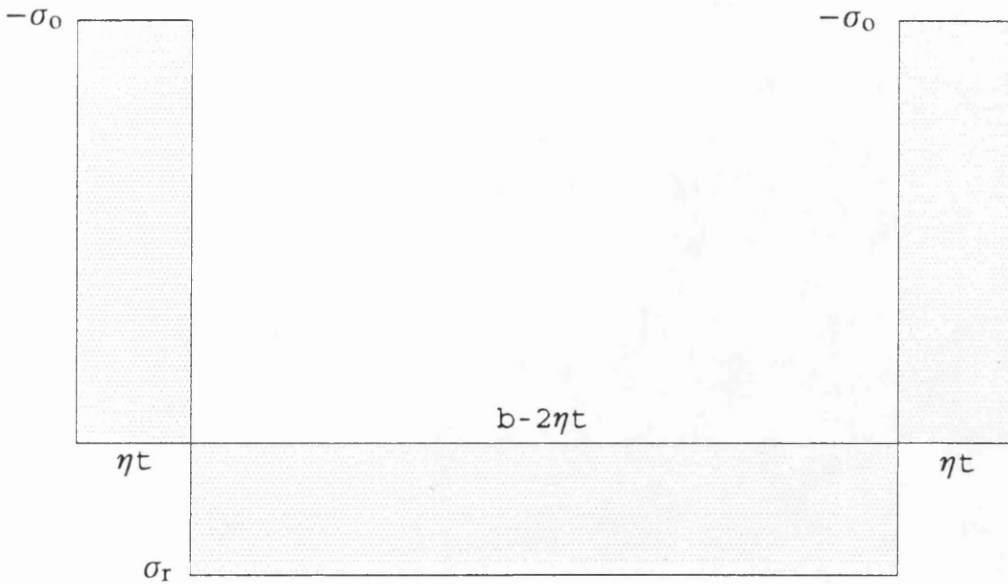


Figure 6 - Residual Stresses Pattern Model
 Model of residual stresses distribution on a plate due to welding of the edges.

where the tangent modulus is related to the slenderness by:

$$\frac{E_t}{E} = \begin{cases} \left(\frac{3.62 \cdot \beta_0^2}{13.1 + 0.25 \cdot \beta_0^4} \right)^2 & \text{for } 0 < \beta_0 < 2.7 \\ 1 & \text{for } \beta_0 > 2.7 \end{cases} \quad (13)$$

in the case of simply supported plates. Guedes Soares and Faulkner⁴ have proposed a simpler expression which was shown to be accurate for practical purposes:

$$\frac{E_t}{E} = \begin{cases} 0 & \text{for } \beta_0 < 1 \\ \frac{\beta_0 - 1}{1.5} & \text{for } 1 < \beta_0 < 2.5 \\ 1 & \text{for } \beta_0 > 2.5 \end{cases} \quad (14)$$

From the equilibrium of the plate, the residual stresses relate to the width of tension strips by:

$$\frac{\sigma_r}{\sigma_0} = \frac{2\eta t}{b - 2\eta t} \quad (15)$$

which recognises the existence of two distinct regions: a central one of width $b-2\eta t$ subjected to a compression stress σ_r , confined laterally by two strips of width ηt each, at yield stress in tension, $-\sigma_0$ (see figure 6).

In order to obtain the desired strength reduction for each strain, there is a need to generalise this theory, assuming that equations (12) and (13) are valid for every strain and using for this purpose the slenderness β instead of the nominal slenderness β_0 in equation (13), fig. 7 and 8.

As a consequence of this generalisation has:

- the ultimate strength of the plate is the same as the initial one,

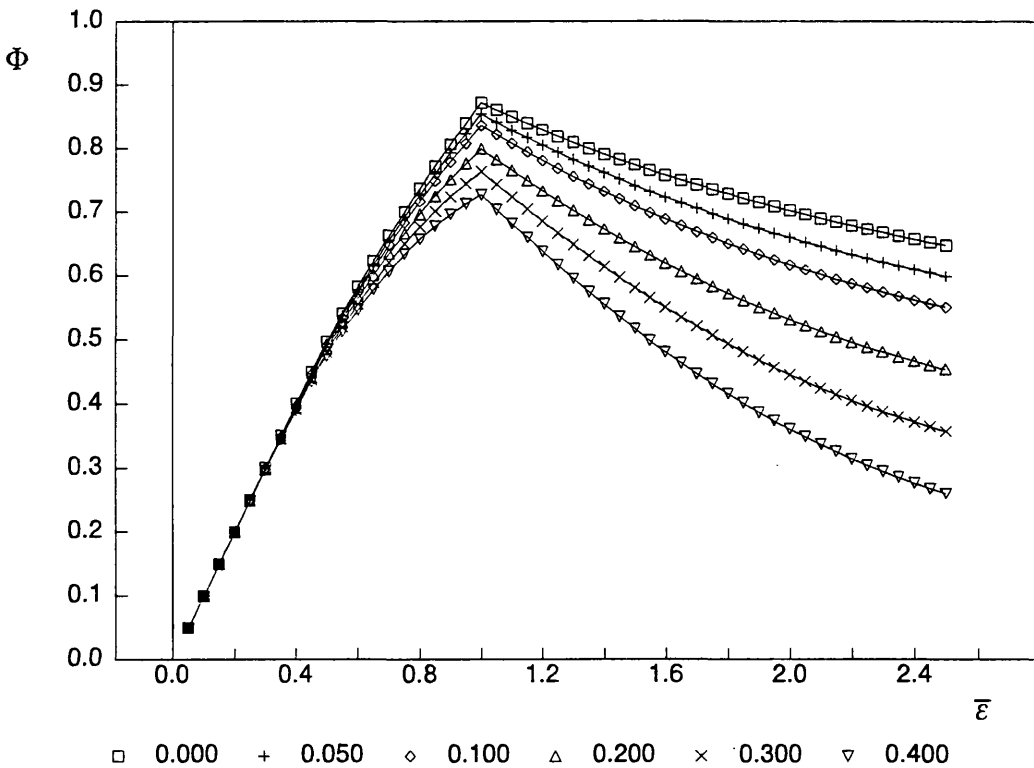


Figure 7 - Residual Stresses Effect using DFM
Average stress-strain curves of plate of $\beta_0=1.557$ with residual stresses using design formula method.

- the reduction in strength increases with the increase in strain,
- the ultimate strength is reached at yield strain ϵ_0 , so that no shift is considered in the strain corresponding to ultimate strength,
- post-buckling strength is different depending on the level of residual stresses $\bar{\sigma}_r$,
- the initial structural tangent modulus of the welded plate, in tension and compression, is independent of the level of residual stresses.

The third and fourth points are of questionable validity, since most studies concluded that the strain at which ultimate strength occurs increases with residual stresses and the strength is almost independent of σ_r

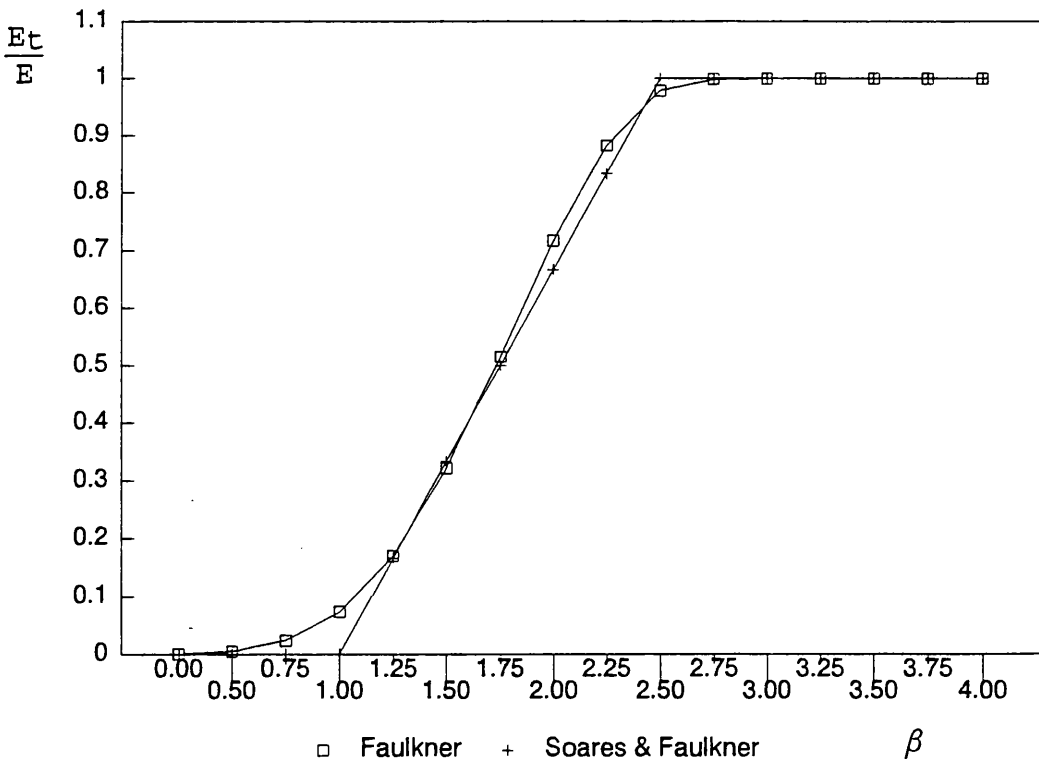


Figure 8 - Tangent Modulus Ratio

Comparison of tangent modulus ratio between the proposal of Faulkner, eq. (13), and G. Soares and Faulkner, eq. (14).

beyond this strain^{8,9}.

The last point creates some incompatibility, in tension, between the adopted model (figure 6) and the resulting curve.

2.2.2 Physical Approach Method (PAM)

Crisfield considered separately the regions of the plate under compression and tension. For this last one he considered a linear elastic behaviour from $\bar{\epsilon}=0$ to 2. Beyond this strain the strip yields in compression.

In the central zone, initially under compression, he considered that the behaviour is similar to the one of an elastic plate without residual stresses and with a pre-strain of $\bar{\epsilon}_r$. So this zone reaches its maximum loading capacity at a strain of $1-\bar{\epsilon}_r$.

In this present formulation it is considered that the plate with residual stresses has a strength given by:

$$\Phi_{rp} = \Phi_w \cdot \Phi_{er} \quad (16)$$

where Φ_w is equation (4) which is not directly affected by the residual stresses and Φ_{er} is nothing more than the representation of elasto-plastic behaviour of the plate corrected by the existence of residual stresses.

This correction is based on the hypothesis that the curve of a perfectly elasto-plastic plate suffers an apparent variation on the tangent modulus at a strain of $1-\bar{\epsilon}_r$ mainly due to the yielding of the central region of the plate. Beyond that strain the only contribution for the increase on strength is from the edges strips. These strips can be loaded until $2\epsilon_0$ from where the plate behaves plastically, as shown in figure 9.

Analytically the straight line between points A and B of figure 10 is given by:

$$\Phi_{er} = \frac{\bar{\sigma}_r \cdot \bar{\epsilon} + 1 - \bar{\sigma}_r}{1 + \bar{\sigma}_r} \quad (17)$$

and so the function Φ_{er} might be written for the whole range of strain as:

$$\Phi_{er} = \max \left\{ -1, \min \left\{ 1, \bar{\epsilon}, \frac{\bar{\sigma}_r \cdot \bar{\epsilon} + 1 - \bar{\sigma}_r}{1 + \bar{\sigma}_r} \right\} \right\} \quad (18)$$

This expression represents a rough approximation to the behaviour of plates in tension, $\bar{\epsilon} < 0$, because there does not exist a perfect identification between the model with residual stresses and the function Φ_{er} , in respect to the tangent modulus.

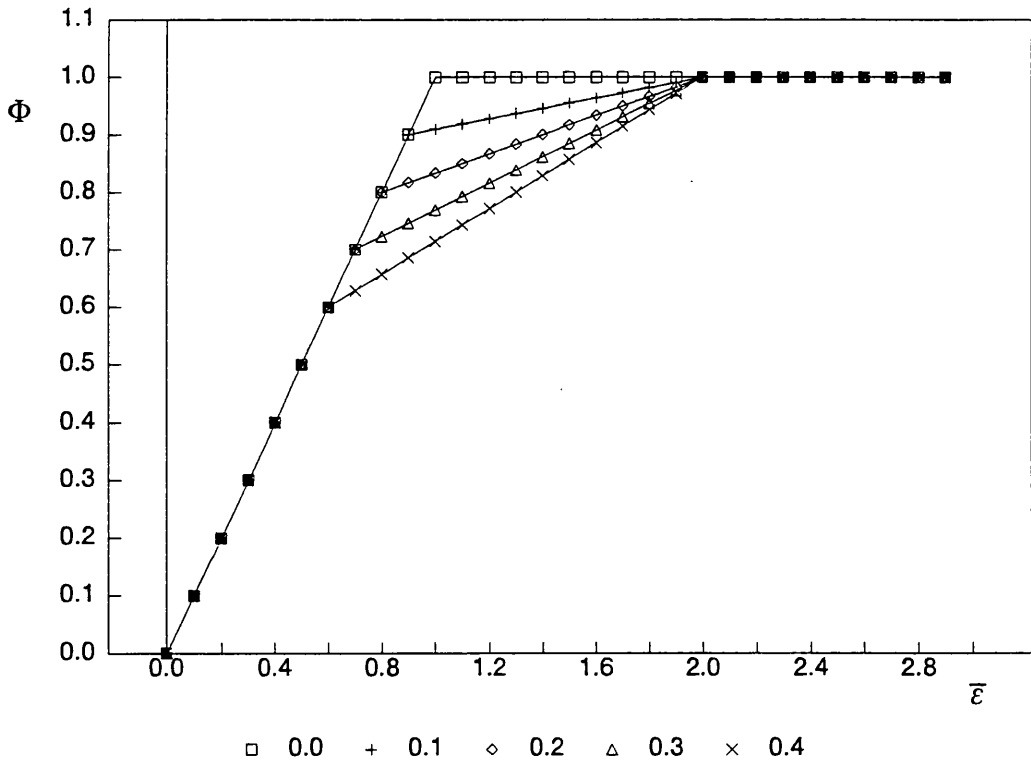


Figure 9 - Residual Stresses Effect in Perfect Plates
stress-strain curves of plates behaving elasto-perfectly plastic with residual stresses

In fact, if one analyses the model, it can easily be shown that the tangent modulus must be $E_t = \frac{b-2\eta t}{b} \cdot E$ when the plate is in tension ($-1 < \bar{\epsilon} < 0$), but at Φ_{er} , $E_t = E$. This solution is considered to be better since it ensures the continuity of tangent modulus at $\bar{\epsilon} = 0$ and it seems to represent better the real plate.

The practical consequence of the use of one or other interpretation is in the flexibility of the overall section and so one obtains a higher value for effective section modulus with the model adopted.

Two important points must be highlighted about the adopted model:

- Φ_w is not affected by the level of residual stresses, which is the same as saying that the

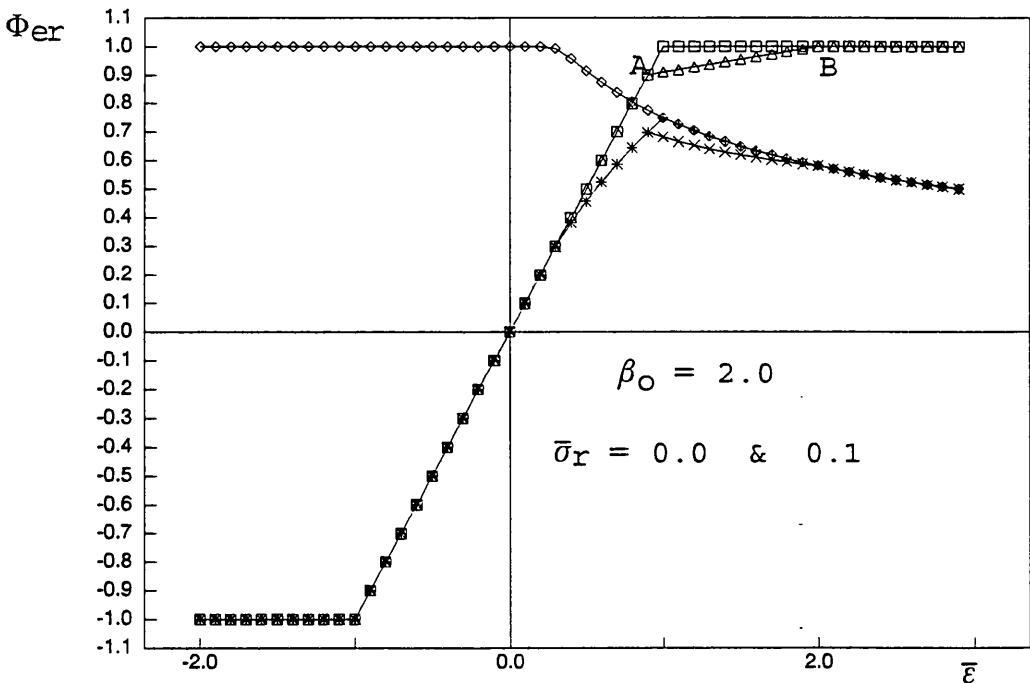


Figure 10 - Example of a Plate with Residual Stresses
Construction of average stress-strain curves for a plate with residual stresses, under uniaxial compression.

eventual loss of effectiveness of the plate caused by the presence of residual stresses is only due to the plastic behaviour of the material.

- the imposition of the continuity in the tangent modulus at $\bar{\epsilon}=0$ is an attempt to reproduce what happens in reality. However, the model might be too rigid for strains near yielding in tension. More realistic solutions may be achieved by considering sophisticated patterns for residual stresses distributions, as a parabolic curves on the tension strips.

From now on these two methods of incorporate residual stresses effects will be designated by Design Formula Method (DFM) and Physical Approximated Method (PAM).

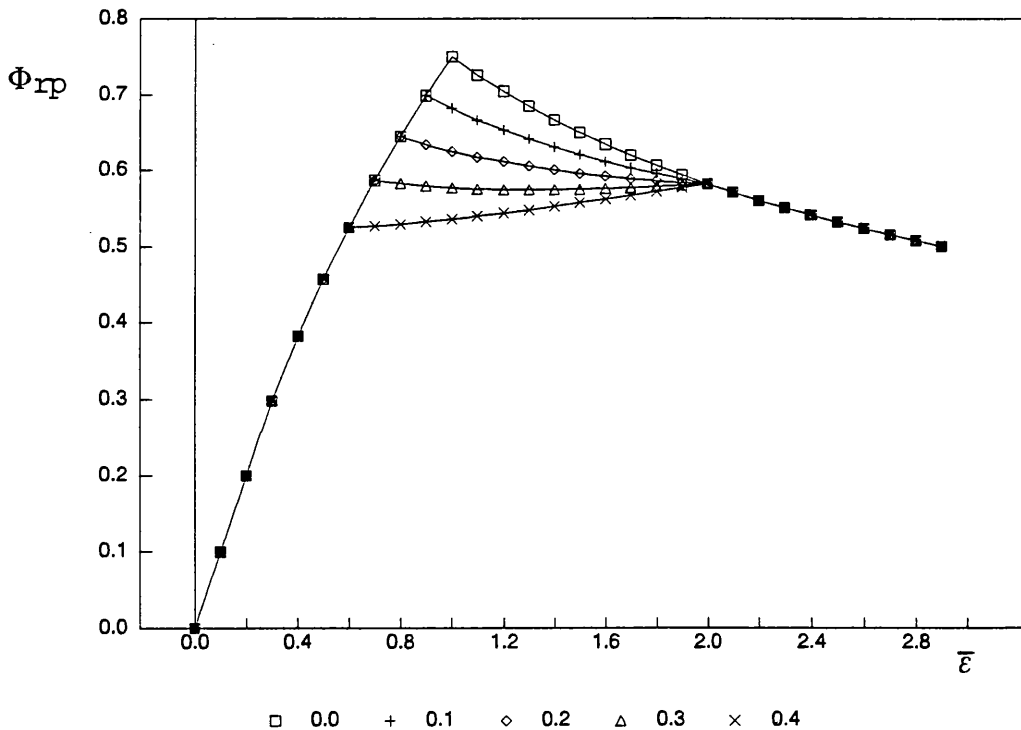


Figure 11 - Curves for several levels of residual stresses

Average stress-strain curves for several levels of residual stresses ($U_r = 0.0, 0.1, 0.2, 0.3$ and 0.4), in a plate of $\beta = 2.0$ under uniaxial compression.

2.2.3. Comparison between models

Some of the principal differences between the two models were already pointed out in the last two sections. However, it is important to compare quantitatively the models in respect to the predicted ultimate strength and the corresponding strain, because it gives information about the rigidity or flexibility of the models which will influence the prediction of ultimate bending moment.

Figure 12 shows the ultimate strength predicted by both methods for a typical bottom plate of a VLCC with $\beta_0=1.55$. The reduction in ultimate strength due to residual stresses is much more marked on the physical model (PAM) than on the design method (DFM). At low levels of residual stresses, the reduction in ultimate strength from the

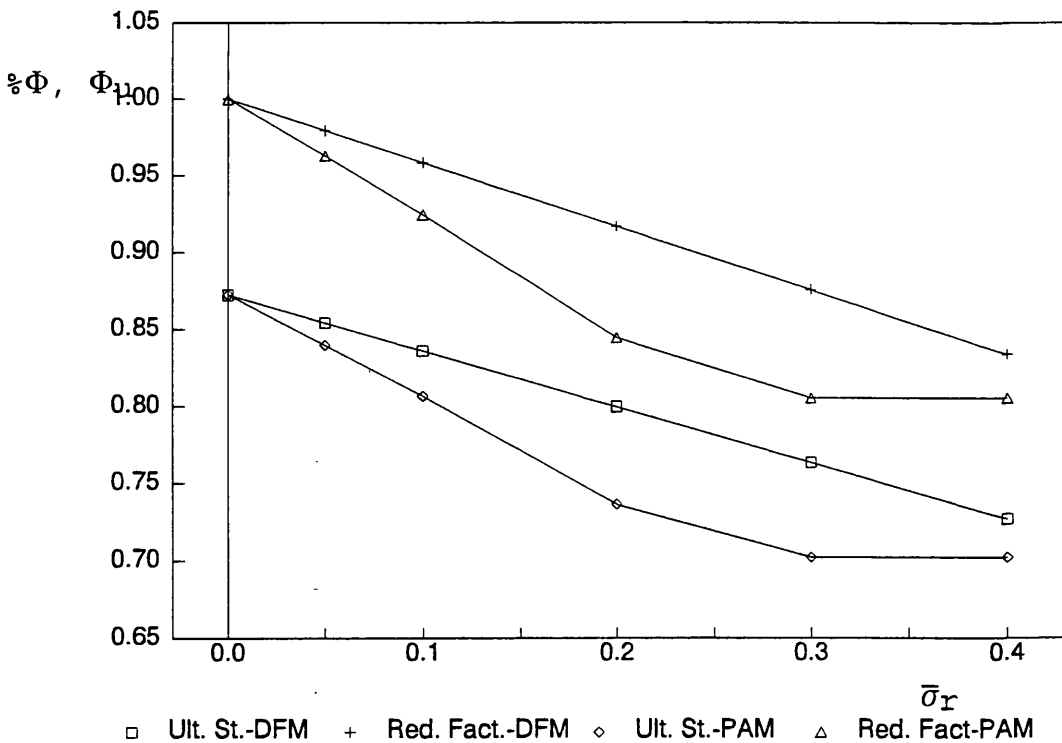


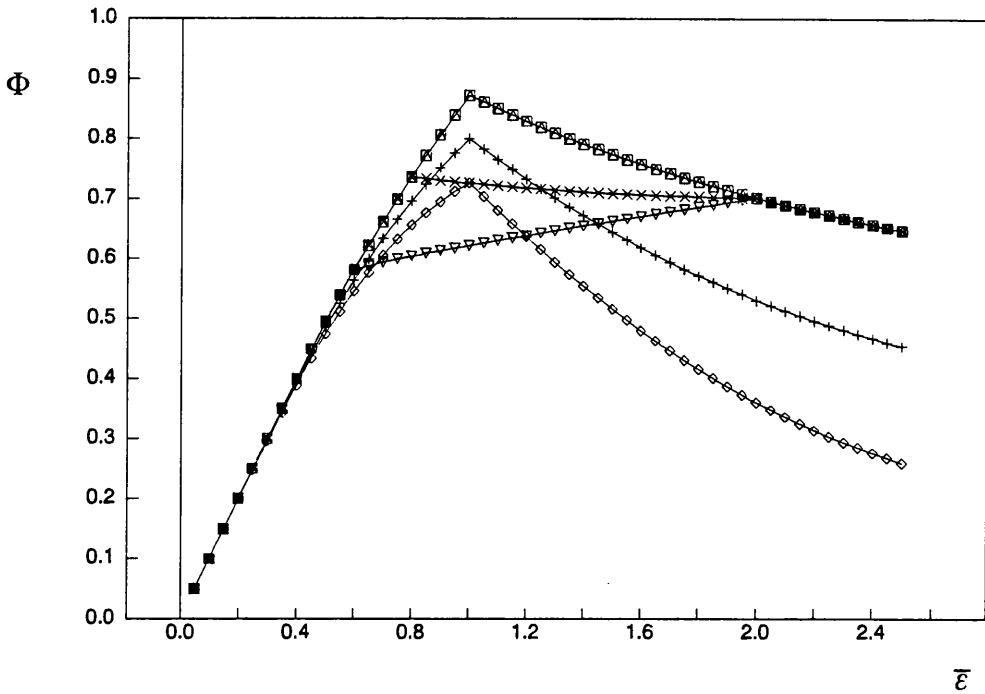
Figure 12 - Ultimate strength and residual stresses comparison of ultimate strength and reduction factor of a plate with $\beta_0=1.55$ predicted by DFM and PAM.

residual stress free plate is almost the double from one method to the other. However, for high levels of residual stresses, say $\bar{\sigma}_r > 0.3$, both methods tend to predict similar reduction factors.

Furthermore, the methods give very different load shedding patterns after buckling and predict different strains at which ultimate strength occurs for the same plate. In fact, in the first method the strain at ultimate strength (it will be called ultimate strain from now) is kept at yield strain by construction in order to obtain the ultimate strength equal to Faulkner's prediction, equation (5,12).

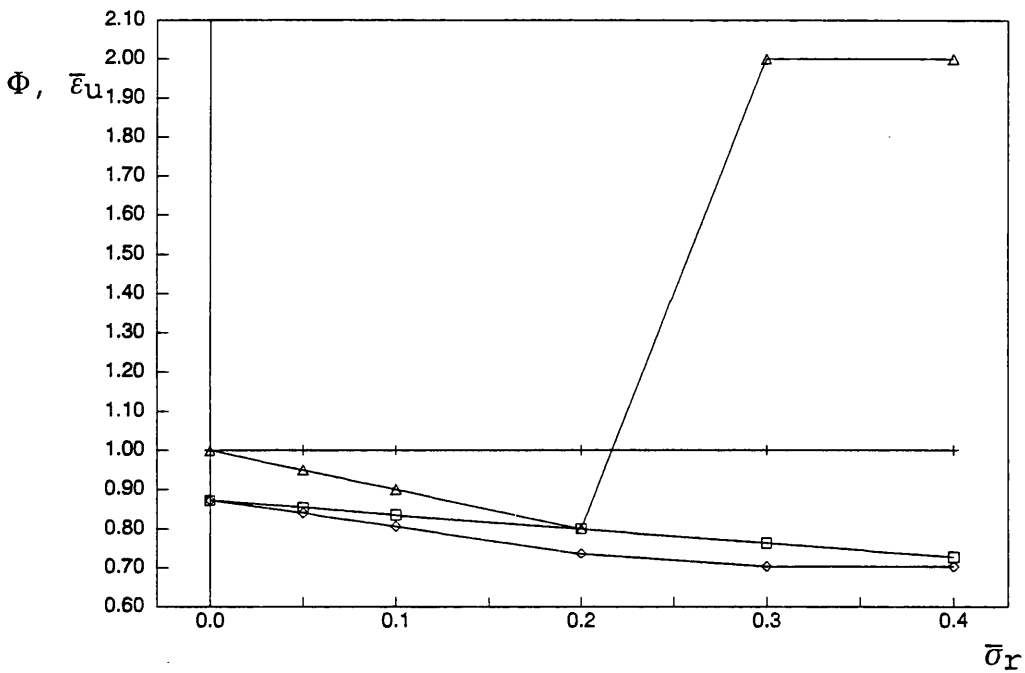
The second method leads to a gradual reduction on ultimate strain at low levels of residual stresses and from a given level it is transferred to $2\varepsilon_0$. The sudden change in ultimate strain results directly from the adopted model for residual stresses distribution, fig. 6, and if a more smooth transition between tension and compression fields is considered than a smoother change is obtain and the curves approach the ones recommended by Smith⁸⁸.

As a consequence of a higher ultimate strain and lower ultimate strength, the predicted rigidity of a section using this last method (PAM) must be lower than that using the design method. On the other hand, the load shedding after buckling is much more marked in the design method and several patterns are obtained depending on the level of residual stresses; Crisfield's method (PAM) gives a load shedding pattern independent of residual stresses specially for high strains, $\bar{\varepsilon} > 2$, as shown in figures 13 and 14.



\square 0.0-DFM $+$ 0.2-DFM \diamond 0.4-DFM \triangle 0.0-PAM \times 0.2-PAM ∇ 0.4-PAM

Figure 13 - Comparison of stress-strain curves
 Comparison of curves for three levels of residual stresses
 (0.0, 0.2, 0.4) of a plate with $\beta_0=1.55$ using DFM and PAM.



\square Ult. Strength-DFM $+$ Ult. Strain-DFM \diamond Ult. Strength-PAM \triangle Ult. Strain-PAM

Figure 14 - Ultimate strength and ultimate strain
 Comparison of ultimate strength and corresponding strain of
 a plate with $\beta_0=1.55$ predicted by Faulkner (DFM) and Crisfield
 (PAM) based approaches.

2.3 Effect of Initial Deformations

The plate elements of marine structures and more precisely of ships show distortions as a result of the fabrication in steelworks, transportation impacts, manufacturing process in shipyards and operating ship service. The first two are corrected in the shipyard, but the third one remains for the entire life of the ship and service increases this until replacement of the plating occurs.

Studies done in ships and civil engineering steel structures have quantified the level of initial deformations on plates, and attempt to correlate it with the geometry of the plate.

One might ask why distortions are important to longitudinal strength of ships. The presence of distortions in plate elements make them behave in a different way both in tension as in compression.

In tension, the dominant aspect is the variation in initial tangent modulus. Due to distortions, the initial tangent modulus has a lower value than Young's modulus. As a consequence the plates in tension will have a lower rigidity than the perfect plate and so the hull section rigidity will be lower. However, for usual levels of distortions, the consequences are minor and may be ignored.

In compression, out-of-plane deformations are much more important. Their presence in plate elements usually cause load-end shortening curves to be smoother near collapse, so there is not a critical collapse load. In other words, the sudden collapse that characterises the almost perfect plates, disappears and the behaviour of the

plates is smoother as the distortions are greater.

On the other hand, the shape and the level of distortions along the plate may influence the mode of collapse and some variations on ultimate strength of the plate may occur. As those variations are frequently negative, it becomes very important to quantify their shape and amplitude.

Faulkner¹ concluded that the amplitude of distortions δ for warships is dependent on β_0^2 , and it is usual to find values between $0.05 \cdot \beta_0^2$ and $0.15 \cdot \beta_0^2$, where δ_D is the maximum distortion normalised by the thickness of plate. He also observed that the shape of the deformations has a marked $m=n=1$ mode. A coefficient of 0.12 was proposed for warships and eventually 0.15 for merchant ships. Of course welding has an important role on the level of deformations achieved and values as high as $0.40 \cdot \beta_0^2$ can be observed in heavily welded plates.

Other measurements are available from the work of Kmiecik and Czujko⁸⁹, as well as from Antonίου²⁹. It should be noted that Kmiecik proposed a dependence on β_0 while the others assumed that this dependence is on β_0^2 .

Guedes Soares³ suggested a mean value of the measurements of Faulkner¹ and Antonίου²⁹ for design purposes, $0.11 \cdot \beta_0^2$.

The effect of initial imperfections on plates strength was studied by several authors. Carlsen and Czujko³⁰ have shown that, in spite of the effect being normally weakening, there are situations where some stiffening might occur, specially when the shape of distortions is rather different than the plate's buckling mode.

Frieze³¹ and Guedes Soares²⁸ pointed out that plates with an aspect ratio higher than 1.0 tend to be stronger than squares plates if the shape of distortions in longitudinal direction approaches half of a wave. This is a usual situation on ships in service during a few years, especially on bottom plates, and also this is the shape of distortions induced by welding¹ as noticed before. However this stiffening is very sensitive to any local deformations and it must not be considered in design³².

Murray³³, Dwight and Little¹⁷ proposed that the weakening effect of distortions must not be considered for $\delta_p < 0.23$ and $\alpha > 4$ but Frieze³¹, Dwight and Ratcliffe²⁰ concluded that it must be considered for $\delta_p > 0.3$.

Guedes Soares³ has quantified the loss on strength of imperfect plates due to initial imperfections or residual stresses or both simultaneously, which is the most common situation. He proposed that the strength of the plate with initial distortions should be given by:

$$\Phi_{\delta p} = \Phi_0 \cdot \Phi_{\delta} \quad (19)$$

where Φ_0 is the ultimate strength of 'perfect' plate, eq. (6), and the degradation due to initial distortions is:

$$\Phi_{\delta} = 1 - (0.626 - 0.121 \cdot \beta_0) \cdot \delta_p \quad (20)$$

However some problems arise when one is trying to transpose and extend this kind of formulation to the whole range of the load-shortening curves of plates.

2.4 Effect of Biaxial Loading

The ship plate elements are always subjected to a biaxial loading, even if the principal loads develop predominantly in the longitudinal direction when the hull is subjected to global bending, some transverse loading is present due to the effect of lateral pressure of the sea water for example.

The study of the plate behaviour under biaxial loading has concentrated on the determination of ultimate strength using associated interaction curves. Much more difficult is to have an explicit way to obtain average stress-strain curves for a generic combination of longitudinal and transverse loading, in particular when the loading goes beyond linear behaviour.

The work on this subject is of two kinds: numerical and experimental. Numerical works^{7,34} are very different from experimental works^{14,35} with respect to the philosophy adopted. The former ones have chosen as normal practice to present constant ratios between the strains in both directions, ε_x and ε_y . The latter have kept the displacement (or the loading) in one direction constant.

For the present work the second kind are more interesting and more important, since it is the behaviour of a plate with a secondary constant low loading that matters for ship plating analysis. Unfortunately there are not many results in this area and the strength still depends on the loading path applied.

Several proposals were presented for the form and constants in the interaction curves between longitudinal and transverse strength. The usual way to do this, is to

normalise the applied stresses by the ultimate strength in each direction, defining R_x and R_y as:

$$\begin{cases} R_x = \frac{\sigma_x}{\sigma_{ux}} \\ R_y = \frac{\sigma_y}{\sigma_{uy}} \end{cases} \quad (21)$$

It is important to clarify that the prediction of strength σ_{ux} and σ_{uy} that is used to calculate R_x and R_y depends of the proposer's opinion, and so for every interaction formulation a different pair of predictions may be used. Also in this area some agreement must be achieved.

Faulkner²⁵ proposed a parabolic interaction curve:

$$R_x + R_y^2 = 1 \quad (22)$$

DNV and BS-5400 recommend a circular interaction:

$$R_x^2 + R_y^2 = 1 \quad (23)$$

Valsgard³⁴ considered a generalisation of the expressions where the curve parameters depend on the geometric characteristics of the plate:

$$R_x^\gamma - \zeta R_x R_y + R_y^2 = 1 \quad (24)$$

with:

$$\begin{cases} \gamma = 2 \text{ (for } \alpha=1) \text{ or } 1 \text{ (else)} \\ \zeta = 0.25 + 0.5 \cdot (\zeta - 0.25) \cdot (3 - \alpha) \end{cases}$$

$$\text{and } \zeta = 3.2 \cdot e^{-0.35 \beta - 2} .$$

For square plates ζ is the same as ζ . Valsgard also proposed the adoption of $\gamma=1$ and $\zeta=0.25$ for plates with $\alpha>3$.

The expression (24) represents the Von Mises curve for very stocky plates ($\sigma_{iu} \cong \sigma_o$) if one puts $\gamma=2$ and $\zeta=1$.

2.4.1 Reduction Factor

The stress-strain curves may be corrected for the effect of biaxial loading by including a reduction factor, C_y , in the global formulation:

$$C_y = \sqrt{1-R_y^2} \quad (25)$$

which is applied to the curve of the plate without transverse loading.

This reduction factor is only valid when used for ultimate strength predictions. However it might be generalised over the whole curve without loss of credibility if the ratio R_y/R_x is kept low. Generally, for the longitudinal hull strength the relationship that matters is between longitudinal loading and longitudinal shortening of plates under an almost constant transverse loading, but no systematic study has been done yet under these conditions. The stress-strain curve under biaxial loading will be given by:

$$\Phi_{ba} = \Phi_a \cdot C_y \quad (26)$$

From this equation it is possible to deduce the reduction in tangent modulus due to biaxial compression:

$$E_{tb} = C_y \cdot E_t \quad (27)$$

It was impossible to prove this relationship since all available studies used a proportionality between ϵ_x and ϵ_y and equation (27) is supposed to be valid only for a constant σ_y . The inverse behaviour may be detected in Dowling⁷ work and it results from the Poisson effect by the simultaneous increase on ϵ_y and ϵ_x . Due to this simultaneous increase, the relation between σ_x and ϵ_x has

a derivative higher than the tangent modulus and even higher than the Young's modulus in the elastic range of strain. So, in the cases where the ratio $\varepsilon_y/\varepsilon_x$ is kept constant, the correction must be positive instead of negative.

2.4.2 Formulation Adopted

Guedes Soares and Gordo²¹ have developed an interaction formulation based on experimental and numerical results. They concluded that a circular formulation, associated with a normalisation based on Faulkner's formula (5) for longitudinal stresses and Valsgard's one (10) for transverse strength, gave the best fitting for available numerical^{7,38} and experimental results^{14,35,37}. It has also been found convenient to divide plates into two main groups: stocky plates, with $\beta_o < 1.3$, and slender ones, for $\beta_o > 1.3$, so as to represent their distinct strength characteristics.

For the stocky plates the best fitting is achieved when both longitudinal and transverse stresses are normalised by equation (5). Physically this means that the strength of a stocky plate of any aspect ratio is the same as the square plate with a similar slenderness and the plate failure is mainly a result of yielding.

The calculation of C_y , equation (25), implies the definition of R_y . Equation (21) is used where σ_{uy} is:

$$\sigma_{uy} = \Phi_{ux} \cdot \sigma_o \quad \text{for } \beta < 1.3 \quad (28a)$$

$$\sigma_{uy} = \Phi_{uy} \cdot \sigma_o \quad \text{for } \beta > 1.3 \quad (28b)$$

To incorporate the effect of residual stresses and distortions, equation (25) must be modified according to:

$$C_y = \sqrt{R_{rd}^2 - R_y^2} \quad (29)$$

where²¹:

$$R_{rd}=1.11-0.16\cdot\bar{\sigma}_r-2.01\cdot\bar{\sigma}+0.27\cdot R_x^* \text{ for } \beta < 1.3 \text{ (30a)}$$

$$R_{rd}=1.12-0.58\cdot\bar{\sigma}_r-0.07\cdot\bar{\sigma}+0.04\cdot R_x^* \text{ for } \beta > 1.3 \text{ (30b)}$$

$$R_x^* = \frac{R_x}{\sqrt{R_x^2 + R_y^2}} \quad (30c)$$

Residual stresses and distortions have also a different influence on the strength of these two groups of plates. Distortions are much more relevant in stocky plates (three times more than in the slender group) while residual stresses are more relevant for slender ones (3.5 times more important on average than in the stocky group) as it can be seen from equations (30a) and (30b).

2.5 Effect of Lateral Pressure

Lateral pressure affects directly and indirectly the behaviour of ship plates. Its presence causes changes in ultimate strength because it increases the initial imperfections developing the half wave mode ($m=n=1$) along the plate in both principal directions. This increase in the amplitude of the first mode can improve or weaken the strength depending whether the mode of collapse coincides or not with the principal mode of deformation induced by lateral pressure. Simultaneously it creates a state of stresses along the plate edges which adds to the predominant in-plane stresses increasing the onset of local yield.

The persistence of lateral pressure during a ships' life often causes permanent deformations with an symmetric mode in adjacent plates. These modes of deformation usually make the plate stronger because the permanent deformations have a lower mode ($m=1, n=1$) than the critical collapse mode ($m=\alpha, n=1$) and symmetry of adjacent plates near collapse provides rotational restraint.

Dier and Dowling³⁸ and Becker et al.³⁹ studied the behaviour of plates under combined biaxial compression and lateral loading. The former used numerical techniques on plates of aspect ratio 1 and 3 with several boundary conditions. The latter conducted tests on square tubes.

Work on combined uniaxial loading and lateral pressure were performed by Yoshiki et al⁴⁰, Yamamoto et al.⁴¹ and Okada et al.⁴².

A compilation²¹ of the results of these works tried to quantify the effect of lateral pressure on ultimate

strength. The non-dimensional parameter $Q_L = q_o E / \sigma_o^2$ proved to be the most representative to account for the influence of lateral pressure.

Equation (23) was modified to incorporate this effect assuming the form of:

$$\sqrt{R_x^2 + R_y^2} + R_Q = 1 \quad (31)$$

where R_Q is given by:

$$R_Q = 0.117 Q_L \beta_o^2 \quad (32)$$

The coefficient of variation associated with this analysis is 0.14 and it might be compared to the deviation under biaxial compression, 0.13, or uniaxial compression, which is about 0.05 (from ref. 21 and 1).

For use in average stress-strain curves, equation (25) must be extended to incorporate a coefficient C_{yQ} which includes simultaneously the contribution of transverse loading and lateral pressure.

$$C_{yQ} = \sqrt{(1 - R_Q)^2 - R_y^2} \quad (33)$$

Finally the curves are given by:

$$\Phi_{bQa} = \Phi_a \cdot C_{yQ} \quad (34)$$

where the coefficient C_{yQ} replaces completely C_y from (25), since on the absence of lateral pressure both are coincident.

A similar procedure of applying these reduction factors was used by Smith⁴³ and Davidson⁴⁴ where lateral pressure was found to have little effect on the shape of the stress-strain curves of plate elements.

2.6 Effect of Edge Shear

In normal ship operation, plate elements are always subjected to combined loads such as compression or tension, bending and shear. However, in the sections where the bending moment achieves a maximum value the shear loads vanish, if the ship is looked upon as a simple beam, and so it is not very relevant to include the effect of shear stresses on the ultimate strength of ships under bending.

The other reason that reduces the importance of the inclusion of shear in this analysis is because if one looks at a particular section where the longitudinal normal stresses have their maximum value, shear stresses have a minimum, and vice-versa, due to the nature of their distributions around the section.

So this section is included only to complete the analysis of the strength of plate elements.

Using a finite differences method by dynamic relaxation that accounts for plastic effects, Harding et al.⁴⁵ studied the behaviour of square plates subjected to uniaxial loading and shear.

The models had considered two particular boundary conditions, restrained and unrestrained, and covered a range of slenderness from 1.037 (stocky plates) to 8.298 (extremely slender). Initial imperfections were considered through three levels of distortions and residual stresses in both principal directions.

It must be highlighted that distortions in this work were chosen which obeyed a linear relation with β_0 , and so a qualitative classification is not recommended since stocky plates have amplitudes of distortion above the mean

value and slender ones are below (see figure 15), according to references mentioned in 2.3.

Harding et al found an independency of the ultimate shear stress relative to the slenderness β_0 for restrained plates, while unrestrained ones were found to be dependent. The insensibility to the level of distortions might be justified because the shape of distortions and the shear collapse mode are very different. The sensitivity of ultimate shear stress to residual stresses can not be neglected, especially in slender plates.

In particular, for reinforced panels it is very difficult to say if boundary conditions correspond or not to a restrained situation, or whether they are dependent on loading itself, i. e., the mode of collapse might represent a preferential place for the development and location of plastic hinges on stiffeners.

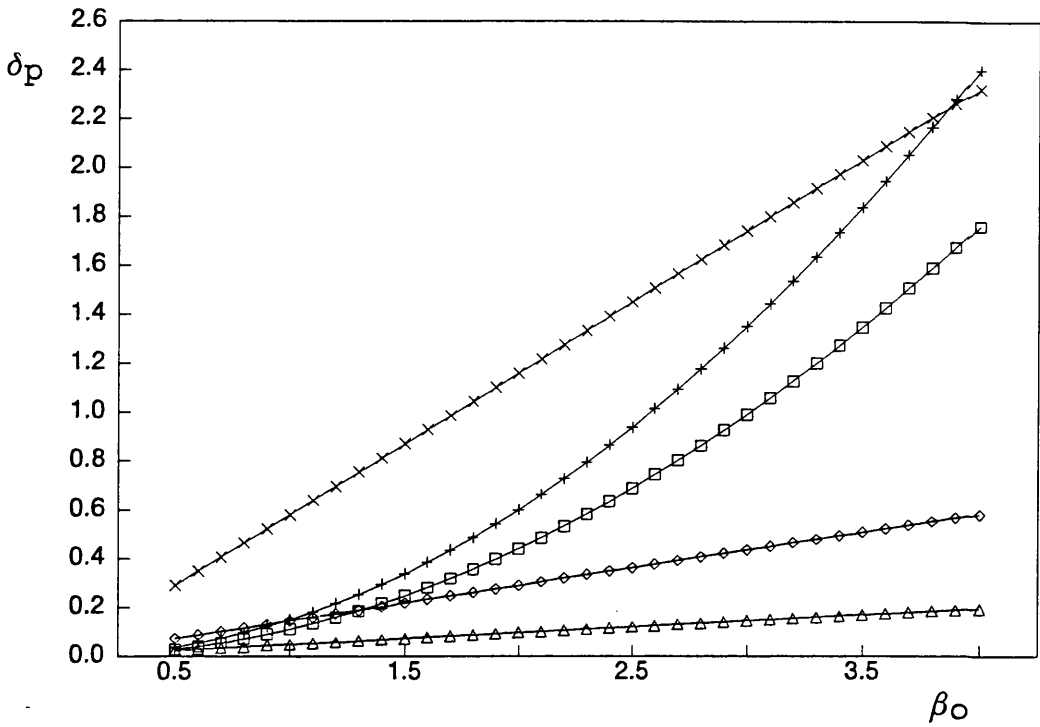
Applying a correction due to shear to the average longitudinal stress-strain curves developed in 2.1.1., is only justified if it is considered to have restrained conditions, otherwise the concepts will not be valid. In effect, this is the same as saying that only a small shear load is allowed to correct curves because the mode of collapse must remain as for uniaxial loading.

In these conditions and considering that a circular interaction is appropriate between longitudinal stress σ_x and shear stress τ normalised by σ_{xu} e τ_0 respectively²¹, the correction will be:

$$C_\tau = \sqrt{1 - R_\tau^2} \quad (35)$$

with

$$R_\tau = \frac{\tau}{\tau_0} \quad \text{and} \quad \tau_0 = \frac{\sigma_0}{\sqrt{3}}.$$



□ G. Soares + Faulkner ◇ Harding M △ Harding L × Harding H

Figure 15 - Comparison between Levels of Distortions
 Comparison of levels of distortions proposed by Faulkner ($0.15\beta_o^2$), G. Soares ($0.11\beta_o^2$) and those used by Harding ($M=0.145\beta_o$, $L=0.145\beta_o/3$ and $H=4 \times 0.145\beta_o$).

There are other studies involving plates under shear loads, but they deal specifically with webs of box girders and their application is not very helpful for the ultimate strength behaviour of ordinary ship plating.

3 Strength of Stiffened Plates

Stiffened plates are the most representative components of a ship hull. They can be found anywhere as in bottom structures, side, deck, superstructures and bulkheads. Historically, the first metal ships had usually transverse framed structures, where plates are loaded mainly in their transverse direction. For these ships the overall strength related to bending moment is governed by the plate strength and so stiffened plate theories are not applied. Faulkner et al.²⁶ analysed a transversely framed 1901 warship based on transversely loaded plate theories and the result seemed to be very satisfactory.

Nowadays most parts of conventional ships have a longitudinally framed structure, i. e., a structure where the distances between longitudinal stiffeners are much smaller than between transverse frames.

Longitudinal stiffeners have, as a main function, to provide the necessary support to the plates to ensure that they retain the required strength. To fulfil this function, stiffeners must have adequate rigidity and the spacing between them must be chosen according to the main characteristics of the plate, namely, thickness and yield stress. The slenderness of the plate has to be designed in such way that the ultimate average stress is kept close to the yield stress for best efficiency.

With an adequate choice of geometric parameters appreciable savings in steel can be achieved. As a consequence, the construction will be cheaper and the cargo deadweight increased. Moreover, the relation between steel

weight and initial cost of the ship is not linear and it must be taken into consideration that a decrease in plate width, i. e., in spacing between stiffeners will result in greater shipyard work cost (mounting, welding and inspection costs) and eventually a greater operational cost (for example an increase on crude oil washing in crude carriers).

Once the required plate strength is achieved, another problem arises, related to the behaviour of the stiffened plate as a beam-column on the hypothesis that one isolated stiffener with associated plate is representative of the whole panel behaviour. Behind this hypothesis there are many questions for which different researchers give different answers:

- is this hypothesis a valid one?
- which is the width of the associated plate that must be considered?
- how does the stiffener interfere with boundary conditions of the associated plate if an effective width concept is considered?
- must residual stresses and distortions be considered in the effective width of the associated plate in beam-column analysis or must they be considered in the overall behaviour of the beam-column?
- what is the best model to represent the flexural rigidity near buckling?
- does the compressive loading follow the shift of the neutral axis in a panel of a section under bending?
- must one compute the heavy frame rotational restraining on the effective span of the column?

and many others could be asked. This chapter attempts to

answer them, highlighting the weaknesses of the choices.

3.1 Review of the literature

3.1.1 Theoretical approaches

The analysis of stiffened plates was performed by several researchers and many solutions to the problem were presented over the years. The prediction of the panel behaviour has led to the development of several techniques such as non-linear finite element methods or more simplified formulations applying the beam-column concept. Common to all of them is the need to apply an incremental end-shortening procedure if a realistic description of the post-buckling behaviour is required. Also common is the use of load-end shortening curves for simply supported plates carried out in separate studies which are able to describe the loss of plate stiffness after buckling.

Finite element analysis was used by Crisfield⁶, Smith and Dow⁵². These last two derived the behaviour of the panel considering that it behaves similarly to a beam-column. Belkaid⁵⁴, using the stress-strain curves proposed by Smith and a finite element program (FABSTRAN) developed at ARE, Scotland, presented analytical equations for strength and post-buckling behaviour of stiffened plates supported by a parametric analysis. In Poland, a finite element program³⁴ was developed allowing for the explicit inclusion of residual stresses and initial imperfections in the nonlinear analysis of stiffened plates.

Finite difference formulations using dynamic relaxation were developed by Frieze and Lin²², also based on the beam-column approach. The effect of the interaction between longitudinally adjacent panels is taken into account by considering several spans acrossing transverse

frames. A parametric study covering geometric parameters and initial imperfections was carried out. Methods involving the solution of the equilibrium equation were applied by Little⁵⁰, Moolani⁵³ and Crisfield⁶.

Design methods to determine the ultimate load of the panels were presented by Faulkner⁵⁵ based on the Johnson-Ostenfeld column approach, by Carlsen⁵⁶ and Dwight and Little⁵⁷ based on the Perry-Robertson formulation and several others⁵⁷⁻⁵⁹ always considering some variations to Johnson-Ostenfeld or Perry-Robertson formulations.

3.1.2 Tests

Experimental programs are generally the best way to test theoretical approaches to a structural problem. Several tests were conducted on panels subjected to uniaxial compression or compression and lateral pressure. But a lack of information exists for more complicated situations like biaxial compression of panels, compression and shear or compression and in-plane bending. Also most tests on reinforced webs under shear must be judged carefully because it is not evident that results can be extended to marine structural panels for the same reasons already mentioned in 2.5.

3.1.2.1 *Uniaxial compression*

Horne et al.⁵⁹ tested 33 reinforced panels in an directed investigation of the effects of plate slenderness, column slenderness, residual stresses and initial imperfections. Also different boundary conditions were imposed on the loaded edges but unloaded edges were free to deflect out-of-plane. Most of the tests were designed to collapse by plate induced failure while five of them

were expected to collapse by stiffener induced failure. Panels were of single span, where stiffeners were welded to plating in two different modes: continuous and intermittent welding. Two different grades of steel were used: grade 43 and 50.

Faulkner⁶⁰ conducted tests on 48 eccentrically loaded panels. The models were of a single bay construction, representing approximately one-quarter scale inter-frame ship panels. The stiffeners were mainly T-sections and the remainder were bars. All panels had five longitudinal stiffeners except two that were single stiffened plates. Continuous manual single pass fillet weld were used, but different levels of residual stresses were included in order to determine their actions. The models were simply supported on the loaded edges and free to deflect out-of-plane on the unloaded edges. A series of 13 similar models was also tested to assess the level of random errors present. A standard deviation of 10.9% was found.

Smith⁵¹ tested 7 full scale welded steel grillages representative of warships bottom, deck and superstructures with an extensive coverage of measurements of the initial and loaded plate deformations. Special care was taken to reproduce shipyard welding procedures.

Dorman and Dwight⁶¹ examined the influence of residual stresses and distortions in 12 tests. It was specified that initial deformations were consecutively upwards and downwards in adjacent spans, which is not the normal situation in ship structures and also can lead to conservative results since the shape of distortions is similar to the mode of collapse.

3.1.2.2 *Compression and lateral pressure*

Smith⁵¹ used lateral pressure in four of the eleven experiments that he had carried out. The geometry of these grillages were similar to those without pressure, allowing for comparison and analysis of the effect of lateral pressure. The levels of pressure applied were of the same magnitude of those found in ships.

A few more tests may be found on experiments conducted by Kmiecik⁸⁷, Kondo⁴⁶, Dean⁴⁷ and Dubois⁴⁸.

Kondo and Ostapenko⁴⁶ tested 2 small simply supported panels with the same lateral pressure but different plate and column slendernesses. The material used was steel of about 275 MPa yield stress and the panels were fabricated by welding.

Dean and Dowling⁴⁷ tested 3 simply supported panels reinforced by 8 stiffeners. The panels were fabricated of mild steel by welding. Transversely there were two frames and the end bays were stiffened to force failure in the middle bay. Two levels of pressure were used.

Dubois⁴⁸ conducted 5 tests, two of them on transversely stiffened panels. Each series used geometrically similar panels where different levels of lateral pressure were applied. The yield stress of the material was of 295 MPa and panels were fabricated by welding.

Kmiecik⁸⁷ tested 3 simply supported panels made of high tensile steel NAV-36 with plating having $\alpha=3$ and a width-thickness ratio of 55. The panels had 4 longitudinal stiffeners (two of the panels were stiffened with bar elements while the other with T stiffeners). The lateral pressure was applied with a column of water in two specimens and one was tested without lateral pressure.

3.2 Modes of failure

Failure of panels is usually classified as:

- plate induced failure
- column-like failure
- tripping of stiffeners
- overall grillage failure.

This last one is normally avoided ensuring that transverse frames are of adequate size and so it is not considered in this study. The first one occurs when the stiffener is sufficiently stocky and the plate has a critical elastic stress lower than yield stress. The second mode is mainly due to excessive slenderness of the column (stiffener and effective associated plate acting together) and failure might be towards the plate or towards the stiffener depending on the column's distortions shape and the type of loading considered, i. e., eccentrically applied or not, following the shift of the neutral axis or not. In a continuous panel, it is usual that the failure is towards the plate in one span and towards the stiffener in the adjacent span. The third mode of failure is consequence of a lack of torsional rigidity of the stiffener; interaction with plate buckling might also occur inducing premature tripping.

Sometimes the first and second modes are incorporated in the same group because the buckled shape of the panel is similar and normally towards the stiffener.

3.2.1 Plate induced failure

In this mode of failure the stiffener is able to

sustain stresses near yield but the plate only can sustain its ultimate stress, σ_u . Thus the ultimate strength of the column is:

$$\Phi_{uc} = \frac{A_s + b_e t}{A_s + b t} \quad (36)$$

where A_s is the stiffener area, b and b_e are, respectively, the width and effective width of the plate, and t the thickness of the plate.

In order to obtain the average load-end shortening curves of the column it is assumed that the stiffener has an elastic-perfectly plastic behaviour, equation (1), and the plate behaves according the relations in chapter 2 and so equation (31) is changed to:

$$\Phi_{ac} = \Phi_e \cdot \frac{A_s + \Phi_w(\bar{\epsilon}) \cdot b t}{A_s + b t} \quad (37)$$

where Φ_e is the edge stress (1) and $\Phi_w(\bar{\epsilon})$ the effective width of the plate for every strain level (4).

3.2.2 Flexural buckling of columns

Two methods for flexural buckling are considered in order to compare the differences in the ultimate bending moment of a ship that each one predicts, the first one proposed by Faulkner⁵⁵ and the second by Carlsen⁵⁶, both using the concept of effective width for plate behaviour and oriented towards marine structures.

3.2.2.1 *Faulkner's method*

Based on the Ostenfeld-Bleich formulation which accounts for inelastic effects of column buckling allowing for residual stresses, Faulkner proposed a model for thin-stiffened plates where it is considered that both the

stiffener and a effective strip of the associated plate are subjected to a edge stress, σ_e . The maximum edge stress that this column can sustain is related to yield stress by the Ostenfeld-Bleich approach, equation (39a,b), but the model used to calculate the buckling flexural rigidity of the column must consider the tangent effective width of the associated plate (41) in order to include the reduction in the tangent modulus or stiffness of the effective material.

Using this approach, the ultimate strength of the column is given by¹:

$$\Phi_{uc} = \frac{\sigma_{ue}}{\sigma_o} \cdot \left\{ \frac{A_s + b_{et}}{A_s + bt} \right\} \quad (38)$$

and assuming the structural proportional limit stress is $0.5 \sigma_o$, the maximum edge stress ratio is related to the column and material properties by the Johnson parabola:

$$\frac{\sigma_{ue}}{\sigma_o} = 1 - \frac{1}{4} \left(\frac{a}{\pi r_{ce}} \right)^2 \cdot \frac{\sigma_o}{E} \quad \text{for } \sigma_E \geq 0.5 \sigma_o \quad (39a)$$

$$\frac{\sigma_{ue}}{\sigma_o} \equiv \frac{\sigma_E}{\sigma_o} = \left(\frac{\pi r_{ce}}{a} \right)^2 \frac{E}{\sigma_o} \quad \text{for } \sigma_E \leq 0.5 \sigma_o \quad (39b)$$

where σ_E is the Euler stress defined as being equal to $\sigma_E = \left(\frac{\pi r_{ce}}{a} \right)^2 E$. The equivalent radii of inertia is defined by the relation:

$$I_{ce}' = r_{ce}^2 \cdot (A_s + b_{et}) \quad (40)$$

and the tangent effective width which must be used in (40) to calculate the reduced moment of inertia was derived by Faulkner as:

$$\frac{b_e'}{b} = \frac{1}{\beta} \cdot \left(\frac{\sigma_o}{\sigma_e} \right)^{\frac{1}{2}} \quad (41)$$

Guedes Soares and Soreide²⁸ have shown that this formulation predicts the mean strength of stiffened plate accurately, when comparing it with available experiments.

The above relation may be changed and generalised to every strain as was done in 3.2.1, by considering that the Euler stress ratio, Φ_E , has an instantaneous value as a consequence of the actual strain. So, the above equations might be redefined and one obtains for the nominal Euler stress ratio:

$$\Phi_E = \left(\frac{\pi}{\lambda}\right)^2 \quad (42)$$

where λ is the column slenderness, $\lambda = \frac{a}{r_{ce}} \cdot \sqrt{\varepsilon_0}$, and replacing ε_0 by ε , the Euler stress ratio at a strain ε is:

$$\Phi_E(\bar{\varepsilon}) = \frac{\Phi_E}{\bar{\varepsilon}} \quad (43)$$

where the column slenderness λ is varying with the strain level due to the variation of effective widths. Modifying equation (39a,b) in order to extend it to every strain level and assuming that the relation is still valid, one obtains the Johnson contribution which corresponds to the first term of the second member of the equation (38) but now for any strain:

$$\Phi_{j\alpha}(\bar{\varepsilon}) = \frac{\sigma_{j\alpha}}{\sigma_0} = \frac{\sigma_{j\alpha}}{\sigma_e} \cdot \frac{\sigma_e}{\sigma_0} = \begin{cases} \left(1 - \frac{\bar{\varepsilon}}{4 \cdot \Phi_E}\right) \cdot \Phi_e \\ \left(\frac{\Phi_E}{\bar{\varepsilon}}\right) \cdot \Phi_e \end{cases}$$

$$\Phi_{j\alpha}(\bar{\varepsilon}) = \left(1 - \frac{1}{4 \cdot \Phi_E(\bar{\varepsilon})}\right) \cdot \Phi_e \quad \text{for } \Phi_E(\bar{\varepsilon}) > 0.5 \quad (44a)$$

$$\Phi_{j\alpha}(\bar{\varepsilon}) = \Phi_E(\bar{\varepsilon}) \cdot \Phi_e \quad \text{for } \Phi_E(\bar{\varepsilon}) < 0.5 \quad (44b)$$

and finally the expression to calculate the load-end shortening curves including inelastic buckling effects can be written as:

$$\Phi_{ab}(\bar{\epsilon}) = \Phi_{jo}(\bar{\epsilon}) \cdot \frac{A_s + \Phi_w(\bar{\epsilon}) \cdot bt}{A_s + bt} \quad (45)$$

where $\Phi_{ab}(\bar{\epsilon})$ is the average stress of a column composed by a stiffener of area A_s and a plate of area bt under a strain $\bar{\epsilon}$.

As to the last remark it must be said that this approach is only valid assuming that initial deformations are small and load diffusion ensures that no eccentricity of the load is present which seems to be the case²⁵. Allowance for residual stresses and biaxial compression are automatically taken into account from the application of the corrective factors to plate strength already developed in the previous chapter. Improvements are possible if residual stresses in the stiffener are considered.

3.2.2.2 Carlsen's method

In order to incorporate explicitly the initial imperfections of the stiffener, Carlsen⁵⁶ proposed a formula for the ultimate strength of panels which also accounts for the loss of effectiveness of plating by the introduction of a effective width. The basis is the well known Perry-Robertson formulation modified by the introduction of the plate effective width due to the nature of the ships' panels. The prediction of the panel ultimate strength is suggested to be:

$$\Phi_{ub} = \frac{A_e}{A_t} \cdot \frac{(1+\gamma+\xi) - \sqrt{(1+\gamma+\xi)^2 - 4\gamma}}{2\gamma} \quad (46)$$

where

$$A_t = A_s + bt \quad (47a)$$

$$\gamma = \frac{\sigma_o}{\sigma_E} \quad (47b)$$

$$\xi = \frac{A_t \cdot \delta_s}{W} \quad (47c)$$

and the effective area A_e is the sum of the stiffener area and an effective area of the associated plate. δ_s and W are, respectively, the out-of-plane stiffener distortion and the section modulus of the stiffener with associated plate. For the calculation of the effective area it was recommended to use an effective width of:

$$\frac{b_e}{b} = \frac{1.8}{\beta_0} - \frac{0.8}{\beta_0^2} \quad (48a)$$

for plate induced failure and:

$$\frac{b_e}{b} = 1.1 - 0.1 \cdot \beta_0 \quad (48b)$$

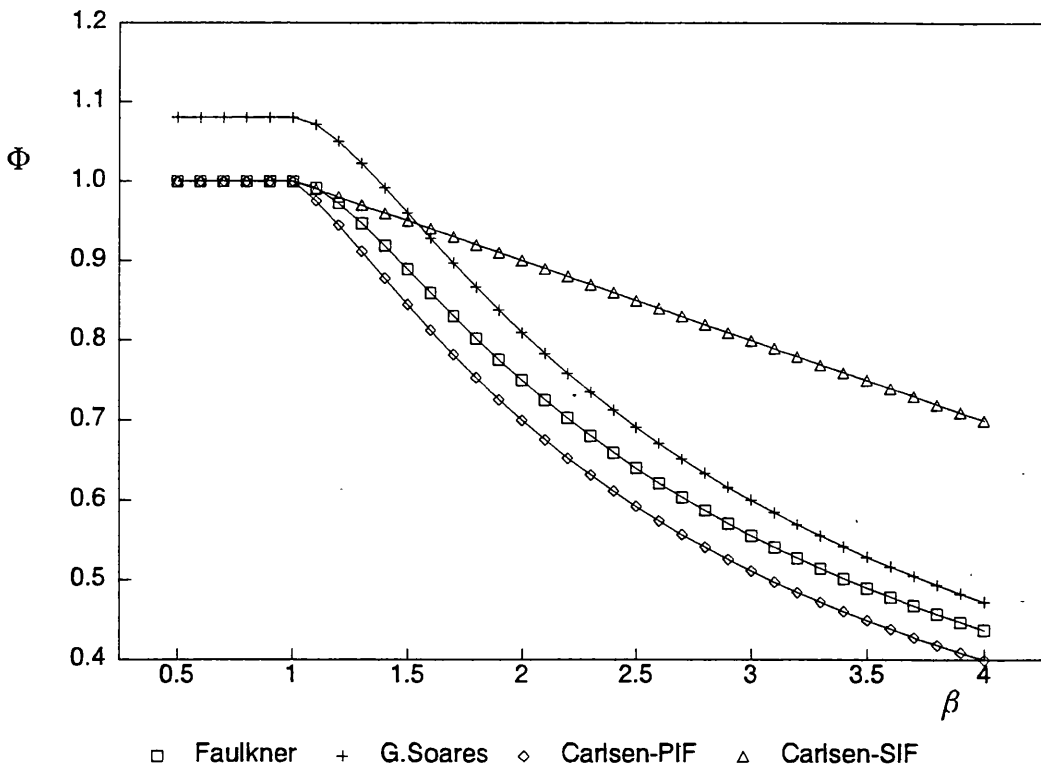


Figure 16 - Comparison between effective width formulas

for stiffener induced failure, both limited to not greater than one. The stiffener out-of-plane distortion could be taken as $\delta_s = 0.0015a$ and a correction for the shift of the neutral axis was recommended in the plate induced failure mode. The calculation of the Euler stress σ_E and the section modulus W used the full width of the plate because it was considered that they have a small effect on the overall strength prediction.

This formulation, as it is explained above, is not very suitable to hull bending moment prediction since it does not estimate the carrying capacity of a panel for a given strain. Also some remarks must be made about some of the assumptions from the point of view of ship structural geometry and the prediction of moment-curvature relationship:

- the correction proposed for the shift of neutral axis due to loss of the plate effectiveness must not be considered in panels belonging to hull sections and subjected mainly to bending moments due to load diffusion,
- in very thin stiffened plates the full width and the effective width are very different, thus the Euler stress is different if the latter is used instead of the former. The same comment can be applied to the calculation of the ξ parameter,
- equations (48a,b) are helpful to calculate effective widths in a buckling situation but not to apply during the loading path, even if they are modified to cover the strain range, because away from the buckling strain region of the panel the plate does not know if it is going to buckle by plate or stiffener induced effects and its effective width at that strain must be only one of these. Also these equations are applicable on a particular level of initial imperfections which is not the objective of this study.

Furthermore, Guedes Soares and Soreide²⁸ have shown that this method is generally conservative by more than 15%. In fact, they pointed out that while this method is a design method because it incorporates a safety margin, Faulkner's method is a strength assessment method predicting the mean panel strength.

In order to consider these remarks and to obtain an average load-shortening curve of the panel, Carlsen's formulation was altered especially in some parameter definitions.

The Ayrton-Perry formula⁶² states that the average buckling stress of a column is given by:

$$\sigma_a = \sigma_{E\mu} - \sqrt{\sigma_{E\mu}^2 - \sigma_o \sigma_E} \quad (49)$$

with

$$\sigma_{E\mu} = \frac{1}{2} \cdot \{ \sigma_o + (1 + \mu) \sigma_E \} \quad (50a)$$

$$\mu = \frac{c \cdot \delta_s}{r^2} \quad (50b)$$

where $r \equiv r_{ce}$ already defined in equation (40) in order to consider loss of effectiveness and rigidity of the plate and c is the distance from the centroid to the most compressed fibre (noting that the centroid is shifting during loading because the geometry of the equivalent column is also changing).

Consider that equations (49) and (50a) are still valid if the edge stress σ_e is used instead of the yield stress, which physically means that for an average shortening of the column, ε , an average column's stress, σ_a , might always be calculated. Using this generalisation the Ayrton-Perry formula becomes:

$$\Phi_{aP} = \Phi_e \cdot \left\{ \Phi_{E\mu e} - \sqrt{\Phi_{E\mu e}^2 - \frac{\Phi_E}{\Phi_e}} \right\} \quad (51)$$

where:

$$\Phi_{E\mu e} = \frac{1}{2} \cdot \left\{ 1 + (1 + \mu) \cdot \frac{\Phi_E}{\Phi_e} \right\} \quad (52)$$

The real average stress ratio of the panel must consider the full width of the plate:

$$\Phi_{ab} = \Phi_{aP} \cdot \frac{A_s + b_e t}{A_s + b t} \quad (53)$$

These equations are similar to those derived by Carlsen, equations (46, 47, 48), but now using only one formula to calculate the effective width of the plate, equation (4). The parameter μ is only dependent on the geometric characteristics of the stiffened panel, if one disregards the small change in the radii of gyration of the section as a consequence of the change in effective width of the plate when the shortening is increasing.

3.2.3 Tripping of stiffeners

This mode of panel's failure is one of the most dangerous because it is always associated with a very quick shedding of load carrying capacity of the column. Lateral-torsional instability may occur alone by twisting of the stiffener about its line of attachment to the plating developing a partial or full hinge at the intersection, or induced by flexural buckling especially if the deflected shape of the column is towards the plate. In that case, the stiffener will be subjected to a higher stress than the average column stress and the critical tripping stress could be easily reached, followed by a rapid load shedding.

Tripping involves a rotation of the stiffener about a hinge, which is usually considered to be located at the connection of the stiffener to the plating, and vertical flexure in the principal direction of the stiffener.

3.2.3.1 Elastic tripping stress

There are not many studies about tripping and the present work will follow the approach presented by Faulkner^{55,63} and by Adamchak⁶⁴, using them to determine the tripping stress and to estimate a pattern for load shedding after tripping. The approach is based on Rayleigh's principle in order to obtain the elastic critical stress for tripping.

Corrections to elastic derived tripping stresses are presented which are intended to incorporate nonlinear behaviour of both plate and stiffener. However with the development of finite element analysis^{65,66,67} it is expected that a more comprehensive understanding of tripping behaviour will be achieved mainly concerned with inelastic solutions and proposals.

The proposed approach balances the torsional, sideways bending, warping, and spring strain energies with the elastic tripping stress energy:

$$I_p \sigma_T = GJ + \frac{m^2 \pi^2 E T_p}{a^2} + \frac{C_s a^2}{m^2 \pi^2} \quad (54)$$

where m is the number of tripping half wavelength along the length a , J is the St. Venant torsional constant, T_p is an appropriate tripping parameter that includes both sideways bending ($I_z \bar{z}^2$) and longitudinal warping (Γ) contributions and is defined as:

$$T_p = I_p \bar{z}^2 + \Gamma \quad (55)$$

and C_s is the elastic rotational spring stiffness per unit length of the toe which can be derived as:

$$C_s = \frac{Et^3}{2.73b} \quad (56)$$

Equation (54) is applicable when considering a constant constraint along the toe, but a more accurate approach can be obtained if one accounts for the destabilising moments induced by the plate's buckling actions.

Faulkner⁶³ proposed that the rotational constraint might be approximated by a linear interaction based on the analogy of dynamic behaviour of ship grillages⁶⁸:

$$\frac{C}{C_s} + \frac{\sigma}{\sigma_{cr}} = 1 \quad \text{for } \frac{\sigma}{\sigma_{cr}} \leq 2 \quad (57)$$

where σ_{cr} is the elastic critical stress of a simply supported plate:

$$\sigma_{cr} = \frac{\pi^2}{12(1-\nu^2)} E \left(\frac{t}{b} \right)^2 \left[\frac{m_o b}{a} + \frac{a}{m_o b} \right]^2 \quad (58)$$

and m_o is an integer representing the mode of possible collapse of the plate element.

Introducing equation (58) into equation (54) the tripping stress can be determined:

$$\sigma_T = \frac{GJ + \frac{m^2 \pi^2 E T_P}{a^2} + \frac{C_s a^2}{m^2 \pi^2}}{I_P + \frac{C_s a^2}{m^2 \pi^2 \sigma_{cr}}} k \quad (59)$$

The coefficient k is an attempt to include the interaction between the plate and the stiffener and Faulkner recommended the values 1.0, 0.0, 0.5 and 0.0 respectively for $m_o/m = 1, 2, 3$ and more than 3.

Theoretically two remarks must be made to this approach. In the first place the third value must be 0.33 because only one third of the plate is destabilising the stiffener. On the other hand if the plate is destabilising the stiffener then the stiffener is stabilising the plate and some degree of rotational constraint is applied to the

plate. Therefore the assumed simply supported plate boundary conditions may seem to be a little conservative. Furthermore any consideration of the plastification of the toe is not taken into account, which may be very important from the point of view of load-end shortening curves of columns since if some plastification occurs than the toe's spring constant will be reduced.

3.2.3.2 *Inelastic effects*

In order to estimate inelastic effects, Faulkner⁶³ recommends the use of the $\sqrt{E_t E}$ modelling instead of the E_t used in column flexural buckling, due to local bending effects, and a tangent modulus defined by the Ostenfeld-Bleich quadratic parabolae:

$$\frac{E_t}{E} = \frac{\Phi \cdot (1 - \Phi)}{p_r \cdot (1 - p_r)} \quad (60)$$

being p_r the proportional limit stress ratio.

The inelastic tripping stress of the stiffener with effective associated plate will become:

$$\Phi_{Ti} = \frac{\Phi_T^2}{\Phi_T^2 + p_r \cdot (1 - p_r)} \quad \text{if } \Phi_T > p_r \quad (61)$$

$$\Phi_{Ti} = \Phi_T \quad \text{if } \Phi_T < p_r$$

where p_r is recommended to be taken as 0.8 because of the presence of largely tensile residual stresses. However for ships in service maybe $p_r = 0.5$ is more relevant because the residual stress level drops quickly in the early stage of a ship's life.

The ultimate average tripping stress of the panel will be finally:

$$\Phi_{Tu} = \Phi_{Ti} \cdot \frac{A_s + b_e t}{A_s + b t} \quad (62)$$

where the effective width b_e must be calculated for a slenderness $\beta = \beta_0 \cdot \sqrt{\varepsilon_{Ti}}$ using equation (4), eventually corrected by the reduction factors developed in chapter 2. The approach used to determine b_e implicitly considers that the stiffener behaves elastically until σ_{Ti} to be reached and so naturally the correspondent strain will be $\varepsilon_{Ti} = \frac{\sigma_{Ti}}{E}$ which is also the plate's average shortening.

3.2.3.3 Behaviour of pre and post tripping

The equations of the last chapter are only used by Faulkner and Adamchak to predict the ultimate tripping stress. But for ultimate bending moment prediction, it is important to have a relationship between the effect of tripping and the end-shortening state of the column.

Thus, the above equations were modified according to the same principles as in section 3.2.2 but now it is only necessary to predict the behaviour of the column after tripping (say for $\varepsilon \geq \varepsilon_{Ti}$) because before tripping the column's behaviour will be governed by flexural bending; assuming that the stiffener has a perfectly elastic behaviour for tripping stress calculations then equations (44a,b) or (51) for flexural behaviour will be always lower than the elastic one (the effective width is the same in both analyses) and thus flexural derived average curves will govern the pre-buckling behaviour.

The criteria followed considers the minimum tripping stress, equation (59), and if this one is lower than the yield stress, it is multiplied by the effective area ratio:

$$\Phi_T(\bar{\varepsilon}) = \Phi_{Tmin} \cdot \frac{A_S + \Phi_w(\bar{\varepsilon}) \cdot bt}{A_S + bt} \quad (63)$$

which does not account for the column's load shedding after tripping but only for the loss of plate's effectiveness.

To approach the shedding of load after tripping one very simple formula is used as a result of a qualitative analysis of the available average load-end shortening curves using finite element methods⁵⁴, which consists of reducing the column's carrying capacity by the ratio of the tripping strain and the actual strain:

$$\Phi_{TC}(\bar{\epsilon}) = \Phi_T(\bar{\epsilon}) \cdot \frac{\epsilon_T}{\bar{\epsilon}} \quad (64)$$

This a rough approximation to the behaviour but it seems to be reasonably realistic and the results obtained with it are very consistent. It must be said, however, that inelastic effects are not taken into account due to two main reasons:

- the first one deals with the nature of the usual ship panels which are designed in such a way that flexural buckling occurs normally early than tripping buckling of stiffeners. Thus, with a quick load shedding model for tripping, this last one will govern the very post-buckling behaviour of column even if the flexural buckling stress is much lower than the tripping stress, but it does not seem to correspond to real panel behaviour;
- the second one is directly related to the nature of tripping of lateral-torsional weak stiffeners. For this kind of stiffener, let us say flat bar stiffeners, tripping occurs prematurely, on the elastic range of stress and so inelastic effects are irrelevant.

In conclusion, the model has a gap in the load shedding assumed for the cases where flexural buckling stress and inelastic tripping stress are very close as in the range of $0.6-0.9\sigma_0$, but this is also a situation where interac-

tions between both modes of failure might lead to several load shedding patterns depending mainly on the shape and amplitude of the imperfections of the stiffeners.

3.3 Load-end shortening curves of beam-columns

The model used to describe the behaviour of columns is based on the superposition of the equations already derived in the previous sub-chapters. Each equation is related to one particular mode of failure and at every end-shortening of the column the average stress to be considered is always the lowest one between the calculated stresses for each mode of failure:

- plate failure using $\Phi_{ac}(\bar{\epsilon})$ from equation (37),
- flexural column failure using $\Phi_{ab}(\bar{\epsilon})$ from equation (45) if Faulkner based method is desired, or equation (53) for Carlsen based method,
- tripping failure of stiffeners using equation (63) or (64).

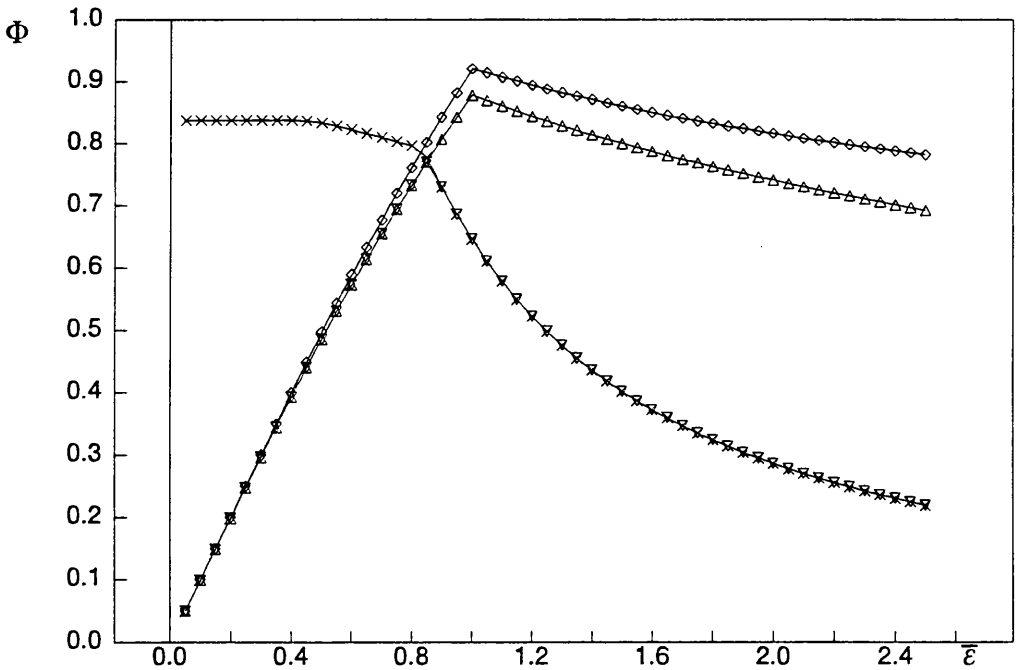
It is evident that the stresses predicted by $\Phi_{ac}(\bar{\epsilon})$ are always higher than those predicted by $\Phi_{ab}(\bar{\epsilon})$, but in spite of this, they are considered in order to allow comparisons between models. These comparisons may be very helpful in the design of panels and provide qualitative information about the 'best' geometry to choose.

Figure 17 plots these curves together in order to demonstrate how a better choice of stiffener geometry that avoids tripping may represent a saving of efficiency of more than 10% in the ultimate strength of the panel. Also a smoother post-buckling behaviour is achieved when avoiding tripping which may be significant for ultimate strength of ships because the ultimate bending moment is reached when some of the panels are already buckled, as will be seen in chapter 4.

The same considerations may be applied to columns with

excessive slenderness. In these cases the plate induced failure and the flexural buckling curves will be well away from each other and so some modifications of the column geometry (its span if possible, and/or the stiffener geometry) may compensate largely an eventual increase in weight.

Four models for column behaviour prediction were developed in order to cover different approaches to the problem. They are a result of the exhaustive combination of Design Formula and Physical Approach methods for residual stresses, with Faulkner's and Carlsen's methods for column behaviour. All the models have also the



◇ plate induced failure △ flexural buckling × tripping ▽ column behaviour

Figure 17-Construction of load-shortening curves
Representation of load-end shortening curves of a column with $\beta_0=1.56$ and $\lambda_0=1.36$, showing the curves corresponding to each mode of failure and the resultant behaviour.

alternative to consider or not a load shedding behaviour after buckling which will be developed in section 3.3.3.

3.3.1 Effect of distortions

Three kinds of distortions coexist in a stiffened panel: initial imperfections of the plate element, out-of-plane deformations of the stiffener and lack of perpendicularity between stiffener and plate along the span.

The first one usually decreases the ultimate strength of the plate and consequently decreases the strength of the panel; the effect on plate behaviour was already discussed on section 2.4.

Out-of-plane distortions of the stiffener induce bending stresses along the span of the stiffener increasing the local stress in the extreme fibres and so, the actual axial carrying capacity of the column will be lower than that with a straighter stiffener because the yield stress will be achieved at a lower axial average stress; these distortions result from the manufacturing process, i. e., mounting defects and especially as a consequence of welding.

The lack of perpendicularity or tilt is mainly a consequence of mounting deficiencies in earlier stages of the hull's construction or of the use of alternate and intermittent welding on light stiffeners. It is especially important in torsional behaviour of the column as it reduces the tripping stress.

3.3.1.1. Consequence of plate imperfections on column strength

The reduction of column strength due to plate distortions may be incorporated in the design through a

reduction of the effective width of the associated plate.

According to Faulkner's method, the strength of the panel is given by equation (38). The reduction on strength due to imperfections of the plate element may be calculated, taking the derivative of Φ_{uc} :

$$\frac{d \Phi_{uc}}{d \delta_p} = \frac{d}{d \delta_p} \left(\Phi_{ue} \cdot \frac{A_s + b_e t}{A_s + b t} \right) \quad (65)$$

$$\frac{d \Phi_{uc}}{d \delta_p} = \frac{d \Phi_{ue}}{d \delta_p} \cdot \frac{A_s + b_e t}{A_s + b t} + \Phi_{ue} \cdot \frac{t}{A_s + b t} \cdot \frac{d b_e}{d \delta_p} \quad (66)$$

which may be rearranged in the form:

$$\frac{1}{\Phi_{uc}} \cdot \frac{d \Phi_{uc}}{d \delta_p} = \frac{1}{\Phi_{ue}} \cdot \frac{d \Phi_{ue}}{d \delta_p} + \frac{b_e t}{A_s + b_e t} \cdot \frac{1}{\Phi_p} \cdot \frac{d \Phi_p}{d \delta_p} \quad (67)$$

This derivative has two components: the first one relates directly to the influence of plate distortions on column strength of the model, Φ_{ue} , and the second one relates to the reduction in average carrying capacity due to the effectiveness of the associated plate. The effect of distortions on Φ_{ue} is expected to be very small because imperfections only affect the radii of gyration of the cross section and this last one is very insensitive to small changes in associate plate effective area.

Therefore, the main reduction is obtained from the second term of equation (67) and neglecting the first term this equation is simply:

$$\frac{1}{\Phi_{uc}} \cdot \frac{d \Phi_{uc}}{d \delta_p} = \frac{b_e t}{A_s + b_e t} \cdot \frac{1}{\Phi_p} \cdot \frac{d \Phi_p}{d \delta_p} \quad (68)$$

which shows clearly the most important parameter to consider: the ratio between effective plate area and effective total area, and the percentage of plate strength reduction due to distortions.

Another important conclusion is that the overall reduction in column strength is always lower than that in plate strength because the first parameter, area ratio, is always lower than one. Thus, in very thin stiffened plates this effect may be disregarded.

Finally the effects of plate imperfections on column strength can be resume by the expression:

$$\Phi_{uc\delta p} = \Phi_{uc} \cdot \Phi_{\delta p} \quad (69)$$

where the reduction factor is given by the following equation:

$$\Phi_{\delta p} = 1 - \frac{b_{et}}{A_s + b_{et}} (0.626 - 0.121\beta_0) \cdot \delta_p \quad (70)$$

which is supported by equation (20).

3.3.1.2 *Consequence of out-of-plane imperfections of the stiffener*

The Faulkner based method does not account for this kind of imperfections. However, the Carlsen based method includes it explicitly, in section 3.2.2.2. Two different situations were considered for design purposes: plate induced failure (PIF) and stiffener induced failure (SIF). The distortion recommended in SIF ($\delta_s = 0.0015a$) is increased, in PIF, by another term that computes the shift of the neutral axis, taking it equal to

$$\delta_s = 0.0015a + z_p \left(\frac{A_t}{A_e} - 1 \right). \quad (71)$$

where z_p is the distance from the neutral axis to the mid-plane of the plate. Comments to this interpretation and its applicability on hull strength were already discussed in the section 3.2.2.2.

With respect to the variation of strength due to stiffener imperfections, it may be computed by the

derivative of equation (46), which gives:

$$\frac{1}{\Phi_{ub}} \cdot \frac{d \Phi_{ub}}{d \delta_s} = -\frac{A_t}{W} \cdot \left((1+\gamma+\xi)^2 - 4\gamma \right)^{-1/2} \quad (72)$$

As can be seen, the influence of distortions decreases when ξ increases (or δ_s). Figure 18 represents graphically equation (72) showing that small imperfections correspond to a large decrease in strength compared with a straight stiffener, but after some level of imperfections the variation becomes very small.

It is also evident that the decrease in strength is more significant in the range $0.75 < \Phi_E < 1.5$. It corresponds to the transition between elastic and plastic behaviour of stiffened plates. Equation (72) becomes undefined for

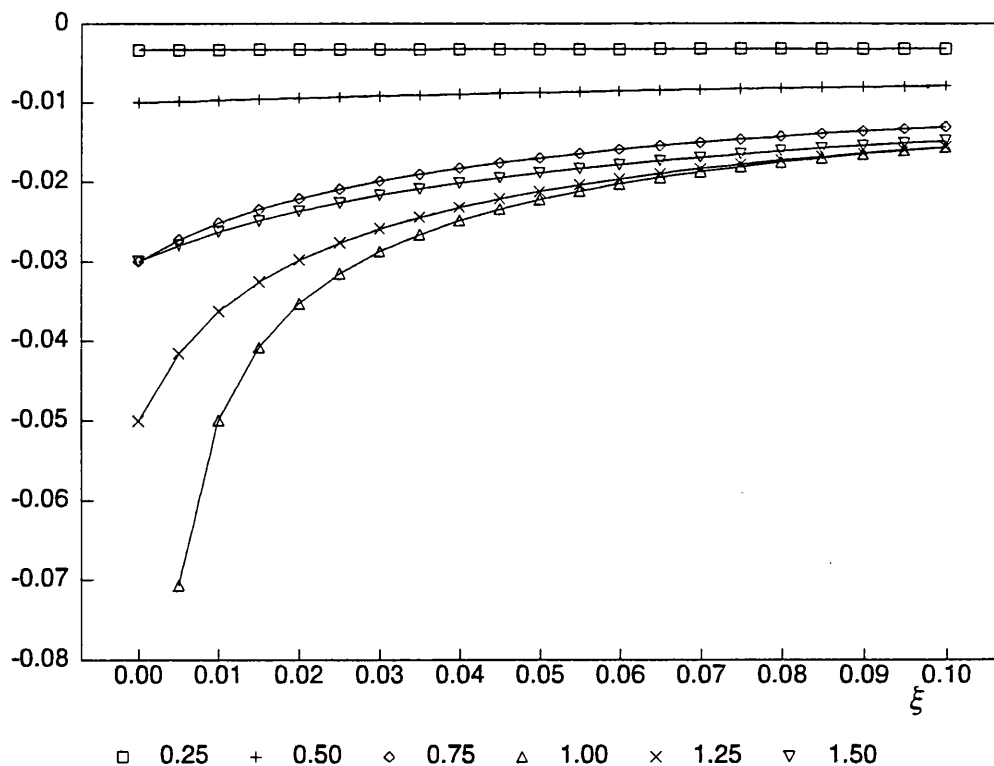


Figure 18 - Effect of Stiffener Imperfections

Percentage variation of panel strength due to out-of-plane imperfections (equation (70)) for $A_t/W=0.01$. Each curve is associated to one value of $\sigma_E/\sigma_0=1/\gamma$.

a straight stiffener ($\xi=0$) when $(1+\gamma+\xi)^2-4\gamma=0$ becomes to $\gamma=1$, and so it confirms the results from figure 18.

In real structures initial imperfections are always present, and thus the expression

$$(1+\gamma+\xi)^2-4\gamma = (1-\gamma+\xi)^2+4\gamma\xi \quad ($$

is intrinsically positive and consequently there is no critical situation. But, even in this case, the largest reduction in strength will be achieved when γ is near 1, if one recognises that ξ is a very small number compared with γ .

3.3.1.3. *Consequence of lateral rotational distortions*

As was noticed by Faulkner⁶³, the elastic tripping stress of a beam-column is associated with a critical length of lateral wave of the stiffener's deformations about the toe. The half wave length is suggested to be independent of the length of the stiffener span and of the number and position of the so called "tripping brackets". It is mentioned that fitting such brackets can be a rather bad solution because they can magnify the destabilising action of the buckled plating in structures where tripping and plate buckling have similar magnitudes.

This interpretation leads to the conclusion that the presence of initial lateral distortions with a wave length approximately equal to the critical one may cause premature tripping and eventually a significant reduction in strength.

Not many works exist on this subject and due to its complex nature with respect to plate-stiffener interaction, more research is necessary and expected.

3.3.2 Effect of lateral pressure

None of the methods described accounts explicitly for the effects of lateral pressure. This may be a consequence of these methods being oriented to ship structures, where lateral pressure intensity is relative low; and also because low lateral pressure level does not necessarily lead to a significant reduction on ultimate strength, and in some cases may increase it slightly. However, some correction may be introduced in order to account for lateral pressure effects.

In the Faulkner based method (JO) the simplest way to follow is to introduce a correction in plate behaviour which will affect the beam-column behaviour in the same way. The subject related to plate strength was previously discussed in section 2.5. and equations (31 to 34) were recommended to account for this effect.

The Carlsen based method (PR) may be modified by an additional "initial out-of-plane distortion" of the stiffener, ξ_1 , acting together with the effect on plate strength referred to earlier. In the elastic domain of plate behaviour it is evident that the additional distortion must be equal to the elastic deformation from lateral pressure alone. The global effect of this action is the lowering of load-end shortening curves thus decreasing strength and rigidity. The effect of the lateral load on plate strength may result in a negative or positive contribution to strength depending on whether the imposed deformation has the same shape as the buckled plate or not, and on the level of lateral pressure and associated bending stresses.

Finally, the ultimate strength of stiffened plates subjected to uniaxial compression and lateral load will

be the result of a combination of both effects and will depend on plate parameters (plate slenderness β_0 , aspect ratio α , initial imperfections δ_p), on load level Q_L and on column parameters (section modulus W , elastic distortion due to lateral pressure ξ_1 , etc.).

3.3.3 Load shedding after buckling

Two different post-buckling behaviours were considered: with load shedding and with constant carrying capacity after buckling.

Load shedding is predicted assuming that the plate strength still continues to decrease after buckling (section 2.1.1., equations (3,4)). This assumption implies that the term A_e/A_t of equations (45,46) decreases continuously with $\bar{\epsilon}$, after buckling, and, also implies that the column's slenderness λ is affected by the change in the effective radii of gyration. However, this last influence is very small and may be neglected.

Together with this assumption, another one is introduced relating to the behaviour of the idealised effective column model itself. It consists of considering that the Euler stress is dependent of the strain state of the column even beyond buckling (sections 3.2.2.1 and 3.2.2.2). The Ostenfeld and Perry formulations are modified in order to include this extension over the range of strains.

3.3.4 Effect of the residual stresses

In this thesis only the residual stresses in the plate elements are considered, as treated in section 2.2. Their consequence on the behaviour of stiffened plates are shown

in figures 19 to 22. These figures show that the predicted behaviour of a column with residual stresses differs substantially according to the method applied (DFM or PAM) used to account for them, while the methods based on Faulkner (JO) and Carlsen (PR) for ultimate strength are almost coincident.

In DFM, the curves are pushed down with increasing residual stresses but keeping the same pattern as the column without residual stresses.

In PAM, one may detect three points of discontinuity of the derivative of the curve: the first of them at a strain ratio lower than 1, which corresponds to the yielding of the strip of the plate initially in compression; the second one at a strain ratio of 1 represents the initiation of the yielding of the stiffener, which is considered to be free of residual stresses; and the last at a strain ratio of 2 marks the yielding of the two strips of the plate near the stiffener, which are modelled initially in tension.

So when analysing the behaviour of a column with residual stresses, not only are the two event points referred to in section 2.2.2 relevant, but also the assumed residual stresses pattern in the stiffener may determine the occurrence of a new event point between the other two, assuming that the residual stresses in the stiffener are lower than in the plate.

Another interesting conclusion from the analysis of the curves is the increase of the strength at high strain associated with a region where the strength varies slowly and, for certain levels of residual stresses the maximum load is reached at strains greater ϵ_0 , and in the limit these could be $2\epsilon_0$.

The figures 21 and 22 give quite different behaviours for PAM and DFM. These figures are drawn for high levels of residual stresses and the differences in column behaviour are directly related to differences in plate behaviour, figure 13. However the differences are mostly in the shape of the curve than in the ultimate strength of the column. Again this is a consequence of the plate behaviour derived for both methods and the results obtained here are in accordance of those resumed in figure 14, i.e., almost the same strength reduction due to residual stresses but a significant difference in ultimate strain prediction.

In respect to the post buckling behaviour the DFM computes a great decrease in strength with increasing residual stresses, while the PAM predicts an unchanged behaviour for strains greater than $2\varepsilon_0$. These differences in post buckling behaviour will have a direct impact on the ultimate strength of the hull and some attention will be called to this subject in chapter 4.

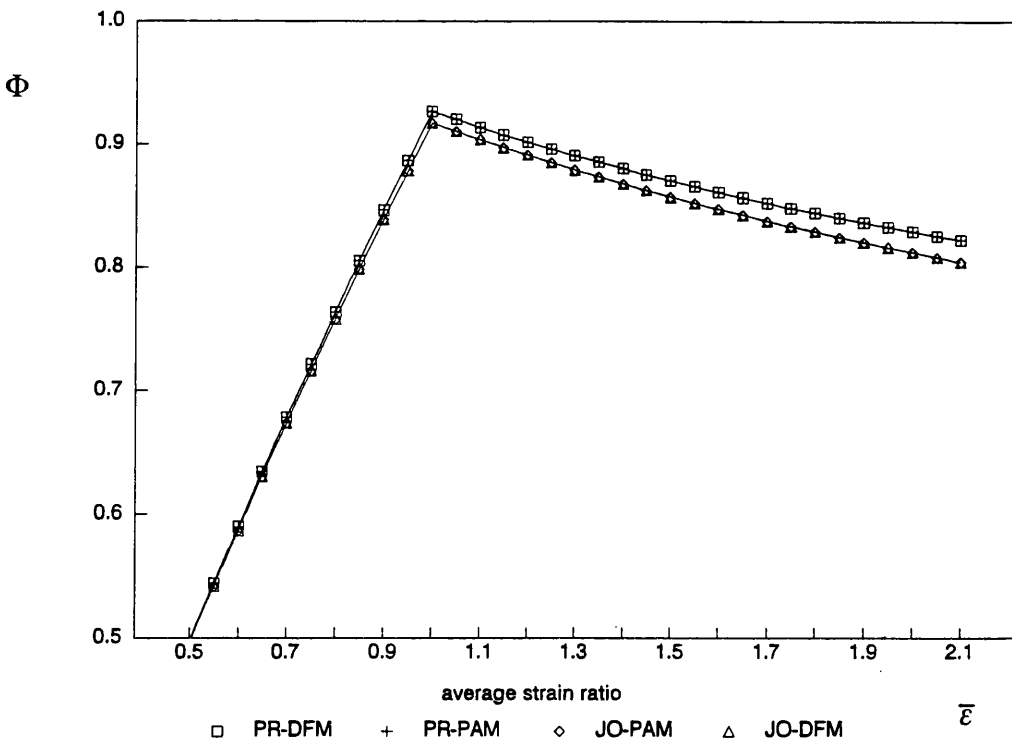


Figure 19-Load-Shortening Curves of Columns

Representation of load-end shortening curves of a column with $\beta_0=1.56$ and $\lambda_0=0.61$ predicted by several methods without residual stresses.

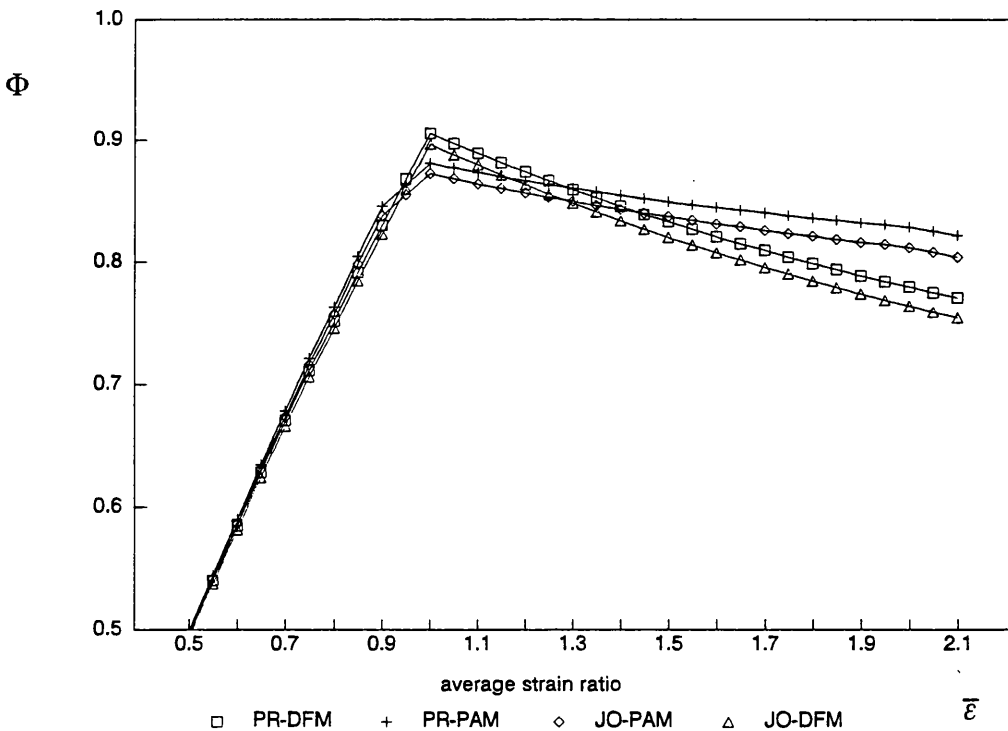


Figure 20-Load-Shortening Curves of Columns

Representation of load-end shortening curves of a column with $\beta_0=1.56$ and $\lambda_0=0.61$ predicted by several methods with residual stresses level of 0.1.

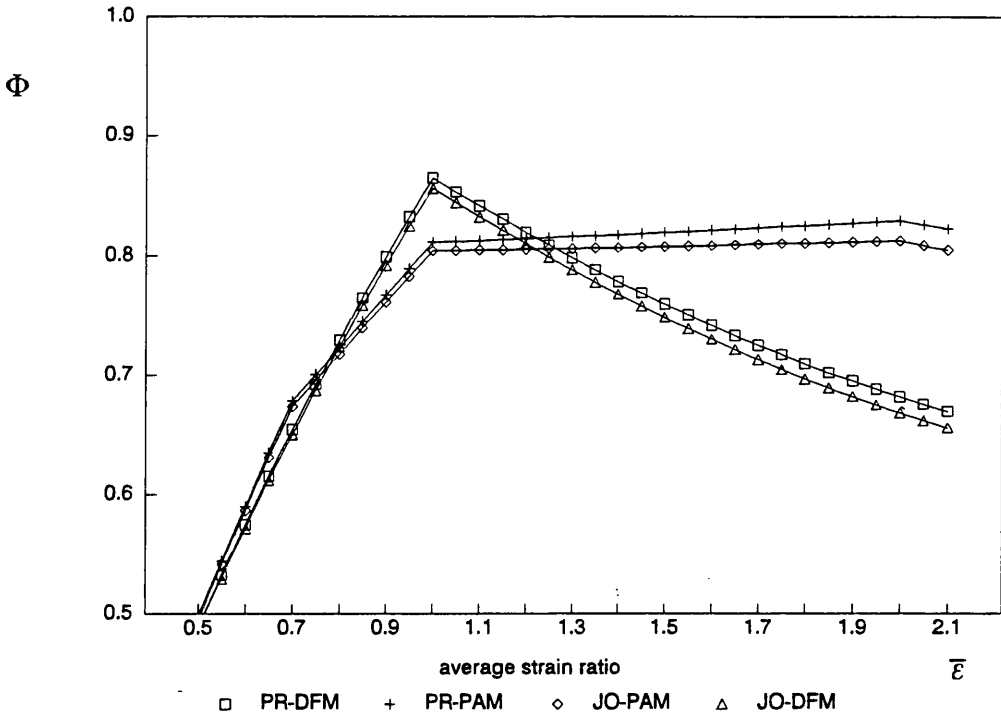


Figure 21-Load-Shortening Curves of Columns

Representation of load-end shortening curves of a column with $\beta_0=1.56$ and $\lambda_0=0.59$ predicted by several methods with residual stresses level of 0.3.

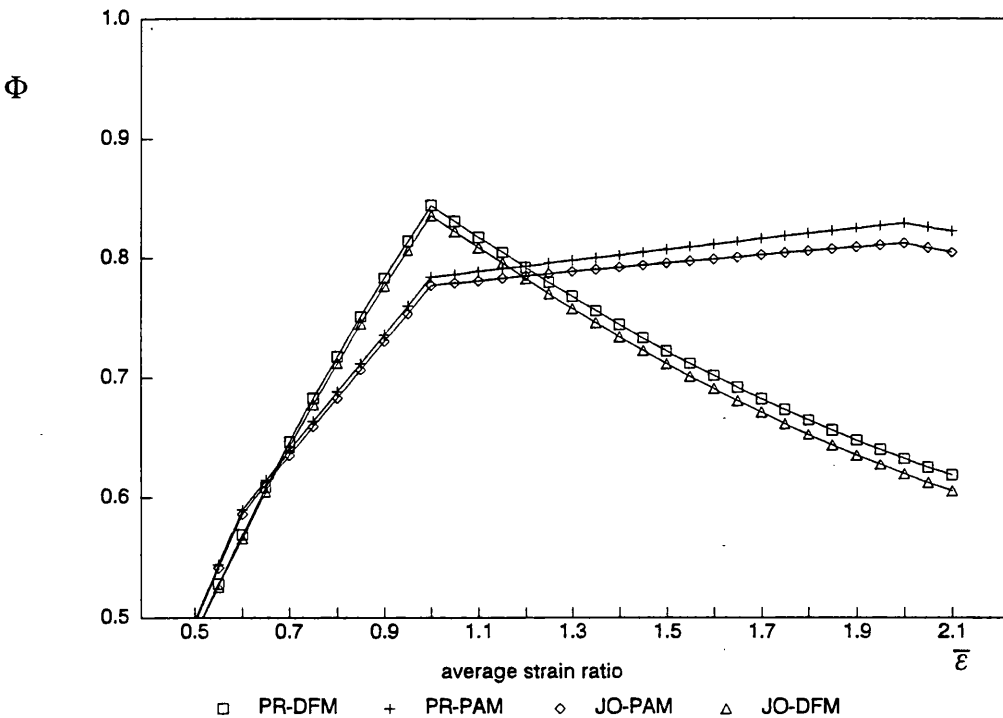


Figure 22-Load-Shortening Curves of Columns

Representation of load-end shortening curves of a column with $\beta_0=1.56$ and $\lambda_0=0.58$ predicted by several methods with residual stresses level of 0.4.

4 Longitudinal Strength of the Hull Girder

The ultimate or maximum bending moment of the ship cross section represents only one part of the knowledge required to understand the behaviour of the ship under bending loads. The philosophy of designers and Classification Societies is nowadays changing and more attention is devoted to the whole curve of the moment-curvature relationship especially the post-buckling behaviour and the differences between sagging and hogging ultimate moment.

As is well known, old rules did not distinguish between these two conditions and requirements were mainly referring to inertial moment of the cross section area and its minimum required modulus. Recently some of them began to incorporate in the calculation of the inertial moment, the degree of effectiveness of panels under compression, in order to obtain a more correct value of the strength of the ship under ultimate conditions.

Historically, the earliest attempts to incorporate buckling and its effects on ship strength were made by Caldwell⁶⁹ using a simplified procedure where the ultimate moment of a midship cross section in the sagging condition was calculated introducing the concept of a structural instability strength reduction factor for compressed panels. Faulkner⁷⁰ developed this concept suggesting a design method to calculate this reduction factor.

Adamchak⁷¹ has developed a simplified method, together with a computer program which implements it, where the ultimate strength of each panel includes a flexural-tor-

sional buckling formulation. Curves of moment-curvature are built from a set of discrete points corresponding to the buckling of each panel. The method was also adopted by Hughes⁷² where any reserve of the panel compressive strength after buckling was neglected.

Billingsley²³ used an engineering approach considering a very simplified model for any individual beam-column element. The strength of hull's girder was obtain from the summation of the individual contributions of each element.

Smith^{73,75} and Dow⁷⁴ developed an incremental curvature procedure which allows the derivation of a complete moment-curvature relationship. It is an hybrid method mainly based on a finite element formulation but where the plate element strength is obtain from a set of empirical curves.

Lin²² described a similar method but he has considered a different approach to assess the plate strength and used a dynamic relaxation method for the stiffened panel strength. Several comparisons were made with experimental results and therefore two simplified expressions for ultimate moment prediction were presented.

Rutherford and Caldwell⁷⁶ recently presented a comparison between the ultimate bending moment experienced by a VLCC and the results of retrospective strength calculations in which a simplified approach to stiffened plates was used, but without considering the post-buckling behaviour. Also the importance of lateral pressure, initial deformations and corrosion rates were investigated. The validity of the model and method was confirmed by using a nonlinear finite element program (MARC).

4.1 Moment-Curvature Curves

The present method follows the general approach presented by Billingsley²³ and by Rutherford and Caldwell⁷⁶, but with respect to plate strength and beam-column behaviour, the models developed in this work and reported in the last two chapters were used.

4.1.1 The method

Broadly speaking, the determination of a moment-curvature relationship is obtained from the imposition of a set of curvatures to the hull's girder. For each curvature, the state of average strain of each beam-column element is determined. Entering with these values in the stress-strain curves, the load sustained by each element may be calculated and consequently the bending moment sustained by the cross section is obtained from the summation of the moments of stress loads in individual elements. The derived set of values defines the desired moment-curvature relation.

However, some problems arise in its implementation, namely, the sequence and spacing of imposed curvatures strongly influence the convergence of the method due to the shift of neutral axis. Also the modelling of the ship's section, which will be treated in section 4.2, and the determination of the position of the neutral axis itself are important issues.

The basic assumptions of the method are the following:

- the elements into which the cross section is subdivided are considered to act and behave independently,

directions, respectively denoted as C_x and C_y . The global curvature C is related to these two components by:

$$C = \sqrt{C_x^2 + C_y^2} \quad (80)$$

or:

$$\begin{cases} C_x = C \cdot \cos \theta \\ C_y = C \cdot \sin \theta \end{cases} \quad (81)$$

adopting the right-hand rule, where θ is the angle between the neutral axis and the x axis. The strain at the centroid of any element ε_i is consequently:

$$\varepsilon_i = y_{li} \cdot C_x - x_{li} \cdot C_y \quad (82)$$

or developing:

$$\varepsilon_i = C \cdot (y_{li} \cdot \cos \theta - x_{li} \cdot \sin \theta) \quad (83)$$

where (x_{li}, y_{li}) is the vector from the two neutral axis to the centroid of the element i (stiffener and associated effective plate). The relation between these local coordinates and the global coordinates are:

$$x_{li} = x_i - NA_x \quad (84)$$

$$y_{li} = y_i - NA_y \quad (85)$$

Equations (84) and (85) are still valid if one uses any point belonging to the neutral axis instead of the point resulting from the intersection of the two neutral axis.

Once the strain state of each element is achieved the correspondent average stresses may be calculated according to expressions in chapter 3 and consequently the components of the bending moment at a curvature C are:

$$\begin{cases} M_x = \sum y_{NAi} \cdot \Phi(\varepsilon_i) \sigma_0 A_i \\ M_y = \sum x_{NAi} \cdot \Phi(\varepsilon_i) \sigma_0 A_i \end{cases} \quad (86)$$

where x_{NAi} and y_{NAi} are the distances from the element i to a local axes of a reference datum located in the precise position of the instantaneous centre of gravity CG.

The modulus of the total moment is:

$$M = \sqrt{M_x^2 + M_y^2} \quad (87)$$

This moment is the bending moment on the cross section if the instantaneous CG is placed in the correct location. Along the step by step process, however, this location is shifting and so it is necessary to calculate the shift between the two imposed curvatures. Rutherford and Caldwell⁷⁶ suggested that the shift could be taken equal to:

$$\Delta NA = \frac{\sum(A_i \cdot \sigma_i)}{C \cdot \sum(A_i \cdot E_i)} \quad (88)$$

but it was felt that this expression underestimated the shift and may cause problems in convergence.

For this reason a trial-and-error process was implemented, having as stopping criteria one of the two conditions: the total net load in the section, NL, or the error in the shift estimation ΔNA should be less than or equal to sufficiently low values. Equations (89) and (90) represent analytically these two conditions, where ζ was taken equal to 10^{-6} .

$$NL = \sum(\sigma_i \cdot A_i) \leq \zeta \cdot \sigma_0 \cdot \sum(A_i) \quad (89)$$

$$\Delta NA = k_E \cdot \frac{NL}{C \cdot E \cdot \sum A_i} \leq 0.0001 \quad (90)$$

The factor k_E is a function of the curvature and yield strain introduced to permit a better convergence of the method, and it is a result of the variation in global tangent modulus of the section with curvature.

4.1.1 Modelling of the ship's cross section

As hull strength assessment is based on the strength of stiffened panels, the modelling of the ship's cross section consists of discretising the hull into stiffened plate elements which are representative of panel behaviour. The design philosophy of the shipbuilding industry is oriented, mainly, to longitudinal stiffened hulls. In this kind of ships large panels with similar and repetitive properties (space between stiffeners, thicknesses and stiffener geometry) are common current practice.

As the behaviour of these panels may be represented as the behaviour of n equally stiffened plate elements, then the hull section shall be divided into small elements representing a plate between stiffeners and the corresponding stiffener. Apart the validity of this modelling concerning panel behaviour, already discussed in previous chapters, some others points of the modelling present some problems or approximations, especially related to:

- the validity of the element's stress state as derived from the strain state at the centroid of the element,
- the modelling of side girders when web stiffeners are not present,
- the modelling of corners,
- the modelling of large and reinforced flanges of primary longitudinal girder system and the validity of this subdivision on the overall behaviour of main girders, specially relating to sideways flexural behaviour.

Relating to the first point, figure 24 shows the strain distribution in a reinforced element. The stress state of the components of the element (plate and stiffener) is

computed considering the strain at the centroid ϵ_i . However the real plate strain is higher than that strain and is approximately equal to ϵ_{max} . This error is only relevant when the element belongs to horizontal panels, i. e., deck and bottom, but because in these two structures the distance of the elements from the neutral axis is high compared with the dimensions of the elements, it results in a ratio between these two strains close to one, which makes the approximation acceptable and allows the simplification of the procedures and iterations.

For the contribution of the side girders without longitudinal stiffeners, two solutions are possible: to neglect their contribution due to the low level of the bending moment experienced as a consequence of the low strength and the proximity of the neutral axis, or to calculate approximately the strength using the formula for transversely loaded plates, as given in equations (9), (10) and (11).

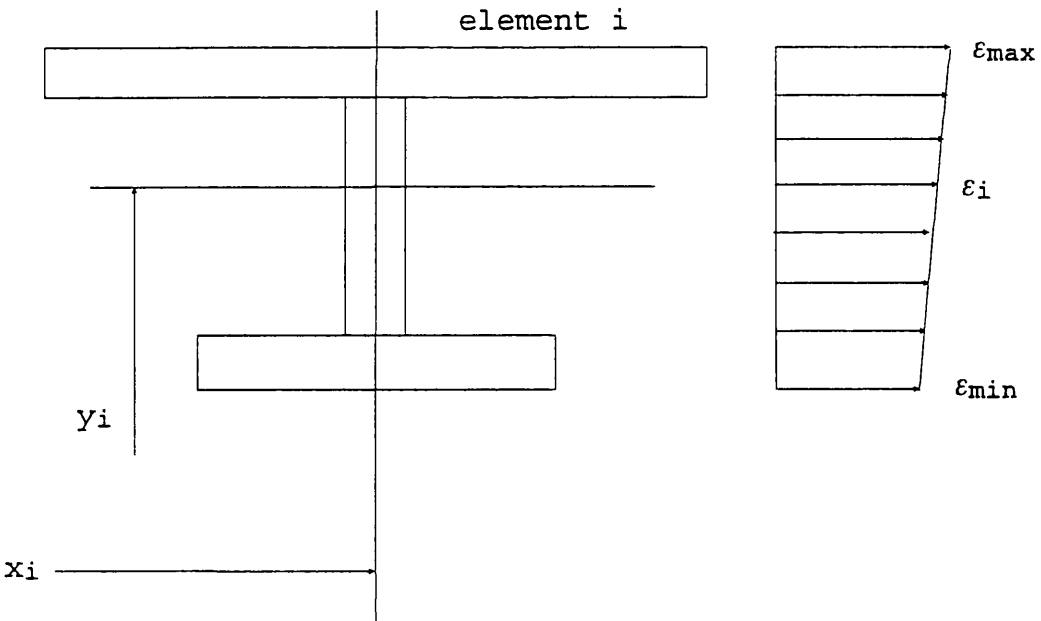


Figure 24-Strain State of a Stiffened Plate Element

In this work the last solution is adopted and the girders are modelled considering three main components: the flange with a stiffener (which is not more than the edge of the girder's web), another stiffened plate on the other side of girder consisting of side plating and part of the web, and a central plate region, figure 25. The extremes are modelled as beam-columns in order to compute their higher rigidity compared with that of plate elements alone; the breadth of the stiffeners (part of the web) must be carefully chosen by the designer in such a way that they behave hardly (low λ_0).

Relatively to the contribution of the corners, normally three situations are considered: first, behaving like hard-corners, i.e., considering that their strength is one ($\Phi=1$) in the plastic domain, second, not taking into account any contribution of the corners on hull's strength, or modelling corners like usual beam-columns. Any of these solutions is formally unsatisfactory because they do not include the influence of the buckled state of

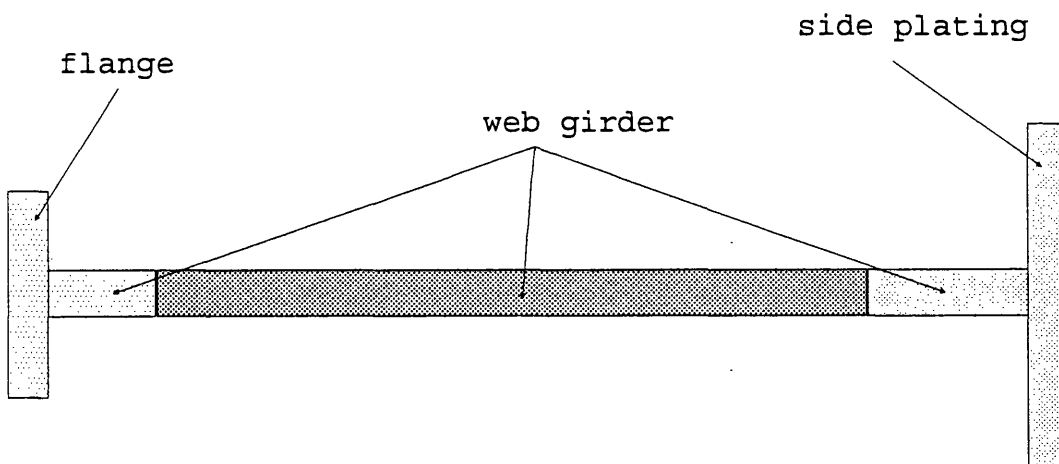


Figure 25-Modelling of Unstiffened Side Girders

adjacent panels on the behaviour of the corner; in section 4.7 this subject will be treated with more detail.

4.2 Analysis of 'Energy Concentration'

In order to test the method and the program developed, the hull of the VLCC-'Energy Concentration' was chosen because there are several studies completed for this ship which permit good comparisons to be made.

This VLCC broke its back in July 1980 during a discharge of oil at Rotterdam. As the ship was discharging in still water and the load conditions were fairly well known, the determination of the ultimate bending moment of the ship could be computed with sufficient accuracy.

4.2.1 The Ship

The ship was ten years old and had been constructed by Kawasaki Heavy Industries, in March 70, in Japan, according to the current design practice at the time for VLCC's and had the following principal dimensions:

Length, overall	326.75 m
Length, between perpend.	313.00 m
Moulded breadth	48.19 m

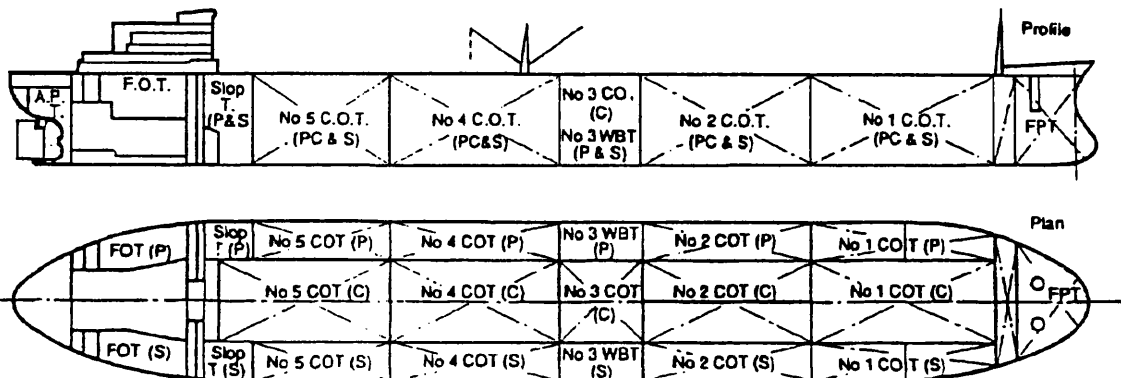


Figure 26-The 'Energy Concentration' plan and profile

Moulded depth	25.20 m
Draft, summer	19.60 m
Deadweight	216,269 tons

Figure 26 shows the profile and plan of the ship and the general arrangement of cargo, ballast and slop tanks, as well as the location of longitudinal and transverse bulkheads. The ship was initially classified by Det Norske Veritas and had changed to Bureau Veritas in 1977. The last survey report found all cargo and ballast tanks in good conditions with the exception of ballast tanks n°. 3 where a greater degree of corrosion was found. The location of these tanks is coincident with the location of the failure.

In the beginning of her last voyage, the ship was heavily trimmed by the stern (1.47 m) and showed a hog deflection of 42 cm. Further calculations performed by

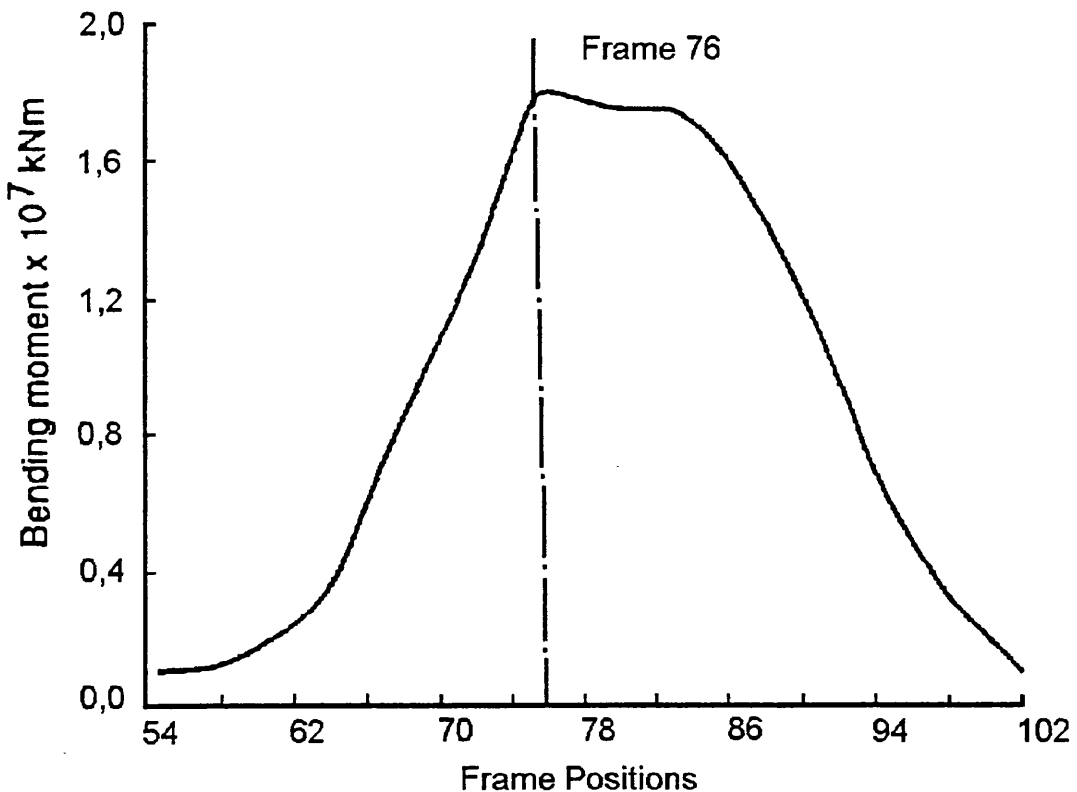


Figure 27-Bending Moment Distribution at Failure

Rutherford and Caldwell⁷⁶, figure 27, concluded that the failure hogging moment should be of about 17940 MN.m. It is also possible to detect a region on the aft side of the frame 76 where very high levels of moment and shear coexist due to the fact that the central tanks were empty.

4.2.2 Modelling of the Ship

In order to perform the analysis of the ultimate carrying capacity of 'Energy Concentration' and to determine of the moment-curvature relationship it is necessary to model the cross-section in stiffened elements as was proposed in section 4.1.1. Figure 28 shows the solution adopted for half of the section, which has 242 reinforced elements and 2 plate elements. Figures 29 and 30 together

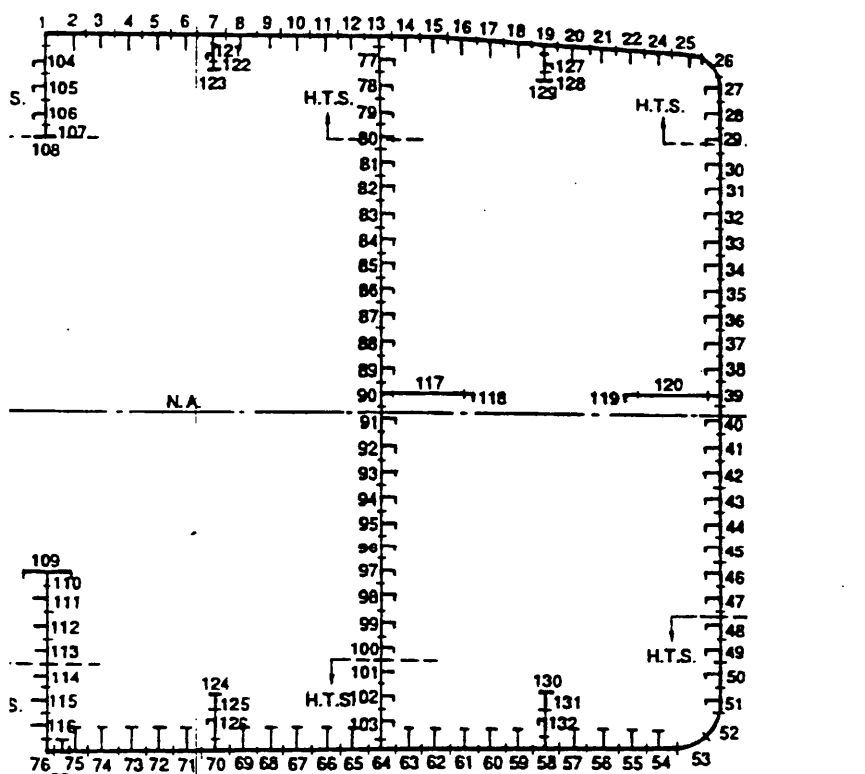


Figure 28-Modelling of the Failure Cross-Section

<u>STF</u>	<u>WEB</u>	<u>FLANGE</u>	<u>STEEL</u>
1	797x15	200X33	HTS
2	297X11.5	100X16	HTS
3	370X16		HTS
4	425X25		HTS
5	480X32		HTS
6	297X11.5	100X16	HTS
7	370X16		HTS
8	447X11.5	125X22	HTS
9	549X11.5	125X22	MS
10	597X11.5	125X22	MS
11	597X11.5	125X25	MS
12	647X11.5	125X25	MS
13	350X25.4		MS
14	647X12.7	150X25	MS
15	697X12.7	150X25	MS
16	747X12.7	150X25	MS
17	747X12.7	180X25	MS

<u>STF</u>	<u>WEB</u>	<u>FLANGE</u>	<u>STEEL</u>
18	797X14	180X25	MS
19	847X14	180X25	MS
20	847X14	180X32	MS
21	847X15	180X25	HTS
22	847X15	180X32	HTS
23	897X15	200X25	MS
24	945X16	200X25	MS
25	897X15	200X25	HTS
26	797X15	180X25	HTS
27	347X11.5	125X22	HTS
28	397X25		HTS
29	300X35		MS
30	230X12.7		MS
31	230X12.7		HTS
32	397X11.5	100X25	HTS
33	-		
34			

Table 1-Scantlings Dimensions and Material Properties

with table 1 give the relevant information about the dimensions and materials properties of the section and elements. As can be noticed the ship uses two different kinds of material in three regions: the deck and bottom are of high strength steel (HTS, $\sigma_o=315$ MPa) and the the main part of side shell, longitudinals and bulkheads are constructed on mild steel (MS, $\sigma_o=235$ MPa). The frame spacing in the zone of interest is 5.10 m and the spacing between longitudinals varies between 925 mm on side and bulkheads to 1000 mm on the deck and bottom.

4.2.3 Moment-Curvature Curve

The programs developed in this thesis are able to predict the moment-curvature relationship for several conditions of heeling, levels of corrosion, residual stresses and distortions, and also to understand the effect of load shedding after the buckling of the panels on the ultimate bending moment of the section.

In this sub-section the results obtained for the initial cross section of the VLCC 'Energy Concentration' are compared with those obtained by the Rutherford and Caldwell⁷⁶ analysis and the calculated moment at the time of failure, Table 2. The results obtained (columns 2 and 3) show that the predictions are 15% above the estimated failure moment of the ship for the 'as built' condition. However, it has been noted that the ship at the time of failure was ten years old and showed some degree of corrosion in the region of failure.

Method	Ultimate Moment (MN.m)			
	Initial	%	Estimate corrosion	%
Failure	17940	100.0	17940	100.0
Rutherford	18979	105.8	17860	99.6
MARC-FEM	20630	115.0	18520	103.2
Faulkner	20618	114.9	18994	105.9
Carlsen	20482	114.2	19025	106.0

Table 2-Results of Hogging Moment

Comparison between methods with the prediction of failure for as built (initial) and for estimate conditions at failure (corrosion effects). The Rutherford analysis considered lateral pressure while MARC included 10% increase in the estimate for yield strength. None of the analyses include residual stresses.

Also, the results of the applied methods (Faulkner and Carlsen) do not account for any level of residual stresses, which seems to be in accordance with reality due to their shakeout. In relation to distortions, Faulkner's equation for plates itself incorporates the effect of average levels of plate distortions and, as it is used on both methods, this effect is accounted for. However the results in the above table do not incorporate stiffener out-of-plane distortions and an increase in their magnitude reduces the ultimate moment.

The last two columns in Table 2 compare the results taking into account a standard level of corrosion of 1mm and the Carlsen method includes a stiffener deflection of $0.0015a$, where a is the span of the stiffeners. The results are all within a band of 6%, which demonstrates the validity of the simplified methods proposed here. It is also relevant to notice how the results from both methods are close to each other (20618 and 20482, and 18994 and 19025 MN.m).

Referring to the moment-curvature curve itself, Figures 31 and 32 show that the curves from both methods are almost coincident in hogging. The maximum moment occurs at an approximate curvature of $1.31 \times 10^{-7} \text{ mm}^{-1}$, and after that point a smooth decrease of the bending moment sustained is present. The curves of the position of the neutral axis show four main regions:

- an elastic region from zero to a curvature of about half the ultimate curvature;
- an elasto-plastic region, which extends almost until the ultimate curvature, where the loss of plate effectiveness due to compression is important and corresponds to a smooth change in the neutral axis position;

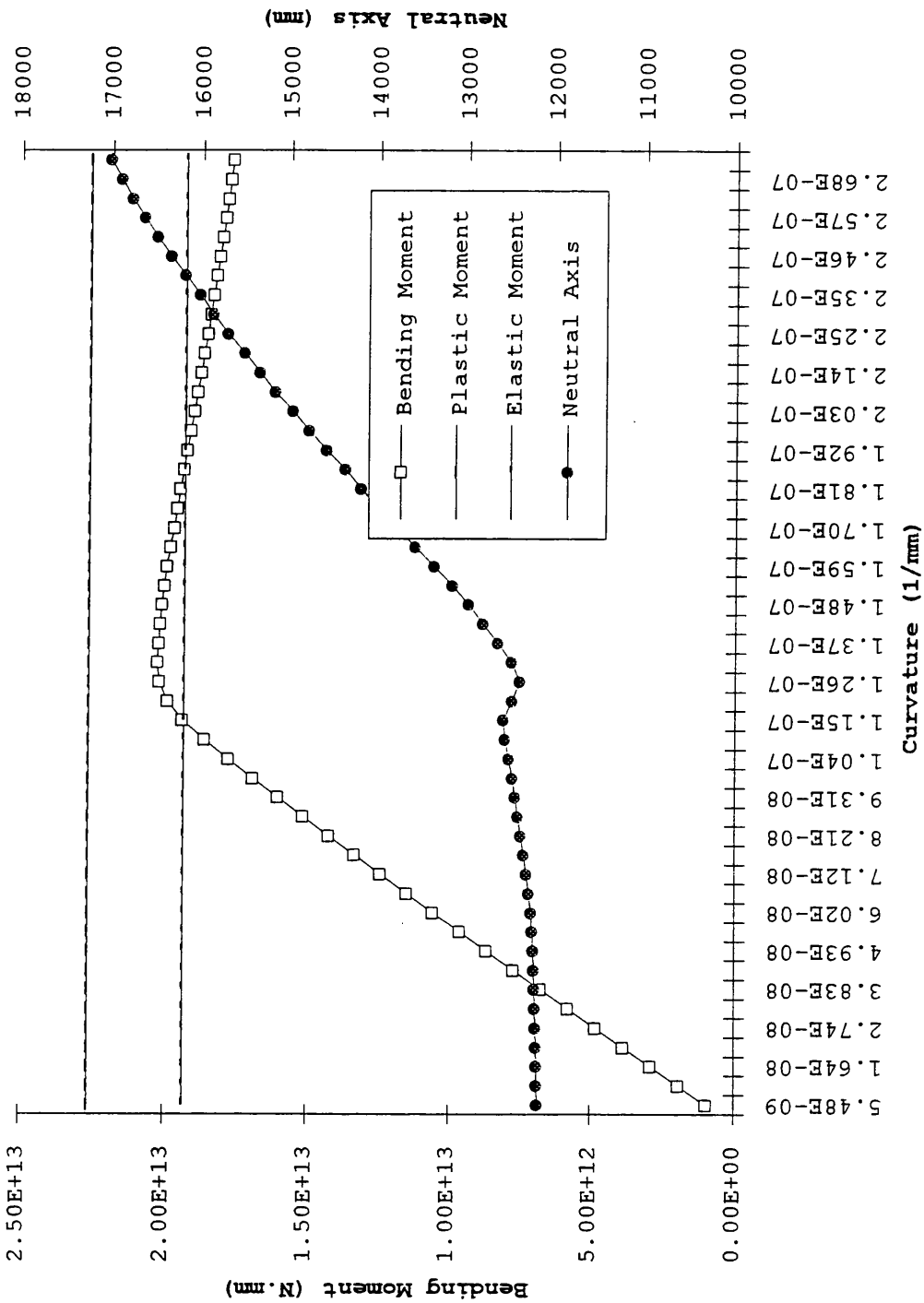


Figure 31-Moment-Curvature Curve of 'Energy Concentration'

Curve of the bending moment and the position of neutral axis against curvature of the 'Energy Concentration', in hogging, using Faulkner's method but ignoring residual stresses and corrosion.

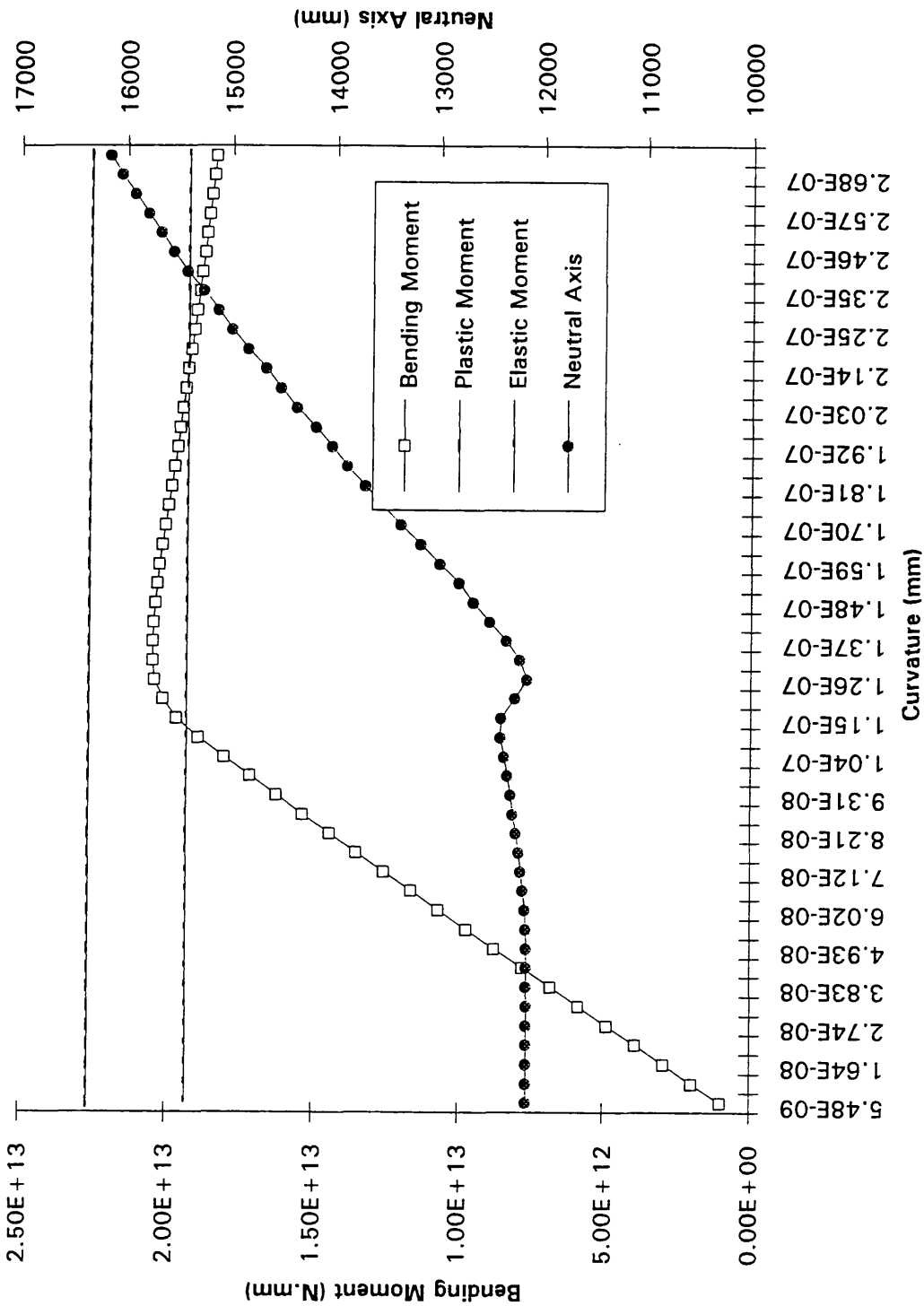


Figure 32-Moment-Curvature Curve of 'Energy Concentration'

Curve of the bending moment and the position of neutral axis against curvature of the 'Energy Concentration' in hogging, using Carlsen's method but ignoring residual stresses and corrosion.

<u>Method</u>	<u>Ultimate Moment (m.MN)</u>			
	Initial	%	Estimate corrosion	%
Elastic M.	19323	100.0	18450	100.0
Rutherford	15450	80.0	14420	78.2
Faulkner	15110	78.2	13878	75.2
Carlsen	15385	79.6	14160	76.7

Table 3-Results of Ultimate Moment in Sagging

Comparison between methods with the prediction of failure for as built (initial) and for estimate conditions at failure (corrosion effects). Rutherford analysis considered lateral pressure. None of the analyses include residual stresses.

- a very narrow band near ultimate curvature, where the effect of the yield of the panels in tension (deck panels in hogging) supersedes the increasing loss of effective width of the plating, and this is represented in the graphs by a sudden change in slope of the neutral axis curve;
- a load shedding region, in which the position of the neutral axis is moving rapidly due to the collapse of the most compressed panels.

Table 3 compiles the ultimate moment results for sagging. It is important to notice that the ultimate bending moment in sagging is about 20% lower than the elastic bending moment for all methods, which demonstrates the weakness of using the elastic theory as a basis for the rules of Classifications Societies. The elastic bending moment is defined as the moment corresponding to the the first yield, normally in the deck, when an elastic analysis of the stresses in the section is performed.

The results from the methods proposed in this thesis are in general one or two percent lower than those calculated with Lloyd's Program n°. 20202 (Rutherford and

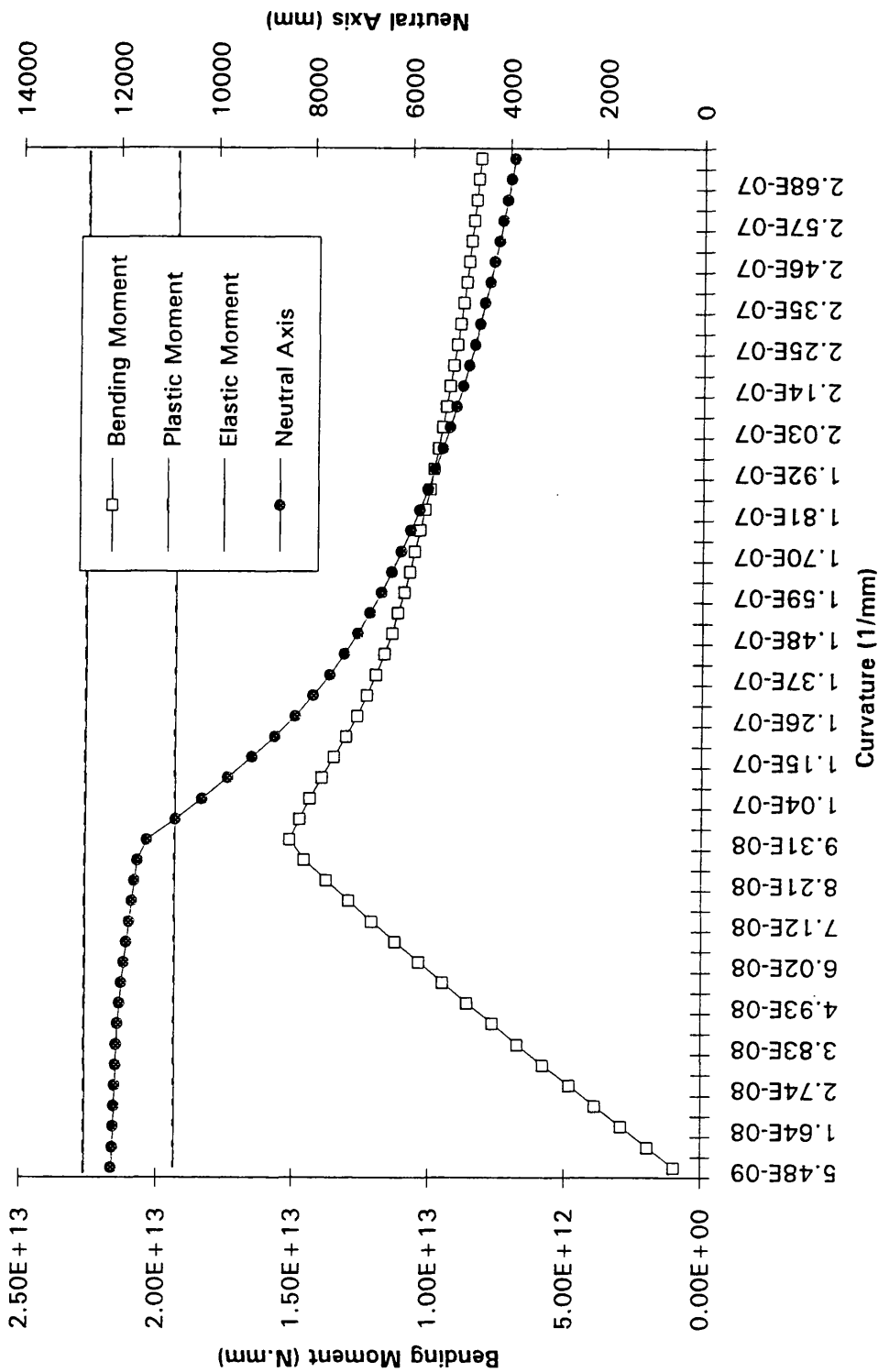


Figure 33-Moment-Curvature Curve of 'Energy Concentration'

Curve of the bending moment and the position of neutral axis against curvature of the 'Energy Concentration' in sagging, using Faulkner's method but ignoring residual stresses and corrosion.

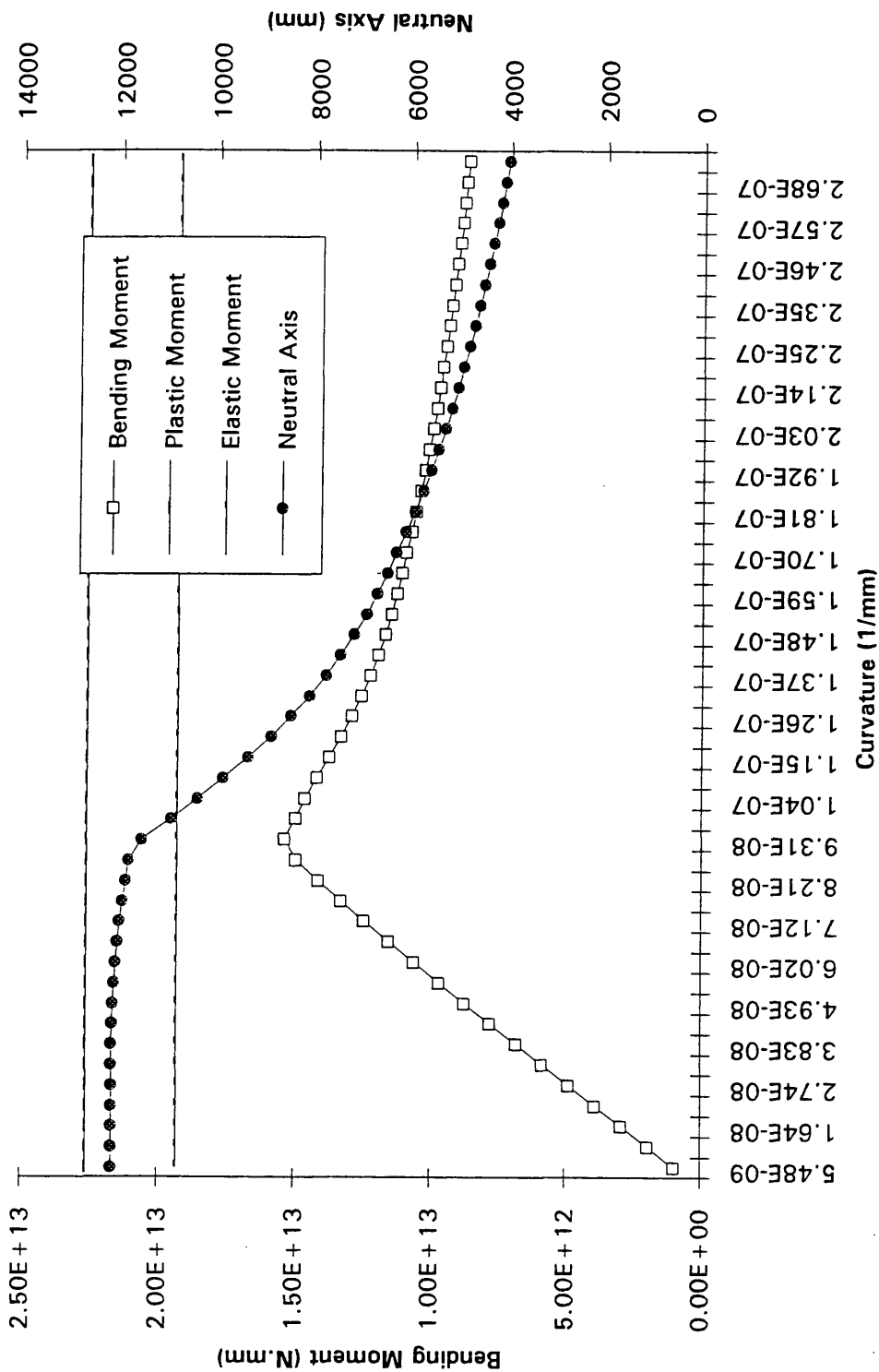


Figure 34-Moment-Curvature Curve of 'Energy Concentration'

Curve of the bending moment and the position of neutral axis against curvature of the 'Energy Concentration' in sagging, using Carlsen's method but ignoring residual stresses and corrosion.

Caldwell results) in sagging while they give higher results in hogging. This discrepancy may be a result of applying different formulations for tripping behaviour of stiffeners and also from the assumed load shedding pattern after buckling. However both of the proposed methods (JO and PR), predict similar behaviour and results for sagging and hogging, the differences between them being lower than 2%.

The analysis of 'Energy Concentration' is very interesting in the validation of these type of analyses because it shows how these simplified methods may predict and identify where the design of the ship may be improved in order to obtain better structural cross-sections.

In this particular case, the ship had very slender panels in the deck and as consequence they promoted the tripping of the stiffeners at an early stage of loading followed by the sudden collapse of the section, as shown in figures 33 and 34, and a very quick change in the position of the neutral axis.

It may be confirmed that there is no problem in the design of the bottom structure in respect to buckling and tripping, because the hogging ultimate moment is between the elastically derived yield bending moment and the plastic one.

4.3 Effect of corrosion

This section attempts to obtain a correlation between the corrosion and the degradation of the hull strength due to it. Comparisons between the methods are also made.

During their lives, ships are subjected to the action of a corrosive environment. The external structures at the water line and upper deck as well as internal tanks structures are the most exposed ones to corrosion. The magnitude of the growing corrosion may be controlled by several methods, but unless plates are replaced, a steady reduction of thickness takes place. Classification's Society rules normally include an allowance for corrosion, between a range of 0.5 and 3mm depending on the position of the scantling, the nature of the tank and surrounding tanks and the type of protection.

The present approach only considers a difference of corrosion rating between webs and flanges/plating, the former having the double of the corrosion rate of the latter. Each level of corrosion reduced the thickness of the plating and flanges by 0.5mm and the web's thickness by 1 mm.

Tables 4 and 5 show the results for the total area, ultimate moment in hogging and sagging for each level of corrosion and compare them with the values for the 'new' ship. Both methods of strength prediction give the same qualitative results and one may conclude that if the panels in compression are stocky (bottom panels in hogging) then 1% reduction on total area promotes a reduction in ultimate moment of about 1.15%. For sections with slender panels in compression (deck in sagging for this ship) the same reduction of 1% promotes a reduction of more than 1.5% in

<u>Corrosion</u>			<u>Ultimate Moment (MN.m)</u>			
Level	Area	%	Sagging	%	Hogging	%
0	7.888	100.0	15110	100.0	20249	100.0
1	7.684	97.4	14452	95.6	19626	96.9
2	7.479	94.8	13878	91.8	18994	93.8
3	7.274	92.2	13328	88.2	18384	90.8
4	7.070	89.6	12422	82.2	17821	88.0

Table 4-Effect of Corrosion (Faulkner Method)

Results of ultimate moment for several level of corrosion in sagging and hogging. Residual stresses are not considered.

<u>Corrosion</u>			<u>Ultimate Moment (MN.m)</u>			
Level	Area	%	Sagging	%	Hogging	%
0	7.888	100.0	15383	100.0	20286	100.0
1	7.684	97.4	14708	95.6	19680	97.0
2	7.479	94.8	14187	92.2	19025	93.8
3	7.274	92.2	13609	88.5	18445	90.9
4	7.070	89.6	12731	82.8	17828	87.9

Table 5-Effect of Corrosion (Carlsen Method)

Results of ultimate moment for several level of corrosion in sagging and hogging. Residual stresses are not considered. Stiffener deformations are in accordance with Carlsen recommendation ($\delta=0.0015a$).

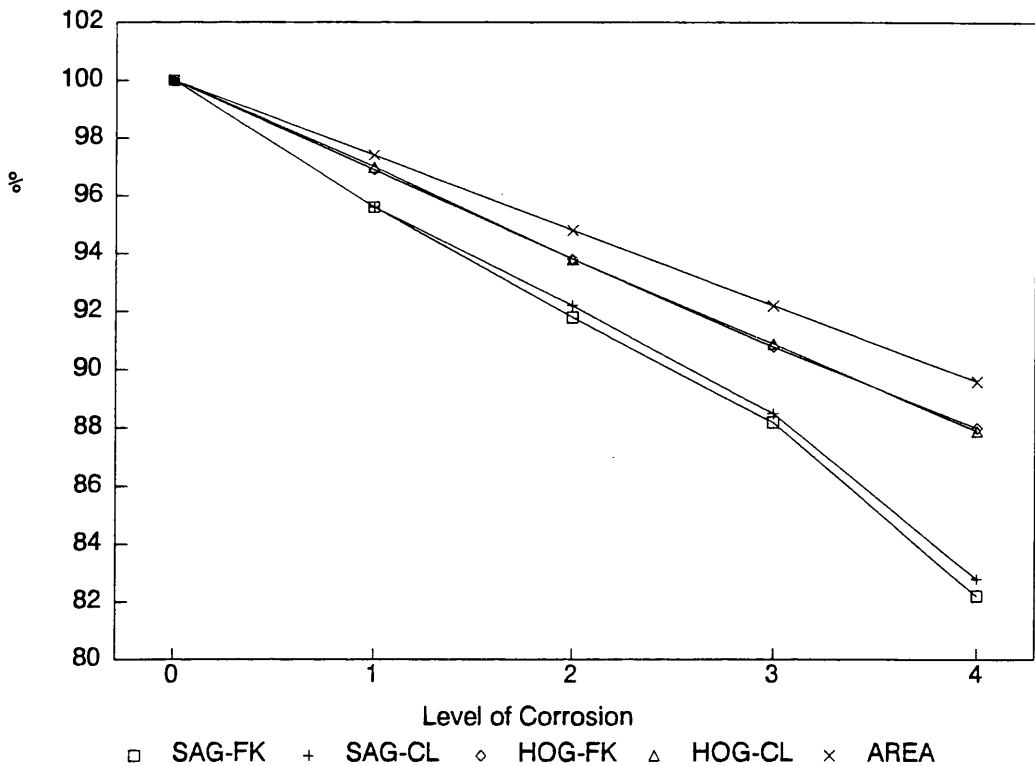


Figure 35-Effect of Corrosion

Ultimate moment normalised for several level of corrosion in sagging and hogging by Faulkner and Carlsen based methods. Residual stresses are not considered.

the ultimate moment.

The results are also plotted in Figure 35, showing the linear correlation of corrosion rate (or reduction of section area) and ultimate moment variation. However, high levels of corrosion in the sagging condition produce more than linear reduction in strength variation, which may result from the change of the type of column failure due to reduction in column slenderness. This means that the best solution to deal with corrosion in design codes must include the dependence of the corrosion allowance on the column slenderness of the stiffener with associated plate of the ship's panels.

4.4 Effect of Residual Stresses

The presence of residual stresses in the plating usually leads to a reduction of the effective width of the plate elements with a consequent decrease in column strength, as was seen in chapters 2 and 3. The present section quantifies the effect on the ultimate moment of a hull girder's cross section.

Residual stresses are classified by levels, each of them corresponding to a tensile zone (figure 6, page 17) with a width of the level times the thickness of the plate. Using this method and assuming that η depends on the welding process, then plates with different thicknesses will have different residual stresses $\bar{\sigma}_r$ to the same level of weld tension block η , according to equation (14).

Table 6 and figure 36 analyse the effect of residual stresses for both sagging and hogging conditions using the Perry-Robertson formulation with the recommended level of stiffener deformation proposed by Carlsen.

In hogging both methods, Design Formula Method and Physical Approach Method for residual stresses, give a linear relation between the ultimate moment and η but the Crisfield based approach (PAM) predicts a reduction in strength which is twice the value if DFM. In order to have a comparison, the level 3 of η corresponds to $\bar{\sigma}_r=0.167$ in a plate having a width-thickness ratio of 40. The bottom plate elements of 'Energy Concentration' have this typical value (1000x25mm) and a reduction of strength of 4.8% (PAM) is predicted.

In sagging the methods predict quite different behaviour in respect to the effects of η . While the DFM

<u>Sagging</u>				
η	DFM	%	PAM	%
0	15383	100.0	15383	100.0
1	15225	99.0	15385	100.0
2	15052	97.8	15409	100.2
3	14861	96.6	15103	98.2
<u>Hogging</u>				
η	DFM	%	PAM	%
0	20286	100.0	20286	100.0
1	20122	99.2	20003	98.6
2	19948	98.3	19681	97.0
3	19751	97.4	19309	95.2

Table 6-Effect of Residual Stresses on Ultimate Moment

Results of ultimate moment for several level of residual stresses in sagging and hogging. Corrosion is not considered. The results are based on Carlsen's approach for column's strength.

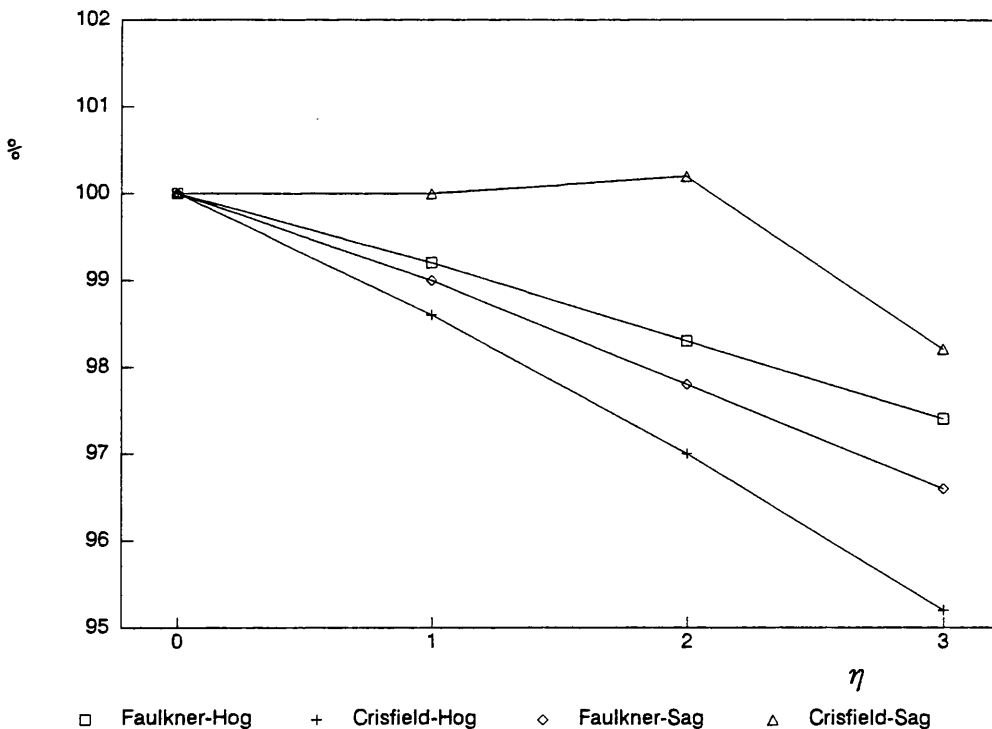


Figure 36- Effect of Residual Stresses

Graphical representation of the results of table 6 based on Carlsen's approach.

equations predict almost the same reduction as in hogging, the PAM method is almost insensitive to low levels of residual stresses. The main reason for this behaviour may be found in the comparison between the tripping stress of deck elements and the stress at which residual stresses act. In this particular case residual stresses do not affect the ultimate strength of the deck panel while the tripping stress is lower than the stress corresponding to yielding in central region of the plate element.

These conclusions are directly related to the design of the deck and bottom panels of this ship. As the column slenderness of the deck is much higher than for the bottom structure and as tripping is present when the deck is in compression, the end-shortening at column failure is lower than the shortening corresponding to yielding.

In DFM this is equivalent to having a reduction factor proportional to the ratio between the end-shortenings, because the ultimate shortening without tripping occurs always at yielding by construction.

In PAM the ultimate shortening is changing with residual stresses and the result in the hull's behaviour is unpredictable because it depends on the combination of several factors. However, for average and higher levels of residual stresses, the rate of strength reduction seems to be the same as in hogging, eg for values between $\eta=2$ and 3 in figure 36 (corresponding respectively to $\bar{\sigma}_r=0.11$ and 0.167 in deck plate elements).

As a main conclusion of this discussion, one may quantify the effect of residual stresses on ultimate bending moment for ships where tripping failure is avoided as being given approximately by:

$$\frac{M_{ur}}{M_u} = 1. - 0.29 \cdot \bar{\sigma}_r \quad (91)$$

according to PAM or by:

$$\frac{M_{ur}}{M_u} = 1. - 0.16 \cdot \bar{\sigma}_r \quad (92)$$

for DFM. These expressions are based on compressed plate elements of $b/t=40$ (bottom panels in hogging) and consequently the dependence on this parameter has to be investigated. In respect of the expressions above, one is based on a specific model for residual stresses as close a possible to reality (PAM) while the other is consequence of a statistical study of the impact of residual stresses on plate elements (DFM). The author has a strong preference to the former, which is recommended for use. This strong preference for the Physical Approach Method is based mainly on the future possibilities of the method by using different patterns of residual stresses distributions.

4.5 Effect of distortions

The influence of distortions on hull strength is directly dependent on their effect in column load-shortening curves, which was discussed on section 3.3.1.

In this section, only the effect of the stiffener's out-of-plane imperfections is investigated, and is summarised in Table 7. The Johnson approach does not account explicitly for distortions, thus only Carlsen's method is used.

According to this method the effect of stiffener's out-of-plane distortions is negligible in sagging because the ultimate cause of cross section collapse is the tripping of the stiffener and its formulation does not incorporate distortions. In hogging (stocky columns in

<u>Distor-</u> <u>tions</u>	<u>Ultimate Moment (MN.m)</u>				
	Level/a	Sagging	%	Hogging	%
	0.0000	15385	100.0	20490	100.0
	0.0005	15384	100.0	20426	99.7
	0.0010	15383	100.0	20357	99.4
	0.0015	15383	100.0	20286	99.0
	0.0020	15382	100.0	20214	98.7
	0.0025	15376	99.9	20144	98.3
	0.0030	15370	99.9	20073	98.0
Faulkner		15110	98.2	20249	98.8

Table 7-Effect of Distortions (Carlsen Method)

Results of ultimate moment for increasing levels of stiffener's out-of-plane deformations in sagging and hogging by Perry-Robertson formulation (Carlsen method). Residual stresses and corrosion are not considered.

compression), the performance of the section is very good, and shows very little dependence with out-of-plane stiffener's imperfections (1% reduction on strength for every 0.0015a increase in δ_s).

However some other types of distortions may have more relevance to hull strength, namely plate distortions due to the reduction of the effective width of the associated plate and the effects of rotational distortions (tilt) of the stiffener on tripping failure or on flexural buckling when lateral pressure is applied from the stiffener side which increases the level of compression stresses in the stiffener.

4.6 Analysis for combined loading

Elastic analysis of the hull girder predicts that the behaviour of a cross section of usual ships under combined vertical and horizontal bending can be described by an interaction equation which is ellipse, where the elliptical distances are respectively $\sigma_0 \cdot W_v$ and $\sigma_0 \cdot W_h$. W_v is the minimum of the section moduli of deck and bottom and W_h is the section modulus of the side relatively to the center line.

The hypotheses to be fulfilled in order to obtain this elliptical behaviour are:

- the distance from the deck and bottom to the neutral axis in the upright position must be constant and sides must be vertical, i.e., there is no rise of floor or camber.
- the yield stress in compression must be the same as in tension.

As usual ships do not fulfill the first requirement because there is always camber and bilge radii, the limit state curve in elastic theory is somewhat different from the ellipse due to the shift of the furthest point from the heeled neutral axis, (x,y) in equation (93).

$$M = \sigma_0 \cdot \frac{I_h \cdot I_v}{x \cdot I_v \sin \theta - y \cdot I_h \cos \theta} \quad (93)$$

The above equation is achieved from the limit stress state, equation (96), and the components of the bending moment in the principal directions are:

$$M_x = M \cdot \cos \theta \quad (94)$$

$$M_y = M \cdot \sin \theta \quad (95)$$

where θ is the angle between the moment vector and the

horizontal axis. These two components generate longitudinal stresses which allow to define the yield limit state due to bending as:

$$\sigma_o = \frac{M_y \cdot x}{I_h} - \frac{M_x \cdot y}{I_v} \quad (96)$$

and the angle of the neutral axis ψ by:

$$\tan \psi \equiv \frac{y}{x} = \frac{I_v}{I_h} \cdot \tan \theta \quad (97)$$

The total bending moment is related to the components by:

$$M^2 = M_x^2 + M_y^2 \quad (98)$$

Faulkner et al.²⁶ deduced from numerical studies a circular failure interaction equation for the HMS Cobra which had rise of floor, camber and assymetry in the cross section. This means that one may calculate the ultimate strength of a ship subjected to combined bending if the vertical and horizontal ultimate moments are known. However some deviation to this circularity may be detect in particular ships and for particular ranges of angles of heel.

When the ship has camber and sucessively increasing heeling angles are considered, the point (x,y) to be used in equation (93) change from the intersection of the center line and deck towards the side corners which corresponds a smaller distance to the actual neutral axis than the initial one. As result, the elastic moment is reduced slighly for small angles of heel when it might normally be expected to increase initially. This explanation is seen from the same behaviour found from the elasto-plastic analysis, Figure 39.

Analysis covering all angles of heeling from sagging to hogging were performed, as shown in Figures 37 and 38

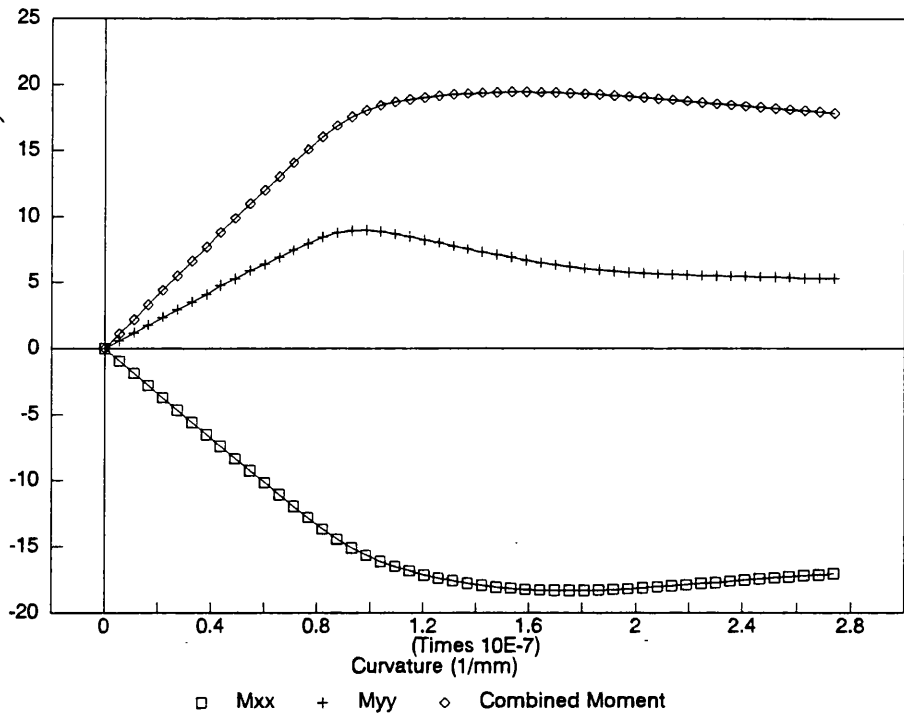


Figure 37-Components of Combined Bending at 165°

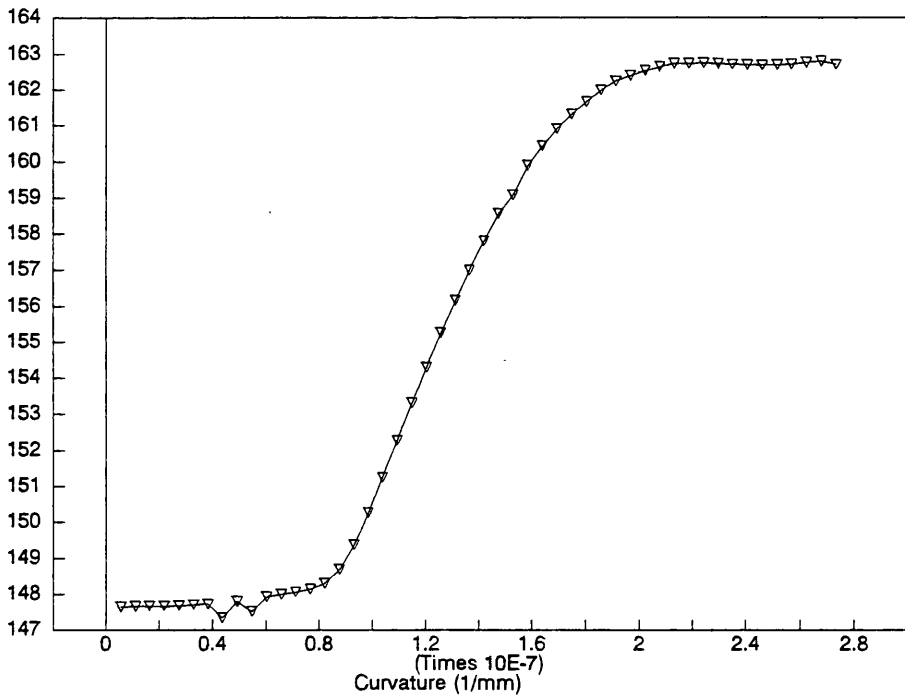


Figure 38-Variation of Moment Angle with Curvature

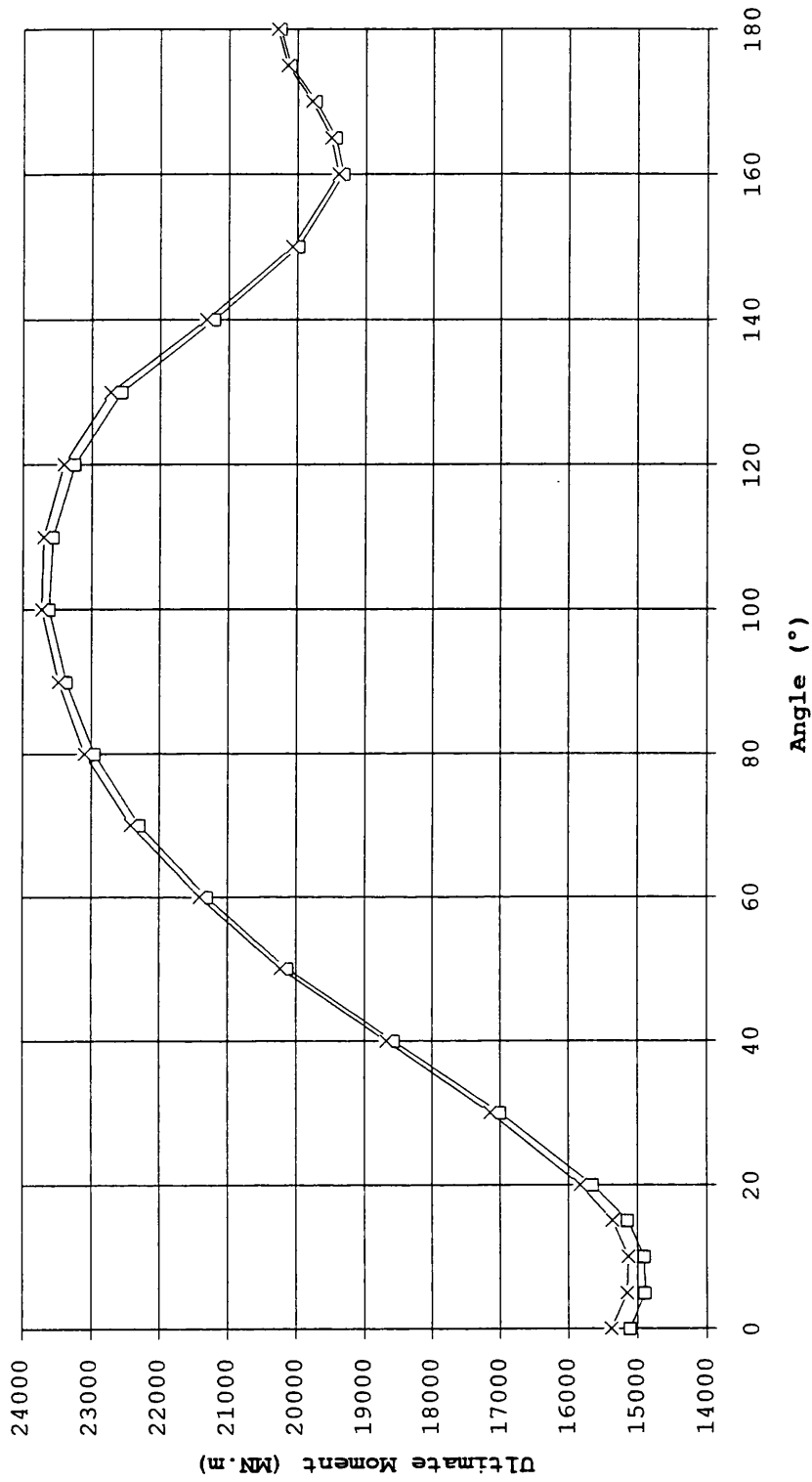
which give results when the neutral axis is kept at an angle of 165° to the horizontal axis (15° apart from pure hogging). It is important to note from these figures the change in the direction of the moment vector and the dissimilar behaviour of its horizontal and vertical components when curvature increases.

Initially the angle is about 148° and this value may be computed with equation (97). When curvature is increased the angle changes slightly toward the neutral axis, but this shift becomes very quick for curvatures near the buckling of the bottom and side plating. After this sudden change the moment vector and the neutral axis have approximately the same direction (163° and 165° respectively).

This behaviour is a consequence of the lack of proportionality between M_x and M_y , which becomes important after the buckling of the first panels, i.e., because bottom and side panels have different column slenderness, the buckling and post-buckling behaviour of the corresponding panels is different, thus the rate of the change of the load carrying capacity of vertical and horizontal moments changes with increasing curvature.

In the present case, at an angle of 165° , a collapse of the section is evident in M_y at a curvature of $9 \times 10^{-8} \text{ mm}^{-1}$, while M_x has its maximum value at a curvature of $17.5 \times 10^{-8} \text{ mm}^{-1}$. The explanation for this is that the side panels near the bilge collapse first and this collapse is more important for the horizontal modulus than for the vertical one due to the greater reduction in effective inertia moment about yy than about xx .

The impact of buckling on the effective moment of inertia is a result of three main contributions:



□ Faulkner × Carlsen

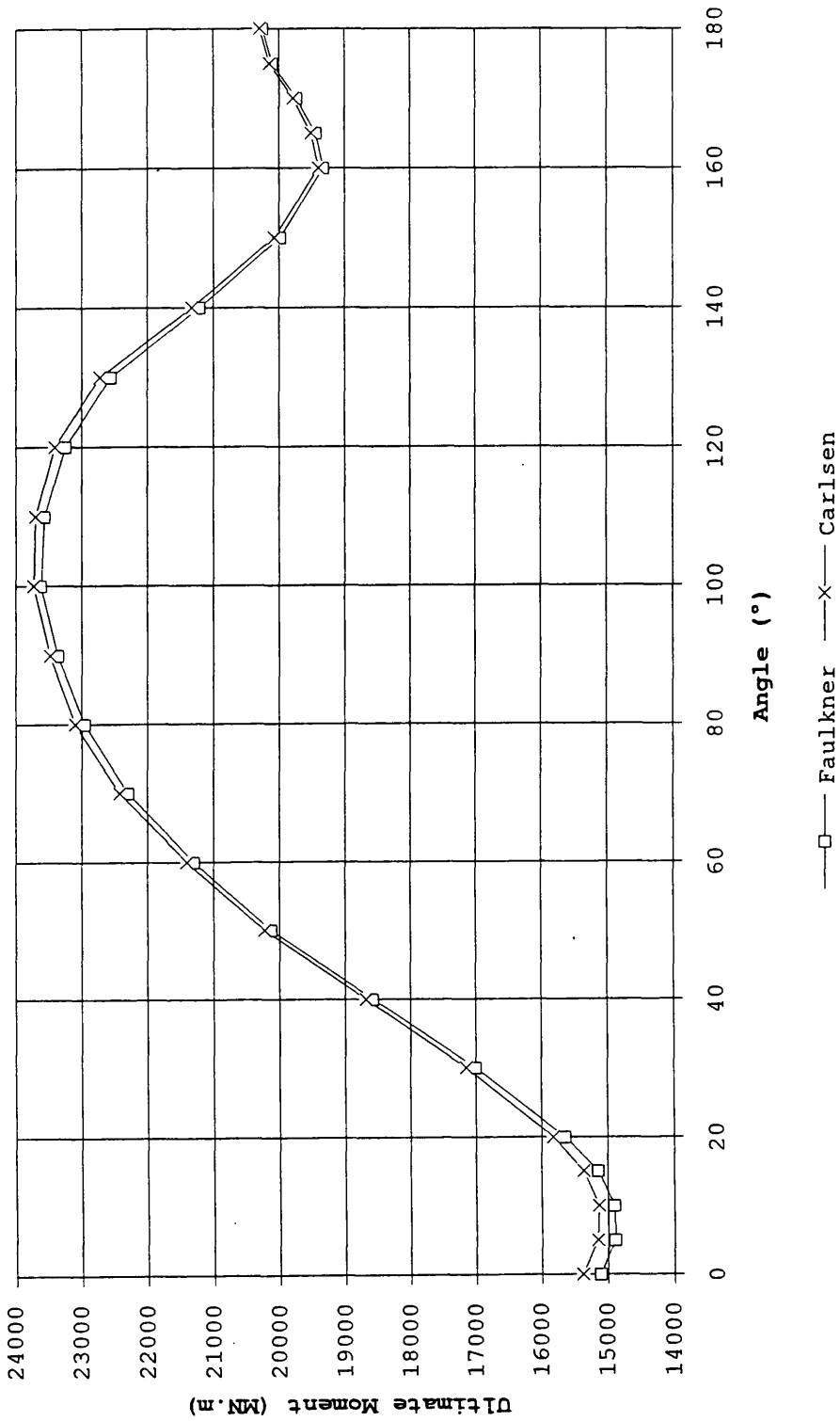


Figure 39- Combined Bending Moment
 ultimate bending moment corresponding to a certain angle of
 the neutral axis about which curvature is imposed.

- the reduction in moment of inertia about the initial axis by an amount proportional to $(1.-\Phi_C) \cdot x^2$ and $(1.-\Phi_C) \cdot y^2$ for y_{NA} and x_{NA} axes, respectively,
- the reduction in effective section area,
- and the shift in neutral axis.

The first is the most important contribution and because y is normally greater than x , the impact on I_h will be greater than on I_v .

Relative to the ultimate moment along heeling the principal conclusions are:

- the different results for hogging (180°) and sagging (0°) due to dissimilar types of collapse as already commented,
- the maximum strength is not located at 90° as expected, but slightly moved toward hogging (110°) due to the presence of more stocky elements in bottom panels,
- the reduction of strength for small heeling angles, with minimums at 5° and 165° for sagging and hogging.

Also worth noting is the coincidence of both formulations over the range of heeling angles. However the Faulkner based method (JO) is more conservative than the Carlsen one (PR), especially when slender panels are in compression.

4.7 Efficiency of high strength steel

High strength steel is one of the many choices at the disposal of the designer when longitudinal requirements are not fulfilled. This solution is extensively used in 'long' ships such as VLCCs and ULCCs.

Apart from some problems with fatigue that are arising in crude carriers which use high tensile steel (HTS), or an eventual degradation of yield stress with aging, the objective of this section is to investigate the efficiency, from the structural point of view, of using HTS instead of mild steel (MS).

The cross section of 'Energy Concentration' was analysed for three situations: using only mild steel of 235 MPa yield, totally built of HTS (315 MPa) and 'as built' using HTS in the bottom and deck and MS on side shell and bulkheads according to the general design practice for VLCCs. Table 8 shows the results of this analysis, by comparing Faulkner and Carlsen methods with the results expected using elastic analysis.

First we note that both methods give very similar results, with differences less than 1%. But the main point to note is the dissimilar effects on the resistance when the panels in compression are stocky (hogging in this example) or slender (sagging).

From the elastic analysis a potential gain of 34% in longitudinal strength is expected when changing from MS to MS+HTS or HTS. In fact only 27% is reached in the 'best' condition of this particular ship, i.e., when the panels in compression are designed to avoid tripping and are sufficiently stocky. If these requirements are not satis-

fied than a very bad increase of 7.5% is obtained and the choice of this solution may be classified as poor.

The potential gain (σ_{HTS}/σ_{MS}) is never achieved because the increase of yield stress increases the slendernesses of the plate β_0 and of the column element λ_0 when the geometry is unchanged, which corresponds to a reduction on average effective stress supported by the panel.

<u>Sagging</u>					
Steel	Elastic	Faulkner	%	Carlsen	%
MS-235	14416	14109	93.4	14246	92.6
MS+HTS	19323	15110	100.0	15383	100.0
HTS-315	19323	15112	100.0	15383	100.0
<u>Hogging</u>					
Steel	Elastic	Faulkner	%	Carlsen	%
MS-235	14416	15879	78.4	15886	78.3
MS+HTS	19323	20249	100.0	20286	100.0
HTS-315	19323	20278	100.1	20336	100.2

Table 8-Influence of High Strength Steel

Ultimate bending moment for a cross section using several grades of steel, in sagging and hogging. Residual stresses and corrosion are not considered.

5 Conclusion and Future Development

The simplified procedure used in this work to predict the behaviour of the hull girder under predominant longitudinal bending seems to be quite accurate when the results are compared with those obtained by different approaches and also in the case of a real ship failure.

On the other hand, if the preparation time of the model and the computational running time is considered and compared with methods using finite element programs, then the developed procedure is far better and more useful for normal design practice. The simplified method takes about three minutes to run and calculate the whole moment-curvature curve in a 386 PC while FE methods need normally a main frame to run the model and spending several hours of CPU time. In relation to the preparation time of the model, FE methods may take more than a month to implement the model while the approximate method only requires about two days of work.

The problem of the prediction of the hull girder behaviour is treated by two methods of treat the stiffened plate approach (JO and PR). The comparison between these two methods have shown that they predict the same kind of behaviour of stiffened plates with very small differences in the ultimate strength if the same unstiffened plate strength formulation is used. However it has to be noticed that one of the stiffened plate formulations accounts explicitly to the influence of the out-of-plane stiffener distortions (PR) while the other 'ignores' this effect (JO).

The above methods, as derived in this thesis, predict a load shedding pattern in the behaviour of the stiffened plate after buckling. This prediction is mainly based on the assumed variation of the effective width of the associated plate and thus it requires the confirmation by other methods: experiments or finite element methods. This confirmation is specially important for the prediction of the ultimate strength of the ship cross-section due to the different state of strain of each stiffened element, where some of them are already in the post buckling region.

Another interesting feature is that the ultimate bending moment in the upright position is greater than at small angles of heel, no matter if the ship is in hogging or sagging. Thus it is necessary to evaluate if this reduction shall be included in the rules of the Classification Societies. In practice, the problem is that if an elasto-plastic analysis of the hull girder is performed and the calculation of the minimum ultimate moment is required then one shall look for the minimum at an angle of heeling of about 10° or more. Alternatively, a reduction to the upright moment shall be considered. However, the last solution seems to be weaker than the first because the degree of the reduction depends on the compressive strength of the deck and side panels.

The use of HTS should be carefully evaluated by the designer because, from the structural point of view, the increase of the yield stress is not fully represented as an increase in the total strength; normally this increase is much lower than expected. If this small increase is judged together with the higher price and the potential fatigue problems of the HTS, then the designer may conclude that HTS shall be avoided in some cases.

Residual stresses and corrosion have a degrading

effect on the ultimate moment. However these effects occur in separate times in the ship life: the residual stresses are present in the early stage of the ship life and the effect tends to reduce with the normal operation conditions, while the corrosion level tends to be increased with the time. So both effects should not be considered together for design purposes, i.e., if an allowance for corrosion is included in the design then reduced allowance for the residual stresses should be considered.

The inclusion of a tripping formulation in the behaviour of stiffened panel is seen to be very important in the particular case investigated here. The deck stiffeners, made of bars, have not much flexural-torsional rigidity and the calculated tripping stress is lower than the flexural buckling stress of the stiffener with associated plate. This fact leads to a very high reduction of the ultimate bending moment in sagging compared with the moment in hogging, where the deck is in tension. Future work is desired in this subject and nowadays it is possible and relatively easy to compare the prediction of the tripping stress using approximate methods and the results of finite element methods for stiffened panels.

The study of the impact of the residual stresses in plate elements developed here (PAM) considered a particular case of stresses distribution. However, a smooth transition between the tension and compression zones may easily be implemented by the modification of the equation that quantifies the change of the 'material' behaviour.

Future development of the approximate methods to predict the hull girder strength should include the implementation of an explicit method to account for transverse strength of the hull and overall buckling of large panels. But, before, it is very important to test

extensively over the practical range of plate and column slenderness the derived load - end shortening curves of unstiffened and stiffened plates, investigating carefully the agreement in the post buckling range.

REFERENCES

1. Faulkner, D.: "A review of effective plating for use in the analysis of stiffened plating in bending and compression", J. of Ship Research, 19, 1975, pp. 1-17.
2. Valsgard, S.: "Numerical design prediction of the capacity of plates in in-plane compression", Computers and Structures, n. 12, 1980, pp.729-739.
3. Guedes Soares, C.: "Design equation for the compressive strength of unstiffened plate elements with initial imperfections", J. Const. Steel Research, 9, 1988, pp. 287-310.
4. Guedes Soares, C. and Faulkner, D.: "Probabilistic modelling of the effect of initial imperfections on the compressive strength of rectangular plates", Proc. Third International Symposium on Practical Design of Ships and Mobile Units (PRADS), Trondheim, vol. 2, 1987, pp.783-795.
5. Frieze, P.A., Dowling, P.J. and Hobbs, R.E.: "Ultimate load behaviour of plates in compression", Steel Plated Structures, Dowling, Harding & Frieze eds, Crosby Lockwood Staples, London, 1977.
6. Crisfield, M.A.: "Full range analysis of steel plates and stiffened plating under uniaxial compression", Proc. Inst. Civil Engrs., 59, 1975, pp. 595-624.
7. Dowling, P.J., Harding, J.E. and Slatford, J.E.: "Plates in biaxial compression", CESLIC Report SP4, Eng. Structures Lab., Civil Eng. Department, Imperial College, London, Nov. 1979.

8. Moxham, K.E.: "Theoretical prediction of the strength of welded steel plates in compression", Cambridge University Report CUED/C- Struct/TR2, 1971.
9. Smith, C.S., Davidson, P.C., Chapman, P.C. and Dowling, P.J.: "Strength and stiffness of ships' plating under in-plane compression and tension", Trans. RINA, 130, 1988.
10. Harding, J.E., Hobbs, R.E. and Neal, B.G.: "The elasto-plastic analysis of imperfect square plates under in-plane loading", Proc. Inst. Civil Engrs., 63, March 1977.
11. Little, G.H.: "Rapid analysis of plate collapse by like-energy minimisation", Jnl. of Mech. Sciences, 19, 1977.
12. Crisfield, M.A.: "Large deflection elasto-plastic buckling analysis of plates using finite elements", Proc. Inst. Civil Engrs., 59, Dec 1975.
13. Moxham, K.E.: "Buckling tests on individual welded steel plates in compression", Report CUED/C-Struct/TR.3, Cambridge University, 1971.
14. Becker, H. et al.: "Compressive strength of ship hull girders, Part I, Unstiffened plates", Report SSC-217, Ship Structure Committee, Washington D.C., 1970.
15. Dwight, J.B.: "Collapse of steel compression panels", Developments in Bridge Design and Construction, Crosby Lockwood, 1971.
16. Dwight, J.B. and Moxham, K.E.: "Welded steel plates in compression", The Structural Engineer, 47, 1969.

17. Dwight, J.B. and Little, G.H.: "Tests on transverse welded box columns", Report CUED/C-Struct/TR24, Engin. Depart., Cambridge University, 1972.
18. Bradfield, C.D.: "Tests on plates loaded in in-plane compression", J. Construction Steel Res., 1, 1980.
19. Little, G.H.: "The collapse of rectangular steel plates under uniaxial compression", The Structural Engineer, 58 B, 1980.
20. Dwight, J.B. and Ractliffe, A.T.: The strength of thin plates in compression, Thin-walled Structures, Crosby Lockwood Staples, London, 1969.
21. Guedes Soares, C. and Gordo, J.M.: "Compressive strength of ship plates under combined loading", Report CEMUL/IST, Lisboa, 1991.
22. Lin, Y.T.: "Ship longitudinal strength", Ph. D. thesis, Dept. of NA&OE, University of Glasgow, Scotland, 1985.
23. Billingsley, D.W.: "Hull girder response to extreme bending moments", Proc. SNAME Spring Meeting, June 4-6, 1980.
24. Rhodes, J.: "On the approximate prediction of elasto-plastic plate behaviour", Proc. Instn Civ. Engrs, Part 2, 71, 1981.
25. Faulkner, D., Adamchak, J.C., Snyder, G.J. and Vetter, M.F.: "Synthesis of welded grillages to withstand compression and normal loads", Computers and Structures, 3, 1973, pp. 221-246.
26. Faulkner, J.A., Clarke, J.D., Smith, C.S. and Faulkner, D.: "The loss of HMS COBRA - a reassessment", Trans. RINA, 1984.

27. Blanc, F.: Discussion to ultimate longitudinal strength, Trans. RINA, 107, 1965, pp. 426-430.
28. Guedes Soares, C. and Soreide, T.H.: "Behaviour and design of stiffened plates under predominantly compressive loads", International Shipbuilding Progress, 30, n.341, 1983, pp. 13-27.
29. Antoniou, A.C.: "On the maximum deflection of plating in newly built ships", Journal of Ship Research, 24, 1980.
30. Carlsen, C.A. and Czujko, J.: "The specification of tolerances for post-welding distortion of stiffened plates in compression", The Structural Engineer, 56 A, 1978.
31. Frieze, P.A., Dowling, P.J. and Hobbs, R.E.: "Ultimate load behaviour of plates in compression", Steel Plates Structures, Crosby Lockwood Staples, London, 1977, pp 24-50.
32. Mansour, A., Yang, J.M. and Thayamballi, A.: "An experimental investigation of ship hull ultimate strength", Trans. SNAME, vol. , 1990, pp..
33. Murray, J.M.: "Notes on deflected plating in tension and compression", Trans. INA, 87, 1945, pp..
34. Jazukiewicz, A., Kmiecik, M., Taczala, M. and Majka, K.: "System of programs for IBM PC/AT for nonlinear analysis of plates and panels by finite element method", Budownictwo i Gospodarka Morska, n. 11-12, 1990 (in Polish).

35. Becker, H. e Colao, A.: "Compressive strength of ship hull girders. part III - theory and additional experiments", Report SSC-267, Ship Structure Committee, Washington D.C., 1977.
36. Valsgard, S.: "Ultimate Capacity of Plates in Biaxial In-Plane Compression", Det Norske Veritas Report n.78-678, Mar 1979.
37. Stonor, R.W.P., Bradfield, C.D., Moxham, K.E. and Dwight, J.B.: "Tests on plates under biaxial compression", Report CUED/D-Struct/TR98, Cambridge University, Engineering Department, 1983.
38. Dier, A.F. and Dowling, P.J.: "Plates under combined lateral loading and biaxial compression", Final Report for the British Ship Research Association, Imperial College, Dep. of Civil Eng., London, CESLIC Report SP8, Sep. 1980.
39. Becker, H.: "Instability strength of poliaxially-loaded plates and relation to design", Steel Plated Structures, P. J. Dowling et al. (Ed.), Crosby, Lockwood and Staples, London, 1977, pp. 559-580.
40. Yoshiki, M. et al.: "Buckling of rectangular plates subjected to combined lateral and edge loads", Transactions Zosen Kyokai, n. 118, Nov. 1965.
41. Yamamoto, Y., Matsubara, N. and Murakami, T.: "Buckling strength of rectangular plates subjected to edge thrusts and lateral pressure", J. Soc. Naval Arch. Japan, 127, Jun. 1970, pp. 171.
42. Okada, H., Oshima, K. e Fukumoto, Y.: "Compressive strength of long rectangular plates under hydrostatic pressure", J. Soc. Naval Arch. Japan, 146, Dec. 1979.

43. Smith, C.S., Anderson, N., Chapman, J.C., Davidson, P.C., Dowling, P.J.: "Strength of stiffened plating under combined compression and lateral pressure", Trans. RINA, 133, 1991.
44. Davidson, P.C., Chapman, J.C., Smith, C.S. and Dowling, J.P.: "The design of plate panels subject to biaxial thrust and lateral pressure", Trans. RINA, 131, 1991.
45. Harding, J.E., Hobbs, R.E., Neal, B.G.: Ultimate load behaviour of plates under combined direct and shear in-plane loading, Steel Plated Structures, J.P. Dowling et al. (eds), Crosby Lockwood and Staples, London, 1977.
46. Kondo, M.R. and Ostapenko, A.: "Tests on longitudinally-stiffened plate panels with fixed ends. Effect of lateral loading", Report 248.12, Fritz Eng. Laboratory, Lehigh University, 1964.
47. Dean, J.A. and Dowling, P.J.: "Ultimate load tests on three stiffened plates under combined in-plane and lateral loading", Steel Plated Structures, P.J. Dowling (Eds.), Crosby Lockwood Staples, London, 1977, pp. 743-763.
48. Dubois, M.: "Tests of flat plated grillages", Bulletin Technique du Bureau Veritas, 1975, pp. 15-20.
49. Fukumoto, Y., Usami, T., Itoh, Y. and Nethercot, D.A.: "A numerical data-base approach to the ultimate compressive strength of unstiffened plates", Stability of metal structures, preliminary report, Paris, 1983, pp. 275-283.
50. Little, G.H.: "Stiffened Steel Compression Panels - Theoretical Failure Analysis", The Structural Engineer, 54, n.12, 1976.

51. Smith, C.S.: "Compressive Strength of Welded Steel Ship Grillages", Trans RINA, 117, 1975.
52. Dow, R.S. and Smith, C.S.: "Fabstran: A Computer Program for Frame and Beam Static and Transient Response Analysis (nonlinear)", ARE Report TR86205, ARE, Dunfermline, Fife, U.K., 1986.
53. Moolani, F.M. and Dowling, J.P.: "Ultimate load behaviour of stiffened plates in compression", Steel Plated Structures, Crosby Lockwood Staples, London, 1977, pp. 51-88.
54. Belkaid, M.: "A Simplified Analytical Approach for the Strength of Longitudinally Framed Vessels and their Components", MSc thesis, University of Glasgow, Dept. of Naval Architecture and Ocean Engineering, UK, 1989.
55. Faulkner, D.: "Compression strength of welded grillages", edited by J.H. Evans, Ship Structural Design Concepts, 1974.
56. Carlsen, C.A.: "A parametric study of collapse of stiffened plates in compression", The Structural Engineer, 56 B, 1980, pp. 33-40.
57. Murray, N.W.: "Analysis and design of stiffened plates for collapse load", The Structural Engineer, 53, 1975, pp. 153-158.
58. Horne, M.R. and Narayanan, R.: "Design of axially loaded stiffened plates", Jnl Structural Div., ASCE, 103, 1977.
59. Horne, M.R., Montague, P. and Narayanan, R.: "Influence on strength of compression panels of stiffener section, spacing and welded connection", Proc. Inst. Civil Engrs., Part 2, 63, 1977.

60. Faulkner, D.: "Compression tests on welded eccentrically stiffened plate panels", Steel Plated Structures, ed. by P. J. Dowling et al., Granada, London, 1977.
61. Dorman, A.P. and Dwight, J.B.: "Tests on stiffened compression panels and plate panels", Proc. International Conference on Steel Box Girder Bridges, Inst. of Civil Engrs., London, Feb. 1973.
62. Perry, S.H. e Chiver, A.H.: "The statistical variation of the buckling strengths of columns", Proc.Inst. Civil Engrs, Part 2, 1976, pp. 109-125.
63. Faulkner, D.: "Toward a better understanding of compression induced tripping", Steel and Aluminium Structures, 3, Ed by R. Narayanan, Elsevier Applied Science, 1987, pp. 159-175.
64. Adamchak, J.C.: "Design Equations for Tripping of Stiffeners under Inplane and Lateral Loads", DTNSRDC Report 79/064, Bethesda, Maryland, 1979.
65. Smith, C.S.: "Elastic analysis of stiffened plating under lateral loading", Trans. RINA, 108, 1966.
66. Smith, C.S.: "Bending, buckling and vibration of orthotropic plate-beam structures", Jnl of Ship Research, 12, 4, Dec 1968.
67. Wittrick, W.J.: "General sinusoidal stiffness matrices for buckling and vibration analyses of thin flat-walled structures", Int. Jnl of Mechanical Science, 10, 1968.
68. Smith, C.S. and Faulkner, D.: "Dynamic behaviour of partially constrained ship grillages", The Shock and Vibration Bulletin, n.40, part 7, Naval Research Laboratory, Washington DC, Dec 1969.

69. Caldwell, J.B.: Ultimate longitudinal strength, Trans. RINA, vol. 107, 1965.
70. Faulkner, D.: Contribution to discussion of ref. 69.
71. Adamschak, J.C.: "ULTSTR: A program for estimating the collapse moment of a ship's hull under longitudinal bending", DTNSRDC Report 82/076, Bethesda, Maryland, Oct 1982.
72. Hughes, O.F.: Ship structural design, chapter 17, John Wiley and Sons, New York, 1983.
73. Smith, C.S., Kirkwood, W.C. and McKeeman, J.L.: "Evaluation of ultimate longitudinal strength of a ship's hull", Admiralty Marine Technology Establishment, Dunfermline, Report AMTE(S)/R671, 1977.
74. Dow, R.S., Hugill, R.C., Clarke, J.D. and Smith, C.S.: Evaluation of ultimate ship hull strength, SNAME, 1981.
75. Smith, C.S. and Dow, R.S.: "Ultimate strength of a ship's hull under biaxial bending", ARE Report TR86204, ARE, Dunfermline, 1986.
76. Rutherford, S.E. and Caldwell, J.B.: "Ultimate longitudinal strength of ships: a case study", SNAME-Annual Meeting, paper n.14, 1990.
77. Carlsen, C.A.: "Simplified Collapse Analysis of Stiffened Plates", Norwegian Maritime Research, n. 4, 1977.
78. Guedes Soares, C. and Kmiecik, M.: "Simulation of the ultimate compressive strength of unstiffened rectangular plates", Proc. Charles Smith Memorial Conference, Dunfermline, published by Elsevier Science Publishers, 13-14 July 1992.

79. Davidson, P.C., Chapman, J.C., Smith, C.S. and Dowling, J.P.: "The Design of Plate Panels subject to In-Plane Shear and Biaxial Compression", RINA, W8, 1989.
80. Dow, R.S.: "N106C: A Computer Program for Elasto-Plastic, Large Deflection Buckling and Post-Buckling Behaviour of Plane Frames and Stiffened Panels", AMTE(s) R80726, July 1980.
81. Faulkner, D. and Sadden, J.A.: "Toward a Unified Approach to Ship Structural Safety", RINA, Spring Meetings, n.3, 1978.
82. Pietzker: "Conceptual Models for Structural Analysis and Synthesis", Ship Structural Design Concepts, J. Harvey Evans, Cornell Maritime Press, 1974.
83. Smith, C.S.: "Imperfection Effects and Design Tolerances in Ships and Offshore Structures", Trans. Inst. Engrs. and Shipbuilders in Scotland, Feb 1981.
84. Smith, C.S.: "Elastic Buckling and Beam-Column Behaviour of Ship Grillages", Trans RINA, vol 110, Jan 1968.
85. Rockey, K. C., Skaloud, M.: "The ultimate load behaviour of plate girders loaded in shear", The Structural Engineer, n. 1, vol. 50, 1972.
86. Rutherford, S.E.: "Stiffened Compression Panels - the analytical approach", Hull Struct. Report n. 82/26/R2, Lloyd's Reg. of Shipp., 1984.
87. Kmiecik, M.: "The load-carrying capacity of axially loaded longitudinally stiffened plate panels having initial deformations", Rapport nr. R-80, Skipsteknisk Forskningsinstitutt, Trondheim, 1970.

88. Smith, C.S.: "Influence of local compressive failure on ultimate longitudinal strength of a ship's hull", Proc. Int. Symposium on Practical Design in Shipbuilding, PRADS, Tokyo, 1977, pp. 73-79.
89. Czujko, J. and Kmiecik, M.: "Post welding distortions of ship shell plating", Report n. 4-S, Ship Research Institute, Technical University of Szczecin, 1975.

